BRIDGE TESTING

Final Report
Project Number ST 2019-12

by

C. H. Yoo
J. M. Stallings

Auburn University Highway Research Center
Auburn University, Alabama

sponsored by

The State of Alabama Highway Department
Montgomery, Alabama

February 1991

DISCLAIMER

The contents of this report reflect the views of the authors who are responsible for the facts and accuracy of the data presented herein. The contents do not necessarily reflect the official views or policies of the State of Alabama Highway Department or Auburn University. The report does not constitute a standard, specification, or regulation.

ACKNOWLEDGEMENT

The material contained herein was obtained in connection with a research project, "Bridge Testing, RP 2019-12," conducted by the Department of Civil Engineering through the Highway Research Center at Auburn University. The research project was sponsored by the State of Alabama Highway Department. The traffic control, test load vehicles, a portable electric generator, bridge inspection vehicles and operators were provided by the Alabama Highway Department's Division and District offices. The cooperation and assistance of personnel from the Alabama Highway Department is gratefully acknowledged. Particular appreciation is expressed to Mr. Mike Harper, Chief of the Maintenance Bureau, and Mr. Fred Conway, Chief of the Bridge Bureau, for their interest in and support of this research project. Mr. Terry McDuffie who was appointed as a state liaison was extremely helpful as he provided prompt and able assistance throughout the project.

The analytical work and field experimentation was assisted by supporting personnel from Auburn University. Mr. Robert Kinchler, Mr. Robert Fulton, and Mr. Chris Reddick, graduate students in the Civil Engineering Department, contributed to the project under the direction of Professors Chai H. Yoo and J. Michael Stallings. Robert Kinchler and Robert Fulton contributed immeasurably to the success of the project through their long hours of analytical work and field experimentation that was frequently done in a very harsh environment.

ABSTRACT

Five steel girder bridges in Alabama, located in Shelby, St. Clair, Blount, and Cullman counties were tested under static and dynamic loading conditions. The primary objective of the project was to determine the load carrying capacity of each bridge. The five bridges selected were rated low by the BARS (Bridge Analysis and Rating System) computer program. Ratings made by BARS were compared with test results. The bridges were also rated manually using the same input information as used in BARS by following procedures outlined in the AASHTO Manual for Maintenance Inspection of Bridges.

An examination of test results permits the following conclusions to be drawn:

(1) All five bridges are capable of carrying loads much higher than the limits determined by the AASHTO rating method.

(2) The AASHTO ratings, calculated using the procedures described in the Manual, were essentially the same as the BARS ratings. Comparison of the ratings, as well as study of the BARS documentation, indicate that BARS is an automated (computerized) version of the AASHTO method.

(3) Grid analysis was performed to compare the various ratings. It appears that the current AASHTO truck wheel load distribution in the simplified rating procedure is frequently conservative.

(4) Although it is impossible to assess quantitatively the degree of unintended composite action between the steel girders and the concrete deck, test results reveal that there exists either partial or full composite action despite apparent lack of any physical shear transfer devises.

(5) Grid analysis results are sensitive to the assumptions made in modeling a bridge. It was found that models developed without test data were not able to accurately represent the observed bridge behavior. Test data was used to refine the grid models through assumptions about effective cross section properties, material properties, and support restraint.

(6) Comparison of measured strains and results from the refined grid models showed improvement. It is expected that with further refinement of the modeling technique grid analysis can produce very accurate results.

TABLE OF CONTENTS

DISCLAIMER i

ACKNOWLEDGEMENT ii

ABSTRACT iii

I. INTRODUCTION 1

Objectives 1

II. FIELD TESTS 4

Testing Equipment 5
Test Procedures 9
Data Reduction 9

Description of Bridges and Test Results 11
Ashville Bridge 11
Description of the Tests 13
Test Results 13
Analysis of the Test Results 13
Vincent Bridge 20
Description of the Tests 20
Test Results 23
Analysis of the Test Results 23
Childersburg Bridge 29
Description of the Tests 29
Test Results 29
Analysis of Test Results 35
Mulberry Fork Bridge 35
Description of the Tests 37
Test Results 37
Analysis of the Test Results 37
Locust Fork Bridge 43
Description of the Tests 43
Test Results 47
Analysis of the Test Results 47

III. BRIDGE ANALYSIS 51

Introduction 51
Modeling the Bridge Deck System as a Grid 52
Development of Grid Models for the Tested Bridges 52
The Ashville Grid Model 54
The Vincent Grid Model 54
The Childersburg Grid Model 58
The Mulberry Fork Grid Model 58
The Locust Fork Grid Model 62

Grid Analyses Performed for the Rating Process 65
Other Analysis Methods 70

IV. BRIDGE RATINGS..... 73

Introduction 73
Dead Loads and Allowable Stresses..... 73
Test Ratings..... 73
AASHTO Ratings 76
Grid Ratings 78
Comparison of the Bridge Ratings 78
Comparisons of AASHTO and BARS Ratings 78

V. CONCLUSIONS 84

VI. REFERENCES 85

APPENDIX A 86

APPENDIX B 113
APPENDIX C 128
APPENDIX D 132
APPENDIX E 135
APPENDIX F 138
APPENDIX G 153

LIST OF TABLES 158

LIST OF FIGURES 160

I. INTRODUCTION

In order to assist highway engineers at the state and local level to comply with the federally mandated program of inspection, rating, and posting of highway bridges, a computer program called BARS (Bridge Analysis and Rating System) has been developed by C.W. Beilfuss and Associates, Inc. under the auspices of AASHTO. The BARS program is used by the Alabama Highway Department to establish bridge ratings. BARS is a versatile program which can handle most highway bridges. The fundamental analysis methodology used in BARS is the AASHTO simplified methods of transverse wheel load distribution. By nature of the versitility of the methods incorporated into BARS, the program tends to give very conservative bridge ratings. Currently the BARS ratings of some steel girder bridges in the state of Alabama are below normal legal truck weights despite the relatively short service life and apparently sound condition of the bridges.

Interest in bridge testing has increased significantly in recent years in part because of the large number of older bridges across the country with posted load limits that are below the normal legal truck weights. Load testing of bridges is an attractive evaluation tool because it can provide a more realistic appraisal of the bridge behavior than analysis. Field load testing frequently offers a means of illustrating that the safe load capacity of a bridge is greater than the capacity calculated by following the AASHTO Manual (1983) or by use of BARS. One reason this is possible is the inability of AASHTO's, and therefore BARS', simplified procedures to accurately model the way that truck wheel loads are distributed among the girders of a bridge. Another reason is that many highway bridges exhibit some degree of composite action even when they were not constructed with shear studs or other devises for transferring shear between the girders and deck. This unintended composite action along with other factors such as unintended support restraint, and the added stiffness of parapets and railings can cause observed strains in the bridge girders to be smaller than predicted by a typical analysis.

Objectives

The primary objective of the project reported here was to perform field load tests on the five bridges identified in Table 1 for the purpose of establishing ratings for the bridges. The five bridges were chosen by the Alabama Highway Department. BARS ratings were performed for each of the bridges by the

Table 1. Bridges Tested

Bridge Name/ Bridge ID No.	Location	No. of Girders	Girder Spacing	Spans Tested	Bridge Type
Ashville 053-58-30.7	St. Clair	5	5'2"	34'	simple span
Vincent 025-59-51.1	Shelby Co	8	3'	27'-27'	two span continuous
Childersburg 038-59-26.6B	Shelby	4	5'-10"	44',77'	simple span
Mulberry Fork 074-22-34.5	Cullman Co.	4	7'	34',44'	simple span
Locust Fork 079-05-9.9	Blount Co.	4	7'-8"	49' 80',100',80'	simple span & three span continuous

Alabama Highway Department before the start of the project. The BARS ratings indicated that each bridge should be posted at load limits below the State of Alabama legal truck weights as illustrated in Figure 40.

A second objective of the project was to perform manual ratings calculations for each of the bridges according to the procedures of the AASHTO Manual (1983). These ratings (referred to as AASHTO ratings) were compared to the ratings based on the test results. Comparisons were also made between the manual calculations and the original BARS results for some of the bridges. These comparisons of BARS ratings and AASHTO ratings illustrate that the BARS program is an automated version of the AASHTO rating procedure.

Another objective of the project, not originally proposed, was to compare AASHTO ratings with ratings determined through grid analyses of the bridges. These ratings were carried out to investigate the relative merits of load testing versus a structural analysis that is more advanced than the wheel load distribution factors used in the BARS program.

II. FIELD TESTS

Introduction

The field tests of each bridge were performed in order to establish the live load capacity of the bridge. By comparing the live load moment capacity with the moment produced by a standard truck loading, a rating can be established as follows:

$$\text{Rating} = \frac{M_{cap}}{M_{abs\ max}} W \qquad (1)$$

where M_{cap} = the allowable live load moment capacity

$M_{abs\ max}$ = the absolute maximum moment produced by an applied load

W = the weight of the standard truck

The purpose of the bridge test is to establish M_{cap}, while analytical analyses are performed to determine $M_{abs\ max}$ for the various standard truck types.

The type of bridge to be tested determines how the bridge should be instrumented. All of the bridges tested for the AHD were short span slab on steel girder bridges. The behavior of these bridges can be characterized by the flexural, or bending stresses, in the girders along the span length. These flexural stresses were determined by measuring the flexural strains in the girders with strain gages at midspan. The strain gages were placed at the extreme fibers of the cross section (or as close as practical) in order to measure the maximum strains at midspan.

The midspan location was chosen as a reference location for test purposes. Two-axle dump trucks were furnished by the AHD to provide the test loading for each bridge. The absolute maximum moment, $M_{abs\ max}$, generally does not occur at the same location for the test trucks and the other standard trucks for which bridge ratings were required. Because the location changes from truck to truck a common reference location, midspan, was chosen. The effects of the various locations of $M_{abs\ max}$ were accounted for in the rating calculations.

The allowable live load moment capacity in Equation 1 can be determined by the following equation:

$$M_{cap} = \frac{\sigma_{all} - \sigma_{dl}}{IF\,\sigma_{ll}} M_{test} \qquad (2)$$

where M_{cap} = allowable moment capacity

σ_{all} = allowable stress

σ_{dl} = dead load stress

σ_{ll} = live load stress

IF = impact factor

M_{test} = moment produced by test truck

The expression in the numerator, $\sigma_{all} - \sigma_{dl}$, represents the allowable live load stress. The live load stress is multiplied by an impact factor in the denominator to account for dynamic effects. If the numerator is larger than the denominator, then the allowable moment capacity is larger than the moment produced by the test truck. If the denominator is larger than the numerator, then the moment produced by the test truck is larger than the allowable moment capacity.

The test results were used to determine σ_{ll} and the impact factor for Equation 2. To determine σ_{ll}, stationary tests were performed. The stress σ_{ll} was taken as the largest of the stresses measured for the individual girders of the bridge. Moving tests were performed to determine the impact factor. In some instances impact factors based on the AASHTO Specifications (1989) were used in the rating calculations.

Values for σ_{all}, determined from the AASHTO Manual (1983), and σ_{dl}, determined from field data and AHD records, are presented in Chapter IV for each bridge. The value of M_{test} was determined from analyses. The analyses are expalined in Chapter III.

Testing Equipment

The live load strains in the girders were determined by using a number of electrical resistance strain gages as illustrated in Figure 1.

Strain gages, manufactured by BLH, were applied to the girders at predetermined positions along the span on either the top flange, bottom flange, or coverplate. Before the strain gages were applied, the

Figure 1. Strain Gage

steel surface was polished and cleaned. The strain gages were attached to the steel with quick drying adhesive. The surface preparation and strain gage installation was usually carried out in one work day. On the next day, the lead wires for the strain gages were soldered to short lengths of shielded cable and the strain gages were waterproofed by waxing. The bridge tests were normally carried out a few days later.

Cable connectors were attached to the short lengths of cable that were soldered to the strain gages. This allowed rapid connection to the lead wires of the data acquisition equipment on the day of the tests. Shielded cable was used for all lead wires to reduce noise transmission.

Deflections at selected locations were measured using deflectometers as illustrated in Figure 2.

The deflectometers were fabricated specifically for the bridge tests. A strain gage was placed on each deflectometer. The deflectometers were calibrated so that the tip deflection could be determined from the strain gage output. Lead wires were fabricated with cable connectors so that they could easily be connected to the data acquisition equipment.

The deflectometers were attached to the bridge by c-clamps on the day of the tests. The deflectometers were pre-deflected before the test using a thin wire and a dead weight. The pre-deflection was partially released as the bridge deflected. Hence, the change in deflection of the deflectometer was equal to the bridge deflection.

A MDGADAC 2200C dynamic strain recorder with cassette storage was used as the primary data aquisition system during the stationary and moving truck tests. The MEGADAC has a 16 channel capacity and is capable of making 20,000 measurements per second. The MEGADAC was controlled through special software that was run on a microcomputer.

A portable generator powered the MEGADAC and computer during the tests. Due to the electrical noise produced by the generator during the first bridge test, a constant voltage transformer was connected to the generator during the remaining tests to reduce the noise signal.

Vishay P3500 and Vishay P350 static strain indicators were used to verify the MEGADAC strain values and to provide immediate data during testing. A switch and balance unit facilitated the use of the static strain indicator by allowing several channels to be read consecutively. Figure 3 displays the measuring and recording eqiupment used during the tests.

Figure 2. Deflectometer

Figure 3. Measuring and Recording Equipment

Two-axle dump trucks, provided by the AHD, were used to load the bridge. Figure 4 displays two of the trucks during a load test. The trucks were loaded with sand and weighed with AHD truck scales. The weight was recorded for each axle. Truck weights used for each bridge test are presented in a later section.

Test Procedures

Testing for all bridge spans followed the same general procedure. On the day of the test, the recording equipment was connected to the gages, deflectometers, and the portable generator. The instrumentation and data acquisiton equipment were tested. Chalk marks were made on the bridge for positioning the trucks during testing.

The bridge spans were subject to loading from stationary and moving test trucks. Because the curb to curb widths of all the bridges was relatively narrow, the test trucks were always positioned in the centers of the traffic lanes.

One lane of the bridge was loaded first by a stationary truck (or trucks). Then both lanes were loaded by stationary trucks. The response of the bridge was compared to calculated strains and deflections after each loading was applied. Based on statisfactory performance of the bridge spans, the moving truck tests were then performed. Moving truck tests were carried out with single and side by side trucks.

Before each of the stationary truck tests, initial strain gage readings were taken for use in reduction of the test data. Recording of the dynamic strain data was started manually during the moving truck tests. Data collection was started two to three seconds before the trucks reached the bridge. The data collected prior to the test trucks reaching the bridge was used to establish initial, or zero, values for the gages and deflectometers. Notes were kept during testing of computer and cassette file numbers corresponding to the various tests that were performed.

Data Reduction

The test data stored on the MEGADAC cassette was analyzed using special software. The MEGADAC data was collected during all testing by reading each strain gage 1000 times per second. By nature of the digital format of the data, constant strains such as initial readings or strains resulting from the

Figure 4. AHD Two-Axle Dump Trucks

stationary trucks must be determined by averaging over some time period. Averaging over a period of two to three seconds was used to establish constant strain and deflection values.

Averaging was required over shorter periods of time for accurate interpretation of the dynamic strains produced by the moving trucks. Averaging was carried out over 0.10 second periods. This time period was determined to be appropriate from comparisons of data reduction at several different period lengths.

Description of Bridges and Test Results

Detailed description of each bridge test are presented below. The discussion of each bridge test includes information regarding bridge geometry, instrumentation, test procedures, and data reduction. Final strain values experienced by each tested bridge span are presented for the different load tests.

Ashville Bridge. The Ashville Bridge, constructed in 1946 and displayed in Figure 5, is made up of a series of simple and continuous spans. There are three 34 ft simple spans and six 22 ft spans. The 22 ft spans are two span continuous construction. Tests were performed on only one of the 34 ft spans. The second span from the North end of the bridge was tested.

A typical cross section through the span is shown in Figure 6. Drawings for this specific bridge are not available. So it was not clear before testing whether shear ties were provided between the steel girders and concrete deck. Hence, the test was planned and carried out assuming that the bridge was designed and constructed as a noncomposite system.

Recently, AHD personnel have located standard drawings for bridges with details like the Ashville Bridge except for the girder spacing. The standard drawings indicate a girder spacing slightly greater than that used for the Ashville Bridge. The standard drawings indicate the use of shear ties. The test results presented below tend to suggest that shear ties were also used in the Ashville Bridge.

To establish a rating for the bridge it is necessary to make some assumptions about the construction details. The cover plates on the bottoms of the girders are not as wide as the flanges of the rolled shapes. Because of this, it is assumed that the cover plates were attached to the rolled shapes at a fabrication shop before the concrete deck was cast. It is also assumed that there are no shear ties between the concrete deck and the girders as mentioned above.

Figure 5. Ashville Bridge

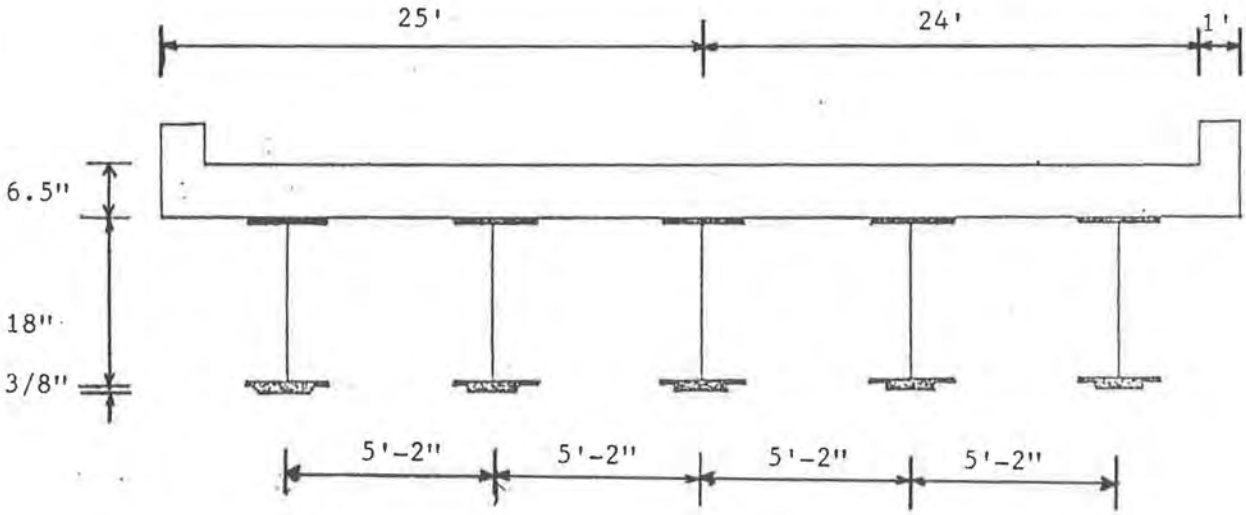

Figure 6. Ashville Bridge Cross Section

The cross sectional properties of the steel girders are listed in Table 2. The steel members are assumed to have a minimum yield strength of 33 ksi as suggested by the AASHTO Manual (1983). The concrete deck is assumed to have a compressive strength of 5000 psi for the purpose of computing composite section properties.

Description of the Tests.

Strain gages and deflectometers were positioned at midspan and located as indicated in Figure 7. The bridge was subjected to loading from stationary and moving test trucks. The axle loads and spacings for the test trucks are illustrated in Figure 8. The bridge was first loaded by one and then two stationary trucks. The longitudinal positions of the truck axles on the bridge deck are illustrated in Figure 9.

Moving truck tests were performed with one truck and then two trucks side by side. The single truck tests were performed at speeds of 20, 40, and 60 mph. Side by side trucks tests were performed at speeds of 20 and 40 mph.

Test Results

Table 3 presents the static and peak dynamic deflections and strains experienced at midspan by each girder. The girder numbers and the locations of the strain and deflection measurements correspond with Figure 7. The strains of Table 3 can be converted to stresses by multiplying by a Young's modulus of 29,000 ksi.

Selected plots of strain versus time from the moving truck tests are presented in Appendix A. Only plots at critical locations for a limited number of tests are shown. It was necessary to limit the number of plots presented in this report because of the enormous amount of data collected during the project.

Analysis of the Test Results

Table 3 indicates that the bridge deck and steel girders behave as a composite section. This is illustrated by the fact that the recorded top flange strains are very small. If the cross section is assumed to be composite the calculated neutral axis location is slightly above the top flange. Hence, strains at the top flange gage locations would be expected to be very nearly zero as was observed. If no composite action is assumed then the strains expected at the top flanges would be about as large as the strains at the cover plates. Also, with no composite action the calculated strains at the cover plates would be significantly

Table 2. Girder Cross Section Properties

Type	S18 x 54.7
Weight (lb/ft)	54.7
Depth (in)	18
Area (in^2)	16.1
Inertia (in^4)	804
Section Modulus (in^3)	89.4

Table 3. Measured Strains and Deflections from Ashville Bridge Test

Test	Location	Girder 1	2	3	4	5
Stat -	C.P	75*	123	120	34	10
1 truck	Bot.	68		83	42	
	Top	22	20	7	-4	
	Defl.	.07	.11"		.06"	
Stat-	C.P.	88	176	197	157	109
2 trucks	Bot.	82		161	153	
	Top	21	-9	7	-19	
	Defl.	.18"	.13"		.08"	
20 mph	C.P.	63	122	112	55	26
1 truck	Bot.	71		94	61	
	Top	24	-6	15	10	
	Defl.	.10"	.12"		.08"	
20 mph	C.P.	90	168	177	161	114
2 trucks	Bot.	93		148	160	
	Top	25	4	9	-12	
	Defl.	.20	.15"		.11"	
40 mph	C.P.	70	129	123	56	22
1 truck	Bot.	72		103	62	
	Top	23	-10	13	10	
	Defl.	.09"	.11"			
40 mph	C.P.	102	201	225	169	113
2 trucks	Bot.	105		178	167	
	Top	32	-10	21	-10	
	Defl.	.20"	.17"		. 12"	
55 mph	C.P.	69	105	92	47	20
1 truck	Bot.	75		81	52	
	Top	21	-6	13	5	
	Defl.	.09"	.09"		.12"	

*units of 10^{-6} in/in

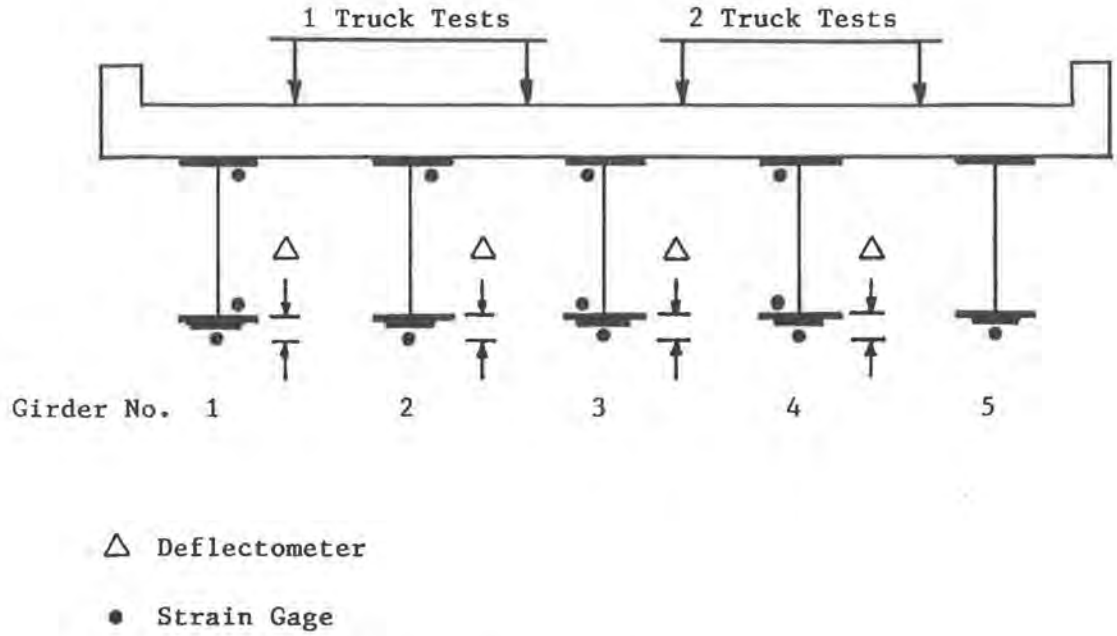

Figure 7. Strain Gage and Deflectometer Locations

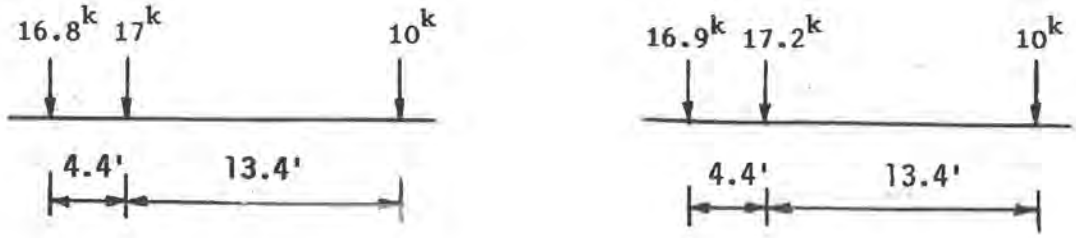

Figure 8. Test Truck Axle Loads and Spacings

greater than those observed.

Inspection of Table 3 also indicates an apparent irregularity in the data. For example, at some locations the strain for the bottom flange is slightly larger than the cover plate strain. This results primarily from electronic noise in the strain gage signals. The irregularity occurs at locations where the strains are relatively small. It should be expected that the magnitude of the error associated with the electronic noise is relatively constant for all the test results. It is estimated that the error in the strains of Table 3 resulting from noise is plus or minus 10 microstrain (10×10^{-6} in/in). This is also considered to be a practical range of accuracy for any static strain recorder such as the Vishay P350. As a percentage, the error decreases as the magnitude of the measured strain increases. It should be noted that after the Ashville tests, a constant voltage transformer was used between the portable generator and the data acquisition system. This greatly reduced the amount of noise in the data.

The strain data of Table 3 indicates that girder 3 experienced the highest strains during the two truck tests. Hence, girder 3 controls the inventory and operating ratings of the bridge. The maximum cover plate strain recorded during the test with two stationary trucks was 197 microstrain. This strain corresponds to a stress of 5.7 ksi. Hence, the stress σ_{ll} used in Equation 2 for the rating calculations was 5.7 ksi.

Impact factors calculated from the test results are shown in Table 4. The impact factors were determined by dividing the strains recorded in the moving truck tests by the strain recorded in the stationary truck test. Impact factors were calculated by using the strains at the bottom flanges and by using the strains at the cover plates. The maximum of the two values is shown in Table 4.

The observed impact factors varied considerably. The large impact factors for girders 4 and 5 are not significant since these girders do not control the rating. The maximum impact factor observed for girder 3 was 1.24 for the 40 mph single truck test. The low value of 0.92 for the 20 mph two truck test resulted from misalignment of the test trucks. The trucks maintained very good side by side alignment during the 40 mph test, and the impact factor of 1.14 appears reasonable.

The observed impact factors provide an indication of the behavior of the bridge when it is subjected to moving traffic loads. The observed impact factor of 1.14 is less than the AASHTO standard value of 1.3.

Table 4. Observed Impact Factors from Ashville Bridge Test

Test	Girder 1	2	3	4	5
20 mph, One Truck	1.04	0.99	1.13	1.61	2.71
40 mph, One Truck	1.06	1.05	1.24	1.64	2.31
55 mph, One Truck	1.11	0.85	0.97	1.37	2.13
20 mph, Two Trucks	1.14	0.95	0.92	1.05	1.05
40 mph, Two Trucks	1.29	1.14	1.14	1.09	1.04

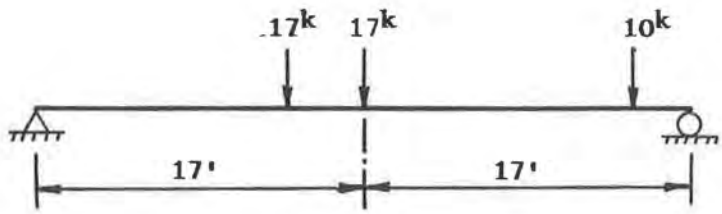

Figure 9. Longitudinal Positions of Test Trucks

This tends to indicate that the bridge behavior is normal for this type bridge. However, the series of moving load tests was not exhaustive, and bridge impact factors are known to depend heavily on truck geometry and details as well as the roadway conditions. Hence, the AASHTO impact factor of 1.3 will be used in Equation 2 for establishing ratings for the bridge.

Vincent Bridge

The Vincent Bridge, displayed in Figure 10, was constructed in 1935 according to Alabama Highway Department records. The skewed bridge is a two span continuous configuration with a total length of 54 ft. The two continuous spans are both 27 ft. Both spans consist of eight steel girders laterally supported along the top flange by embedment in the concrete deck. Tests were performed on both bridge spans.

The overall geometry of the bridge and the member details were determined from information provided by the Alabama Highway Department and from field measurements. A typical cross section through the continuous spans is shown in Figure 11. The available information on the bridge details does not indicate that any shear ties were provided between the steel girders and concrete deck. However, it was observed that the girders were embedded four inches into the concrete deck as shown in Figure 11. The space between the girders was also filled with concrete at the pier and abutments. It is not known whether any reinforcing was provided to produce continuity between the girders and the pier or abutments. The cross sectional properties for the steel girders were taken from Alabama Highway Department records and are shown in Table 5. The steel girders are assumed to have a minimum yield strength of 30 ksi as suggested by the AASHTO Manual (1983). The concrete deck was assumed to have a compressive strength of 3000 psi for the purpose of calculating composite section properties.

Description of the Tests

The north span was instrumented for strain and deflection measurements. The positive moment region was instrumented with strain gages and deflectometers, along a line parallel to the abutment 10.8 ft (0.4 x 27 ft = 10.8 ft) from the abutment. The negative moment region (at the pier) was instrumented with just strain gages. The strain gages and deflectometers were located as illustrated in Figure 12.

Table 5. Girder Cross Section Properties

Type	S12 x 31.8
Weight (lb/ft)	31.8
Depth (in)	12
Area (in^2)	9.35
Inertia (in^4)	218
Section Modulus (in^3)	36

Figure 10. Vincent Bridge

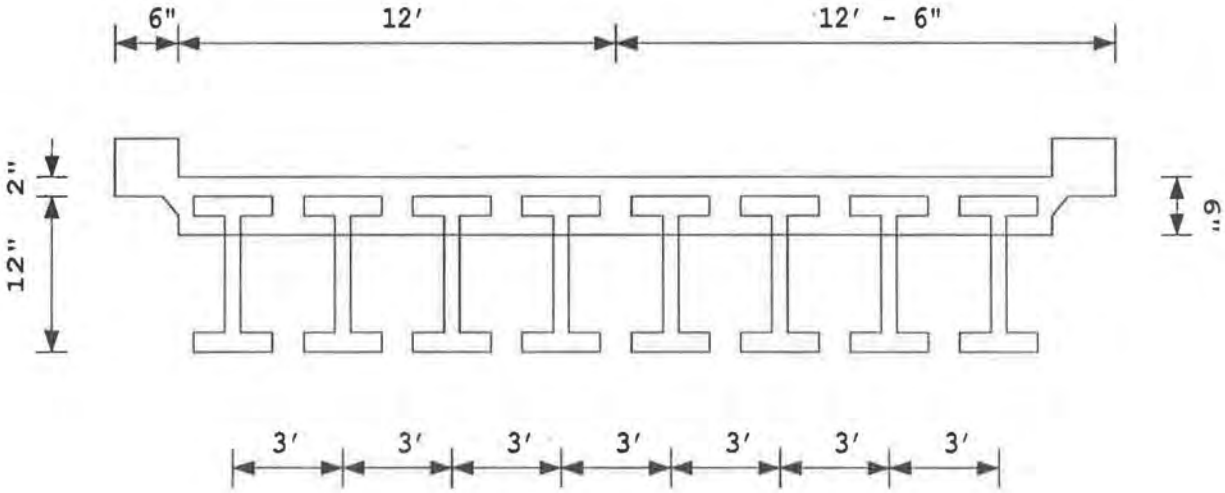

Figure 11. Vincent Bridge Cross Section

Stationary load tests were performed on the north span. The axle loads and spacings for the test trucks are illustrated in Figure 13. The location of the truck axles for the stationary load tests are illustrated in Figure 14.

Moving load tests were performed with one and two trucks at speeds of crawl, 20 and 40 mph. The trucks were staggered during the moving truck tests to maintain approximately the same relative positions as in the stationary side by side test.

Test Results

Tables 6 and 7 present the static and peak dynamic strain data recorded for the bottom flange of each girder in the positive negative moment regions. The strains of Tables 6 and 7 can be converted to stress by multiplying by a Young's modulus of 29,000 ksi. Selected plots of strain versus time from the moving truck tests are presented in Appendix A.

Analysis of the Test Results

An analysis of the test results indicates that the measured strains were lower than expected. The stationary test with two trucks positioned longitudinally were expected to produce the largest negative strain at the pier, but did not. It should also be noted that some of the strains at the pier were positive in the negative moment region as shown in Table 6. It is unclear why this occurred.

Because the bridge was skewed, the stationary tests did not capture the maximum strains for all the girders. However, the moving tests did. The moving tests provide confidence that the strains are low for all truck positions along the span.

The strain data of Table 7 indicate that during the moving truck tests girder 3 experienced the highest strain in the negative moment region with a value of 65 microstrain which corresponds to a stress $\sigma_{||}$ of 1.9 ksi. Girder 3 also experienced the highest strain in the negative moment region during the stationary tests, with a value of 55 microstrain which corresponds to a stress of 1.6 ksi. Therefore, girder 3 will control the test rating of the continuous spans.

For girder 3, impact factors were determined by dividing the peak strains recorded during the 20 mph and 40 mph tests by the peak strain recorded during the crawl speed test. The largest impact factor for girder 3 was found to be 0.94 for the 40 mph test. It is likely that the impact factors were less than one

Table 6. Measured Strains and Deflections from Vincent Bridge Test, Stationary Truck Tests

Test	Girder 1	2	3	4	5	6	7	8
			Positive Moment, One Truck					
+ Moment Strain	13*	42	15	10		3		
- Moment Strain	-22	-38	-40	-22		-7	-11	-22
+ Moment Deflection	.04"				.04"	.03"		
			Positive Moment, Two Trucks					
+ Moment Strain	22	54	25	62		69		
- Moment Strain	-22	-46	-55	-27		-33	-27	-45
+ Moment Deflection	.05"				.07"	.10"		
			Negative Moment, Two Trucks Longitudinally					
+ Moment Strain	32	71	58	67		48		
- Moment Strain	-4	-34	-36	2		11	9	1
+ Moment Deflection	.10				.13"	.15"		

*units of 10^{-6} in/in

Table 7. Measured Strains and Deflections from Vincent Bridge Test, Moving Truck Tests

Test	Girder 1	2	3	4	5	6	7	8
				Crawl Speed, One Truck				
+ Moment Strain	48*	60		75	57	42		
- Moment Strain	-26	-49	-57	-29	-23	-25	-22	-18
+ Moment Deflection	.06"			.06"		.05"		
				Crawl Speed, Two Trucks				
+Moment Strain	55	54		77	98	92		
- Moment Strain	-40	-55	-65	-32	-30	-46	-50	-34
+ Moment Deflection	.06"			.08"		.09"		
				20 MPH, One Truck				
+ Moment Strain	45	56		75	56	39		
- Moment Strain	-27	-38	-56	-30	-24	-26	-24	-18
+ Moment Deflection	.05"			.05"		.04"		
				20 MPH, Two Trucks				
+ Moment Strain	49	58		79	100	89		
- Moment Strain	-31	-52	-57	-11	-23	-44	-46	-30
+ Moment Deflection	.05"			.07"		.08"		
				40 MPH, One Truck				
+ Moment Strain	43	54		109	83	54		
- Moment Strain	-31	-53	-55	-18	-21	-32	-37	-19
+ Moment Deflection	.06"			.08"		.05"		
				40 MPH, Two Trucks				
+ Moment Strain	45	53		100	123	127		
- Moment Strain	-36	-60	-61	-29	-33	-48	-45	-41
+ Moment Strain	.06"			.09"		.10"		

Table 8. Girder Cross Section Properties

	44 ft Span	77 ft Span
Type	Beth B Beam	Beth G Beam
Weight (lb/ft)	110	240
Depth (in)	29.78	36
Area (in^2)	32.45	70.55
Section Modulus (in^3)	314.8	872

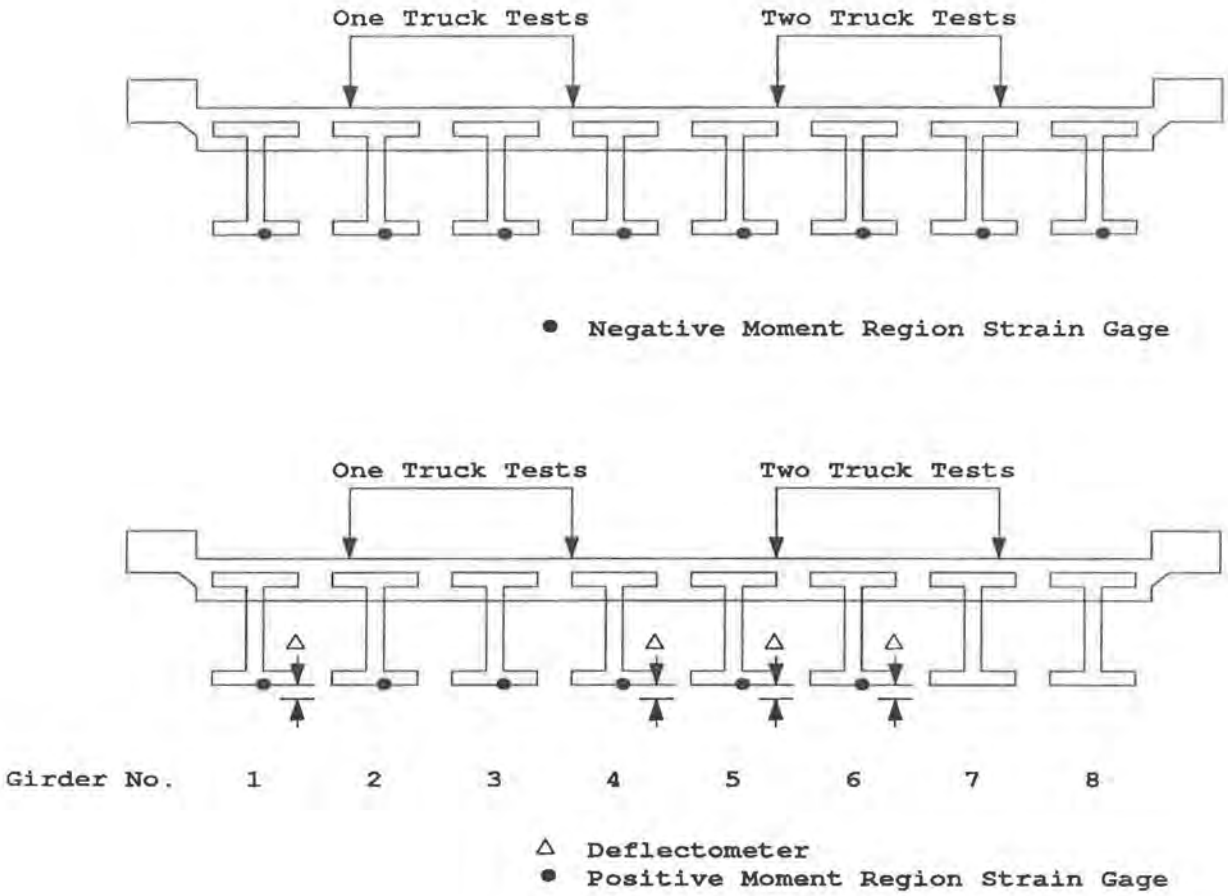

Figure 12. Strain Gage and Deflectometer Locations

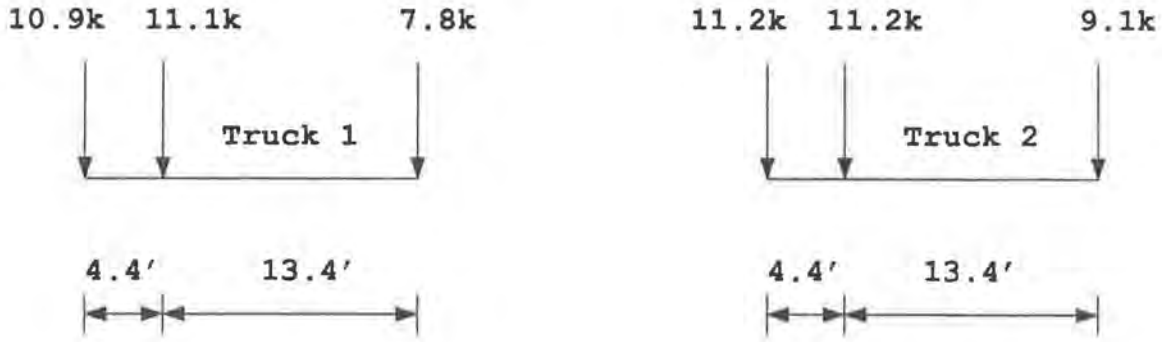

Figure 13. Test Truck Axle Loads and Spacings

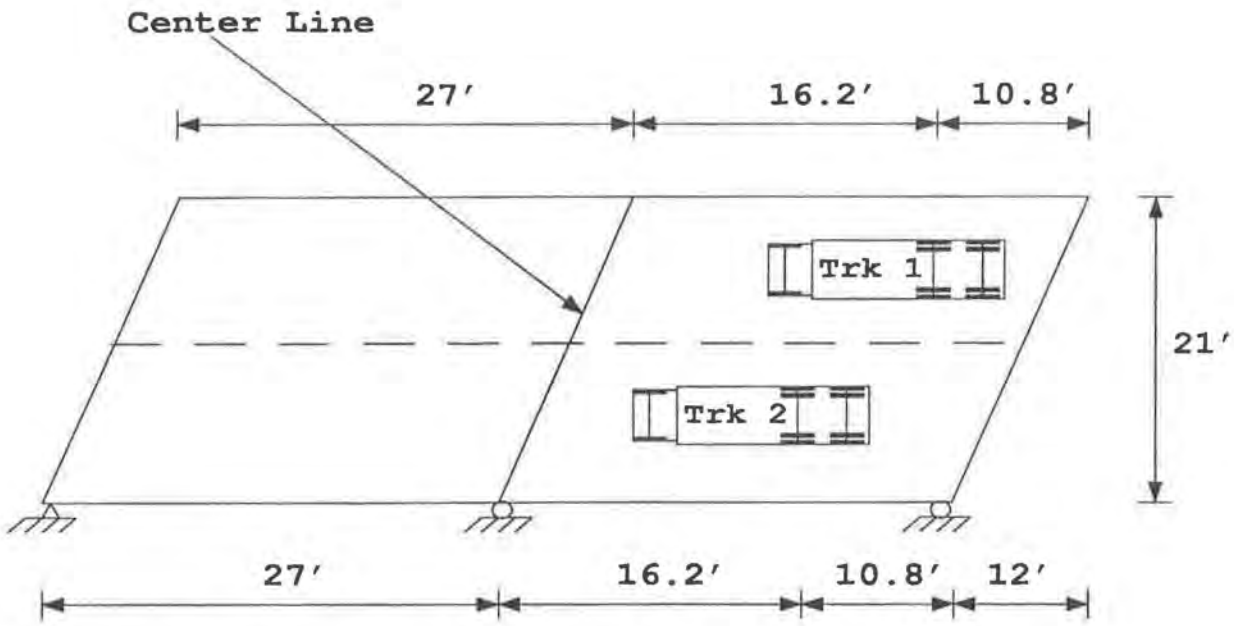

Series 2 - Positive Moment Test

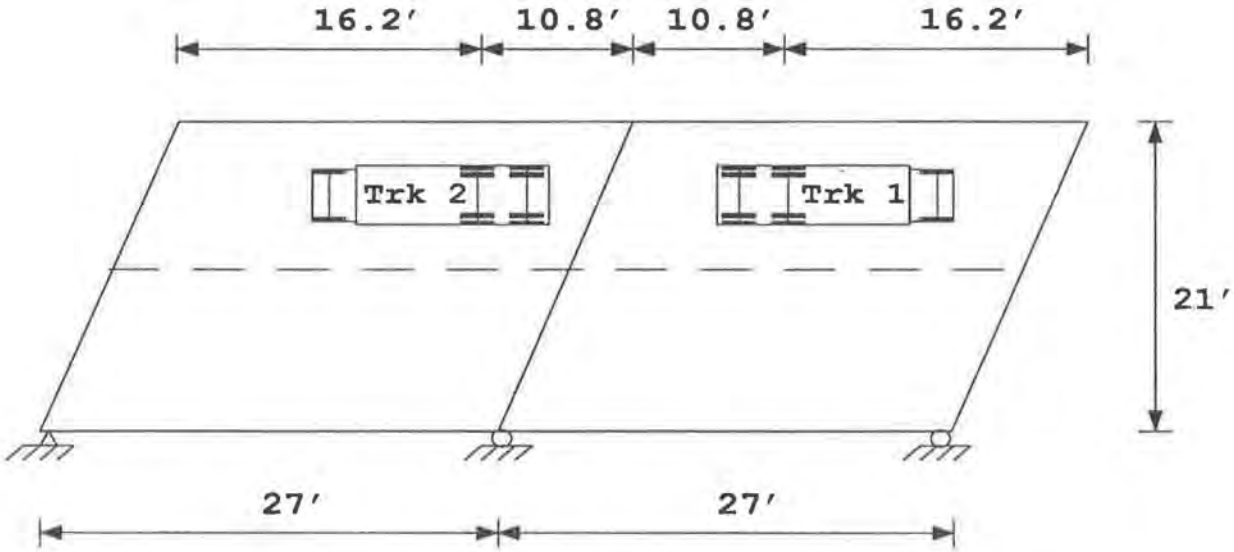

Series 3 - Negative Moment Test

Figure 14. Longitudinal Positions of Test Trucks

because of differences in alignment of the trucks during the crawl, 20 mph, and 40 mph side by side tests. The impact foactor of 0.94 does indicate that impact effects due to normal traffic can be expected to be small. The AASHTO impact factor of 1.3 will conservatively be used in the rating calculations.

Childersburg Bridge

The Childersburg Bridge was constructed in 1930. The main spans of the bridge are steel trusses. The approach spans are simply supported steel girders with a concrete deck. There are three approach spans at the South end of the bridge, and two approach spans at the North end. All the approach spans are either 44 ft or 77 ft between simple supports. The load tests were performed on a 44 ft span and a 77 ft span at the south end of the bridge. The 77 ft span is shown in Figure 15.

A typical cross section through the approach spans is shown in Figure 16. The available details for the bridge spans do not indicate any shear ties were provided between the steel girders and concrete deck. The cross sectional properties for the steel girders listed in Table 8 were taken from a 1930 Bethlehem steel manual. The steel girders are assumed to have a minimum yield strength of 30 ksi as suggested by the AASHTO Manual (1983). The concrete deck is assumed to have a compressive strength of 5000 psi for purposes of calculating composite section properties.

Description of the Tests

Strain gages and deflectometers were positioned at midspan and located as indicated in Figure 17.

The bridge was subjected to loading from stationary and moving test trucks. The axle loads and spacing for the test trucks are illustrated in Figure 18. The bridge was first loaded by one and then two stationary trucks. The locations of the truck axles are illustrated in Figure 19.

Moving truck tests were performed with one truck and then two trucks side by side. The single truck tests were performed at speeds of 40 and 60 mph. Side by side truck tests were carried out at 20 and 40 mph.

Test Results

Tables 9 and 10 present the static and peak dynamic deflections and strains recorded for each girder. The girder numbers and the locations of the strain and deflection measurements correspond with Figure 17. The strains can be converted to stresses by multiplying by a Young's modulus of 29,000 ksi.

Table 9. Measured Strains and Deflections from Childersburg Bridge Test, 44 ft Span

Test	Location	Girder 1	Girder 2	Girder 3	Girder 4
Stat -	Top	-4*	-4	-1	
1 truck	Bot.	6	34	97	71
	Defl.		.06"	.11"	
Stat -	Top	2	1	-2	
2 trucks	Bt.	91	115	138	82
	Defl.		.16"	.14"	
20 mph	Top	6	3	3	
2 trucks	Bot.	130	134	147	85
	Defl.		.15"		
40 mph	Top	-7	0	11	
1 truck	Bot.	32	57	87	84
	Defl.		.09"		
40 mph	Top	0	2	5	
2 trucks	Bot.	115	147	185	112
	Defl.		.15"		
60 mph	Top	-4	0	-5	
1 truck	Bot.	26	64	88	88
	Defl.		.08"		

*units of 10^{-6} in/in

Table 10. Measured Strains and Deflections from Childersburg Bridge Test, 77 ft Span

Test	Location	Girder 1	Girder 2	Girder 3	Girder 4
Stat -	Top	-2*	-7	-12	
1 truck	Bot.	16	41	68	81
	Defl.		.14"	.12"	
Stat -	Top	-10	-18	-22	
2 trucks	Bot.	94	111	104	95
	Defl.		.28"	.18"	
20 mph	Top	2	0	-7	
2 trucks	Bot.	85	92	89	85
	Defl.		.28"		
40 mph	Top	-2	0	0	
1 truck	Bot.	32	51	64	90
	Defl.		.19"		
40 mph	Top	5	-8	-7	
2 trucks	Bot.	118	113	108	106
	Defl.		.34"		
60 mph	Top	-4	-5	-18	
1 truck	Bot.	36	54	70	86
	Defl.		.20"		

*units of 10^{-6} in/in

Figure 15. Childersburg Bridge

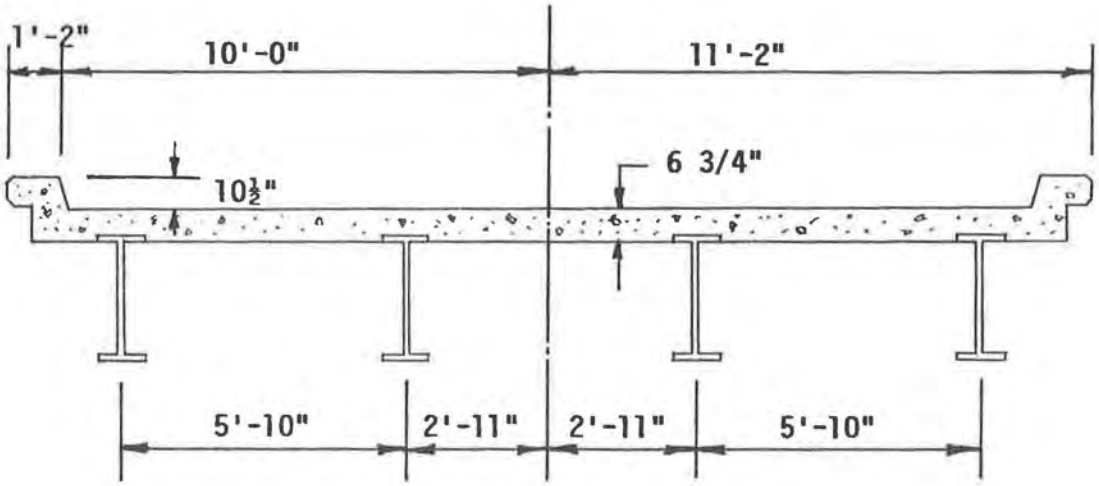

Figure 16. Childersburg Bridge Cross Section

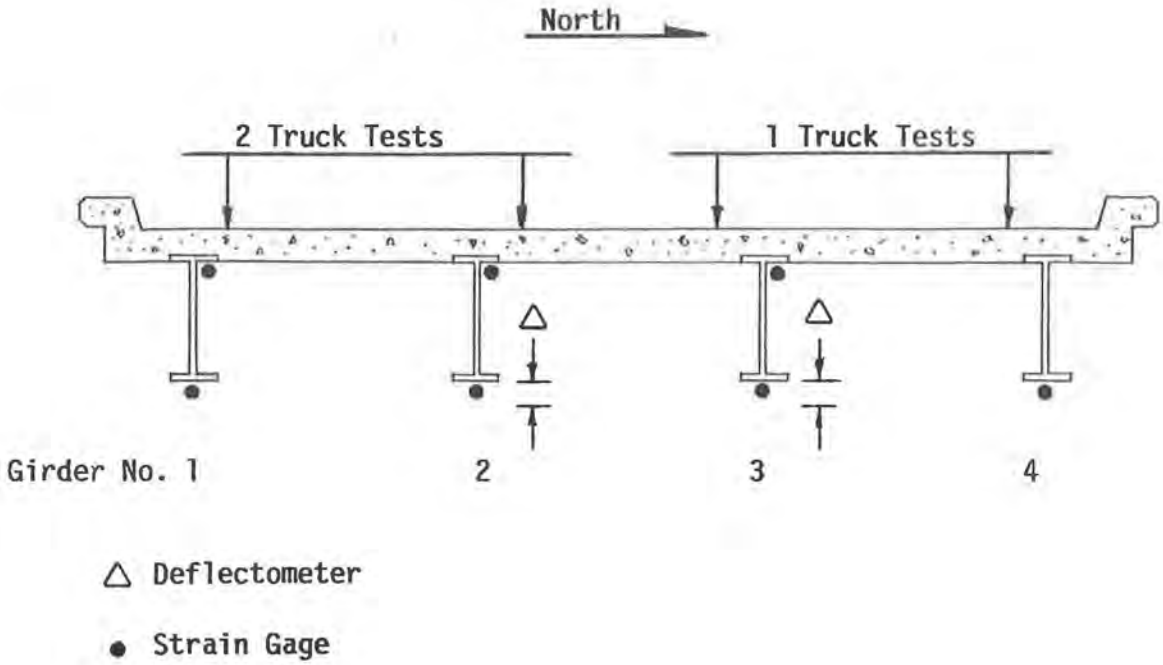

Figure 17. Strain Gage and Deflectometer Locations

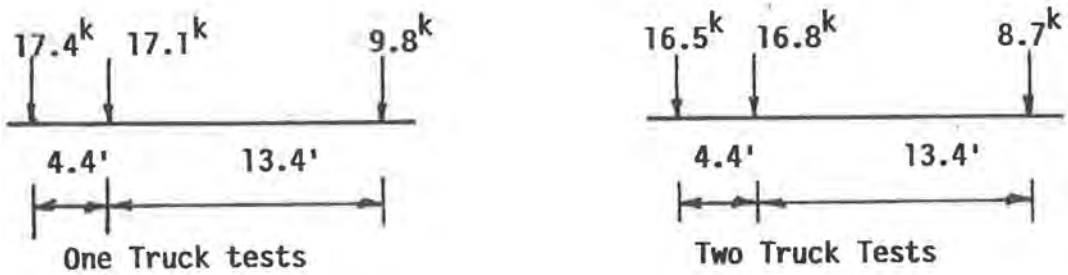

Figure 18. Text Truck Axle Loads and Spacings

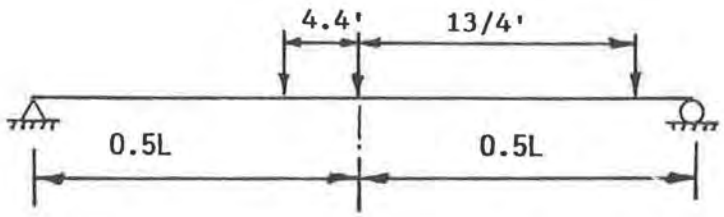

Figure 19. Longitudinal Positions of Test Trucks

Slected plots of strain versus time from the moving truck tests are presented in Appendix A.

Analysis of Test Results

An analysis of the test results for both the 44 ft and 77 ft spans indicates that the bridge deck and steel girders behave as a composite section. This is illustrated by the fact that the recorded top flange strains are very small.

The strain data of Table 9 indicates that girder 3 of the 44 ft span experienced the highest strains in the stationary and moving truck tests with a value of 138 microstrain in the stationary test, and a value of 185 microstrain in the moving truck test. The strain of 185 microstrain resulted from the 40 mph test with two trucks side by side. The ratio of the peak dynamix to static strains (185/138) yields an impact factor of 1.34. This is slightly greater than the applicable AASHTO impact factor of 1.3. In the rating calculations the product ($IF\sigma_{||}$) will be based on the maximum observed dynamic strain of 185 microstrain. Hence, ($IF\sigma_{||}$) will be taken as 5.4 ksi for the 44 ft span.

The strain data of Table 10 indicates that girder 2 of the 77 ft span experienced the highest strain of 111×10^{-6} in./in. during the stationary two truck test. This strain corresponds to a stress of 3.2 ksi. The impact factor calculated according to the AASHTO specifications for the 77 ft span is 1.25. To establish the rating for the 77 ft span the AASHTO impact factor of 1.25 will be applied to the 3.2 ksi stress that was observed in the stationary two truck test. This approach will result in a live load stress including impact due to the test trucks that is somewhat larger than any value actually recorded in the moving truck tests.

Mulberry Fork Bridge

The Mulberry Fork Bridge, constructed in 1953 and displayed in Figure 20, has two 34 ft simple spans and five 44 ft simple spans. All simple spans are skewed, simply supported, and consist of four steel girders laterally supported along the compression flange by embedment in the concrete deck. Tests were performed on the 34 ft span at the West end of the bridge, and the 44 ft span which is the third span from the West end.

A typical cross section through one of the skewed simple spans is shown in Figure 21. The available information for the bridge spans do not indicate that any shear ties were provided between the steel girders and concrete deck. However, it was observed that the concrete deck was cast so that the

Figure 20. Mulberry Fork Bridge

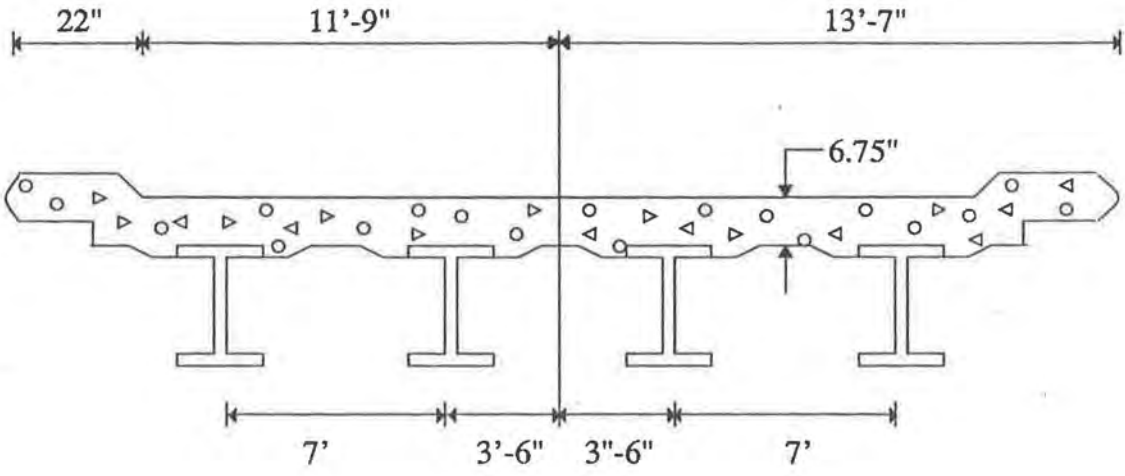

Figure 21. Mulberry Fork Bridge Cross Section

underside of the deck is flush with the underside of the top flanges of the girder as shown in Figure 21.

The cross sectional properties for the steel girders were taken from the AISC Steel Manual (1947) and are shown in Table 11. The steel girders are assumed to have a minimum yield strength of 30 ksi as suggested by the AASHTO Manual (1983). The concrete deck was assumed to have a compressive strength of 5000 psi for the purpose of calculating composite section properties.

Description of the Tests

The bridge girders were instrumented to provide measurements of strain and deflection along a line parallel to the skewed supports at midspan of both spans. Strain gages were placed on the top and bottom flanges. Placement of the strain gages is illustrated in Figure 22.

The bridge was subjected to loading from stationary test trucks only. The strains were recorded using the Vishay P3500 static strain indicator. The axle loads and spacings for the test trucks are illustrated in Figure 23. The bridge was first loaded by one and then two stationary trucks. The locations of the truck axles are illustrated in Figure 24.

Test Results

The strains and deflections measured at each of the girders are given in Tables 12 and 13. The girder numbers and locations of the strain and deflection measurements correspond with Figure 17. The strains can be converted to stresses by multiplying by a Young's modulus of 29,000 ksi.

Analysis of the Test Results

The data of Tables 12 and 13 suggest that the interior girders and deck act non-compositely, while the exterior girders appear to behave in a composite manner. The strain data of Tables 14 and 15 indicate that girder 3 of each span experienced the highest strain during the two trucks side by side tests. The maximum strain at girder 3 of the 34 ft span was 137 microstrain, while the maximum strain at girder 3 of the 44 ft span was 160 microstrain. These strain values correspond to bending stresses, $\sigma_{||}$, of 4.0 and 4.6 ksi for the 34 ft and 44 ft spans, respectively.

To account for the dynamic effects of moving traffic an impact factor of 1.3 will be used for both the 34 ft and 44 ft spans. The impact factor of 1.3 is based on the current AASHTO Specifications (1989).

Table 11. Girder Cross Section Properties

	34 ft Span	44 ft Span
Type	24WF90	30WF116
Weight (lb/ft)	90	116
Depth (in)	24.29	30.0
Area (in^2)	27.63	34.13
Section Modulus (in^3)	220.9	327.9

Table 12. Measured Strains and Deflections from Mulberry Fork Bridge Test, 34 ft Span

Test	Location	Girder 1	Girder 2	Girder 3	Girder 4
Stat -	Top	9*	-75	-17	
1 truck	Bot.	81	76	40	10
	Defl.		.12"	.05"	
Stat -	Top	7	-103	-105	
2 trucks	Bot.	101	124	137	75
	Defl.		.20"	.20"	
Stat -	Top	12	-76	-26	
2 trucks	Bot.	104	95	60	16
Same Lane	Defl.		.17"	.08"	

*units of 10^{-6} in/in

Table 13. Measured Strains and Deflections from Mulberry Fork Bridge Test, 44 ft Span

Test	Location	Girder 1	Girder 2	Girder 3	Girder 4
Stat -	Top		-64*	-29	
1 truck	Bot.	103	94	61	12
	Defl.		.15"	.10"	
Stat -	Top		-121	-133	
2 trucks	Bot.	110	157	160	76
	Defl.		.27"	.30"	
Stat -	Top		-115	-50	
2 trucks	Bot.	126	138	73	21
Same Lane	Defl.		.22"	.16"	

*units of 10^{-6} in/in

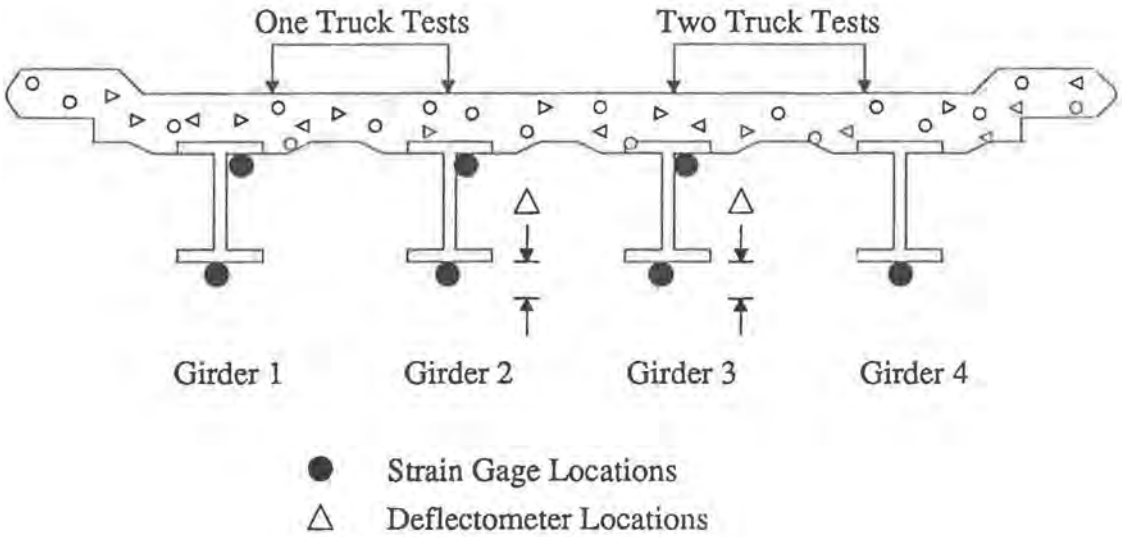

Figure 22. Strain Gage and Deflectometer Locations

Figure 23. Test Truck Axle Loads and Spacings

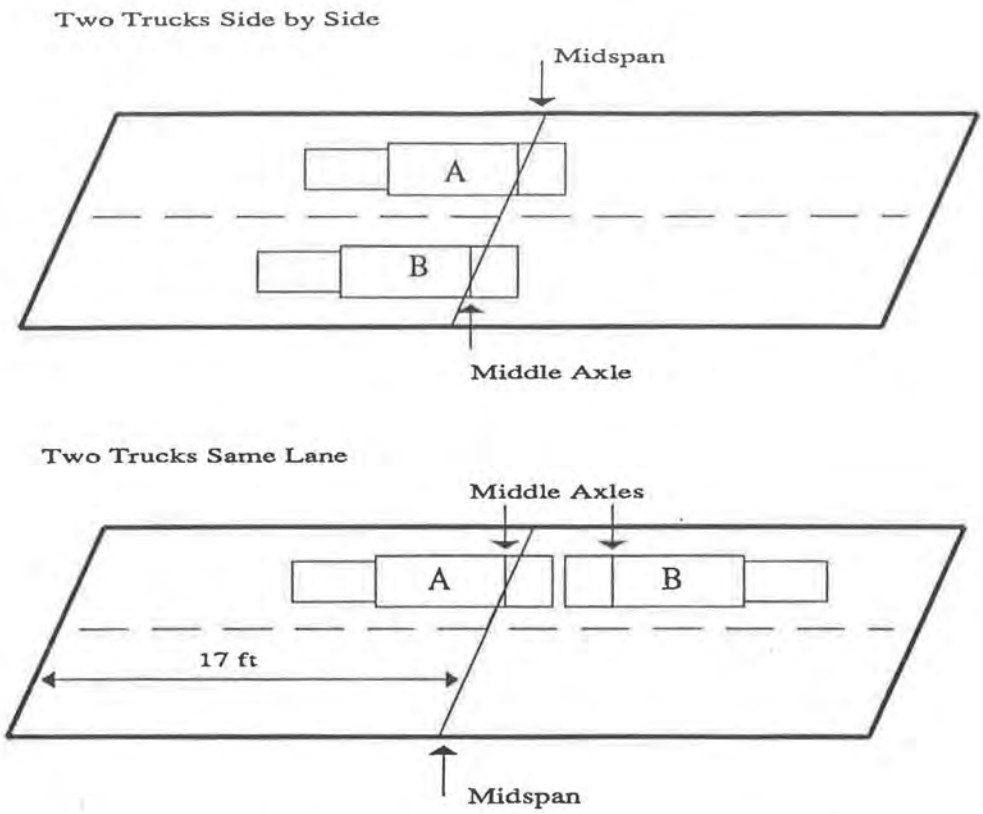

Figure 24. Longitudinal Positions of Test Trucks

Figure 25. Locust Fork Bridge

Locust Fork Bridge

The Locust Fork Bridge, constructed in 1953 and displayed in Figure 25, has five 49 ft simply supported spans and one continuous section 260 ft in length. The continuous span has three spans, two 80 ft exterior spans and a 100 ft interior span. Tests were performed on the continuous span and the second simply supported span from the South side. The bridge consists of a concrete deck resting on four steel girders. Each girder's top flange is embedded in the concrete deck so that the bottom surface of the top flange is flush with the bottom of the deck. Along the continuous spans cover plates are welded to the bottom flanges and are assumed to be welded to the top flanges in the negative moment regions. The positions and lengths of the coverplates are illustrated in Figure 26.

A typical cross section through the bridge is shown in Figure 27. There were no drawings available to determine whether shear ties were used between the steel girders and the concrete deck.

The cross sectional properties for the steel girders were taken from an AISC steel manual by AHD personnel and are shown in Table 14. The steel girders are assumed to have a minimum yield strength of 33 ksi as suggested by the AASHTO Manual (1983). The concrete deck was assumed to have a compressive strength of 5000 psi for the purpose of calculating composite section properties.

Description of the Tests

The bridge girders were instrumented to provide measurements of strain and deflection at midspan of the simply supported span, and at selected locations along the continuous span. Figure 28 illustrates the general instrumentation pattern.

To measure positive moment strains in the continuous spans, gages and deflectometers were placed 32 ft from the end support on the 80 ft span and also placed at midspan of the 100 ft span. For the maximum negative moment strains, gages were placed at the interior support.

Four test trucks were used during the load tests. The axle loads and spacings for the test trucks are shown in Figure 29. The simple span was subjected to stationary and moving truck tests. The simple span was loaded with Truck 3 and Truck 4 as defined in Figure 29. During the stationary truck tests the interior axles of the test trucks were placed at midspan as illustrated in Figure 19. Moving truck tests were carried out with one truck at 20 mph and 50 mph and with side by side trucks at 20 mph.

Table 14. Girder Cross Section Properties

	49 ft Span	Continuous Spans
Type	WF 30 x 132	WF 36 x 160
Weight (lb/ft)	132	160
Depth (in)	30.31	36.01
Area (in^2)	38.9	47.0
Section Modulus (in^3)	380	542

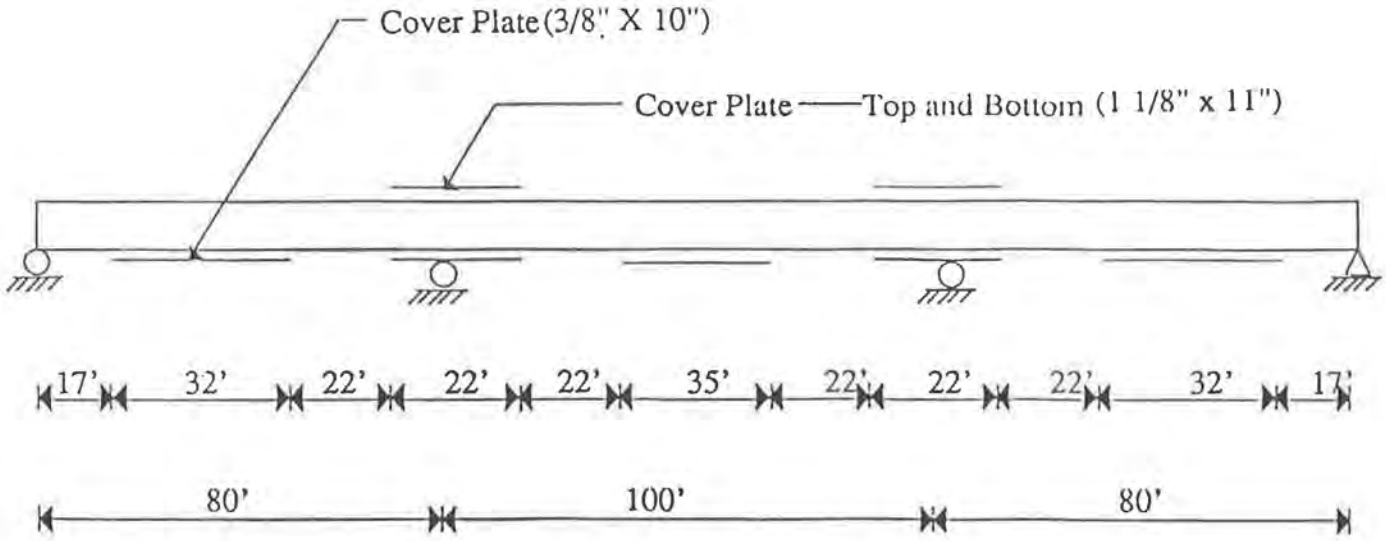

Figure 26. Locust Fork Bridge Cover Plates

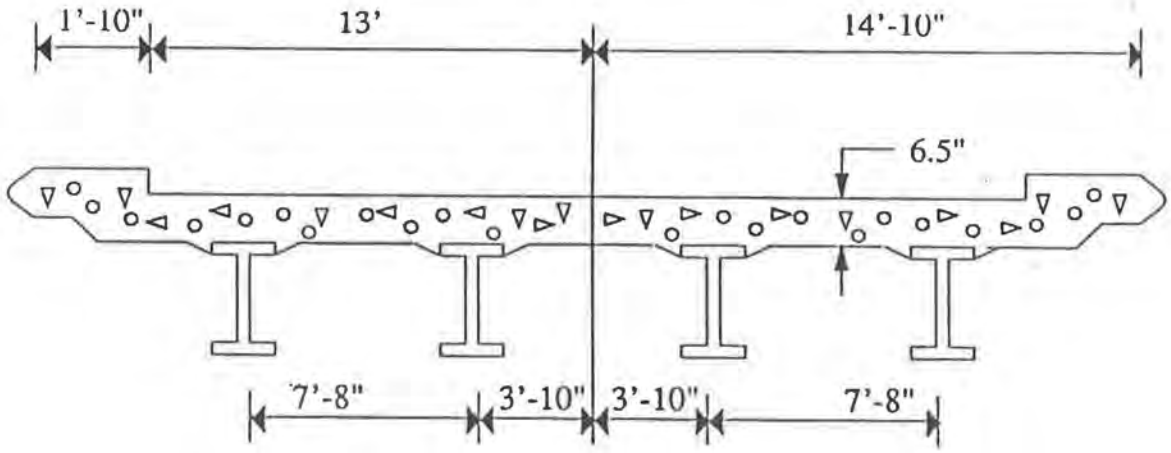

Figure 27. Locust Fork Bridge Cross Section

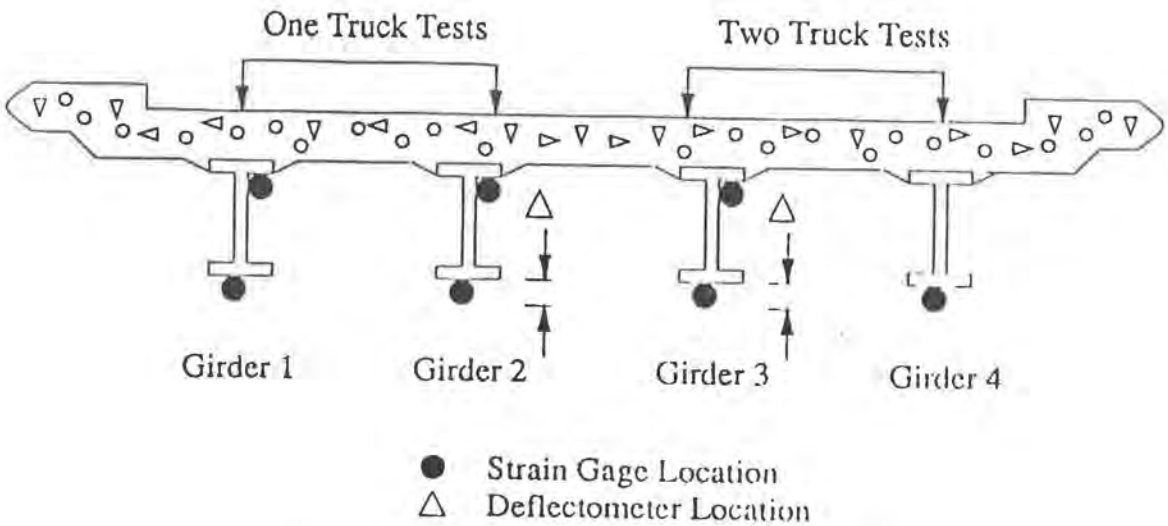

Figure 28. Strain Gage and Deflectometer Locations

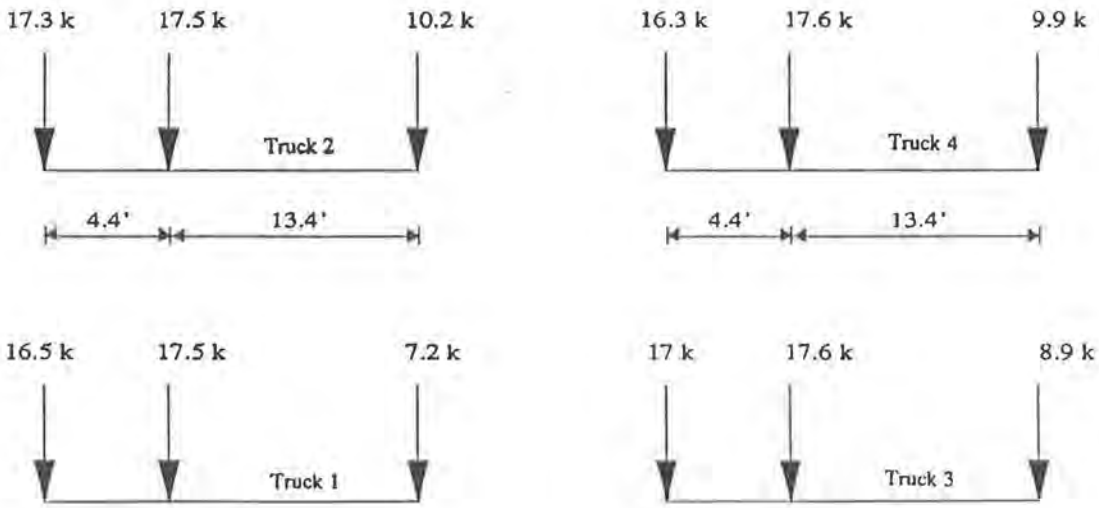

Figure 29. Test Truck Axle Loads and Spacings

Only stationary truck tests were carried out on the continuous spans. Truck positions for the tests are illustrated by Figure 30.

Test Results

The strain and deflection measurements from each of the tests are given in Tables 15 and 16. The girder numbers and locations of the strains and deflection measurements correspond with Figure 28. The strains can be converted to stresses by multiplying by a Young's modulus of 29, 000 ski. Selected plots of strain versus time from the moving truck tests of the simple span are presented in Appendix A.

Analysis of the Test Results

Tables 15 and 16 indicate that the simple and continuous spans exhibit some degree of unintended composite action. For the simple span it appears that the exterior girders exhibit a higher degree of composite action than the interior girders. The simple span strain data presented in Table 15 indicate that girder 3 experienced the highest strain during the moving truck tests with a value of 161 microstrain. The maximum strain during the stationary side by side truck test of 152 microstrain also occurred at girder 3. This corresponds to a stress $\sigma_{||}$ (for Equation 2) of 4.4 ksi. The impact factor calculated from the ratio (161/152) is 1.06. Because only a small amount of moving truck data is available, an impact factor of 1.29 based on the AASHTO Specifications (1989) will be used in rating the simple span.

For the continuous span the strain data of Table 16 indicate that girder 2 experienced the highest strain at the pier during the negative moment tests with four test trucks. The observed value of -185 microstrain corresponds to a static live load stress $\sigma_{||}$ of 5.4 ksi. No moving truck tests were performed on the continuous spans. The AASHTO Specifications (1989) impact factor of 1.23 for negative moment regions will be used in the rating process.

Table 15. Measured Strains and Deflections from Locust Fork Bridge Test, 49 ft Span

Test	Location	Girder 1	Girder 2	Girder 3	Girder 4
Stat -	Top	8*	-40	-9	
1 truck	Bot.	99	89	54	15
	Defl.		.14"	.08"	
Stat -	Top	13	-79	-89	
2 trucks	Bot.	130	152	152	119
	Defl.		.25"	.24"	
20 mph	Top	5	-41	-24	
1 truck	Bot.	92	84	58	18
	Defl.			.09"	
20 mph	Top	11	-95	-131	
2 trucks	Bot.	120	144	161	138
	Defl.			.27"	
50 mph	Top	8	-56	-28	
1 truck	Bot.	103	100	72	28
	Defl.			.11"	

*units of 10^{-6} in/in

Table 16. Measured Strains and Deflections from Locust Fork Bridge Test, Continuous Spans

		Girder		
Test	Location	1	2	3
Stat -	Top			
1 truck	Bot.	108*	90	50
80 ft Span	Defl.		.10"	
Stat -	Top			
2 trucks	Bot.	121	147	166
80 ft Span	Defl.		.33"	
Stat -	Top		-33	
1 truck	Bot.		91	49
100 ft Span	Defl.		.11"	
Static	Top		-49	
2 trucks	Bot.		141	144
100 ft Span	Defl.		.35"	
Static	Top			56
2 trucks	Bot.		-124	-50
At Pier	Defl.			
Static	Top			56
4 trucks	Bot.	-115	-185	-148
At Pier	Defl.			

*units of 10^{-6} in/in

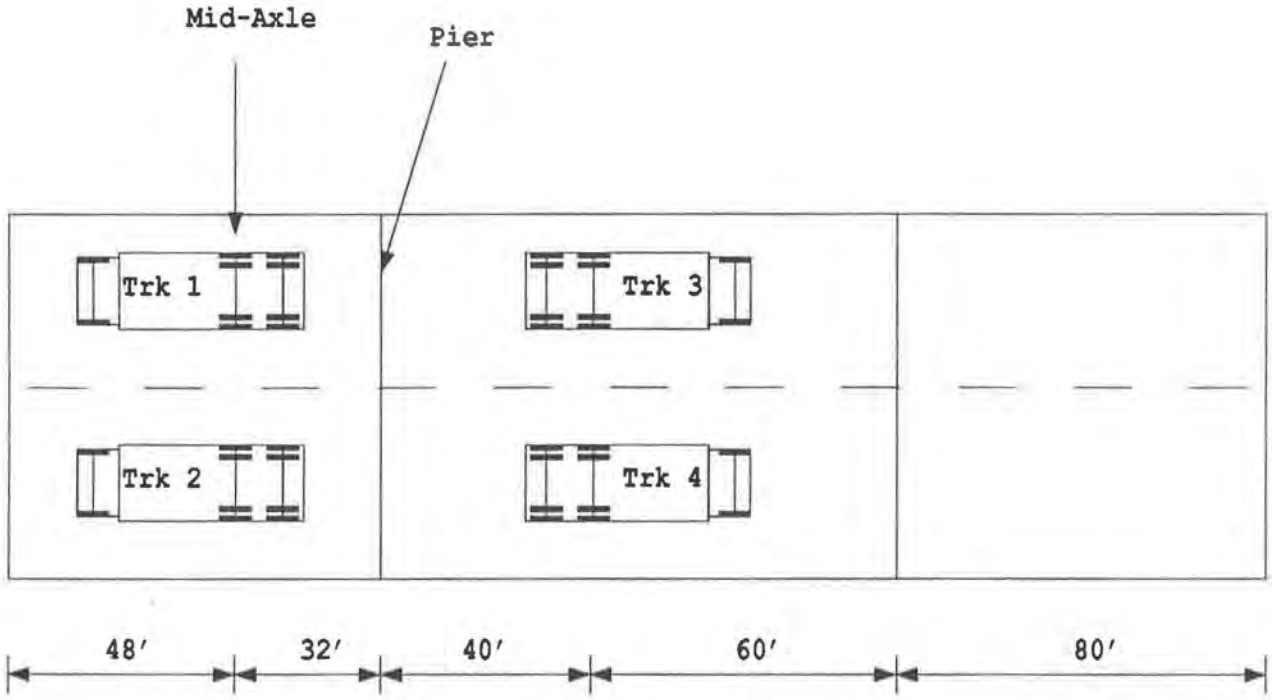

Figure 30. Longitudinal Positions of Test Trucks

III. BRIDGE ANALYSES

Introduction

The determination of the allowable live load moment capacity in Equation 2 involves calculating the moment produced by the test trucks, M_{test}. The rating factor, defined in Equation 1, can then be determined after calculating $M_{abs\ max}$ for any particular loading. Since the AHD uses six standard truck types (as illustrated in Figure 40) to rate bridges, a rating factor, and therefore an $M_{abs\ max}$, was calculated for each standard truck type.

A grid model of each bridge deck was created using geometric information about the bridge along with the test data. To determine M_{test}, the test trucks were positioned on the model in the exact same manner they were positioned on the bridge. The model was then analyzed using the stiffness method. If the behavior of the model closely represented the behavior of the bridge, the stiffness method was used to analyze the model to determine $M_{abs\ max}$ for the AHD's standard truck types.

The stiffness method is a fundamental analysis technique that is readily adaptable to computer analysis. It is applicable to either continuous or discrete structures. Here, the stiffness method was used to analyze the grid models which are discrete framed structures. All framed structures consist of members connected at nodes. Each node has a specified number of degrees of freedom (DOF), or possible displacements. The DOF are considered to be restrained or unrestrained, depending on the structural details and support conditions.

Framed structures can be represented mathematically with a system of simultaneous algebraic equations. These equations when represented in matrix form can easily be manipulated by the computer. The stiffness method employs three primary matrices: a matrix of applied loads, a stiffness matrix, and a matrix of the resulting displacements. The set of matrix equations is solved for the unknown displacements at each node. The calculated displacements are then used to determine the unknown forces and moments at each member end.

For more detailed information about the stiffness method refer to the many available books on matrix structural analysis such as Weaver and Gere (1990) or Przemieniecki (1968).

Modeling the Bridge Deck System as a Grid

Even though the bridge deck and girder system (referred to here as the deck system) is a continuous structure, the analysis of the deck system is simplified by analyzing it as a framed structure. The grid, which is the appropriate type of framed structure for analyzing a bridge deck system, can approximate the flexural and torsional deformations experienced by a deck system to out of plane loads.

The grid is a two-dimensional framed structure consisting of one-dimensional members that either intersect or cross one another. The members are subjected to forces applied normal to the plane of the grid and couples whose vectors lie in the plane of the grid. Axial and shear deformations are usually very small in grid structures and hence are seldom considered. It is assumed that the grid members have two axes of symmentry so that bending and torsion can take place independently.

The grid analysis works well for slab on girder bridges. It is almost instinctive to let the longitudinal members represent the girders and the transverse members represent portions of the concrete deck and/or diaphragms. An example bridge deck system and its grid model are illustrated in Figure 31. The connections, called nodes, between the longitudinal and transverse members are assumed to be rigid. These connections occur where longitudinal and transverse members intersect. A discussion of the details of how to develop a grid model of a bridge is given in Appendix B. Also given in Appendix B is an example input data file for the grid program.

Development of Grid Models for the Tested Bridges

Several models for each bridge were developed. These models were developed using information from test data, field inspections, and assumptions regarding material properties and construction details.

Factors that affected the bridge behavior, such as unintended composite action, were approximated in the models.

Since each model was developed to rate each bridge for the AHD's standard trucks, it was imperative that each model represent the bridge's behavior as closely as possible. The appropriateness of a model for each bridge was determined by placing the test trucks on the grid model in the exact same location that they were placed during the test, and then comparing the calculated strains from the model with the strains experienced during the test. Once the best model was identified, it was used to determine

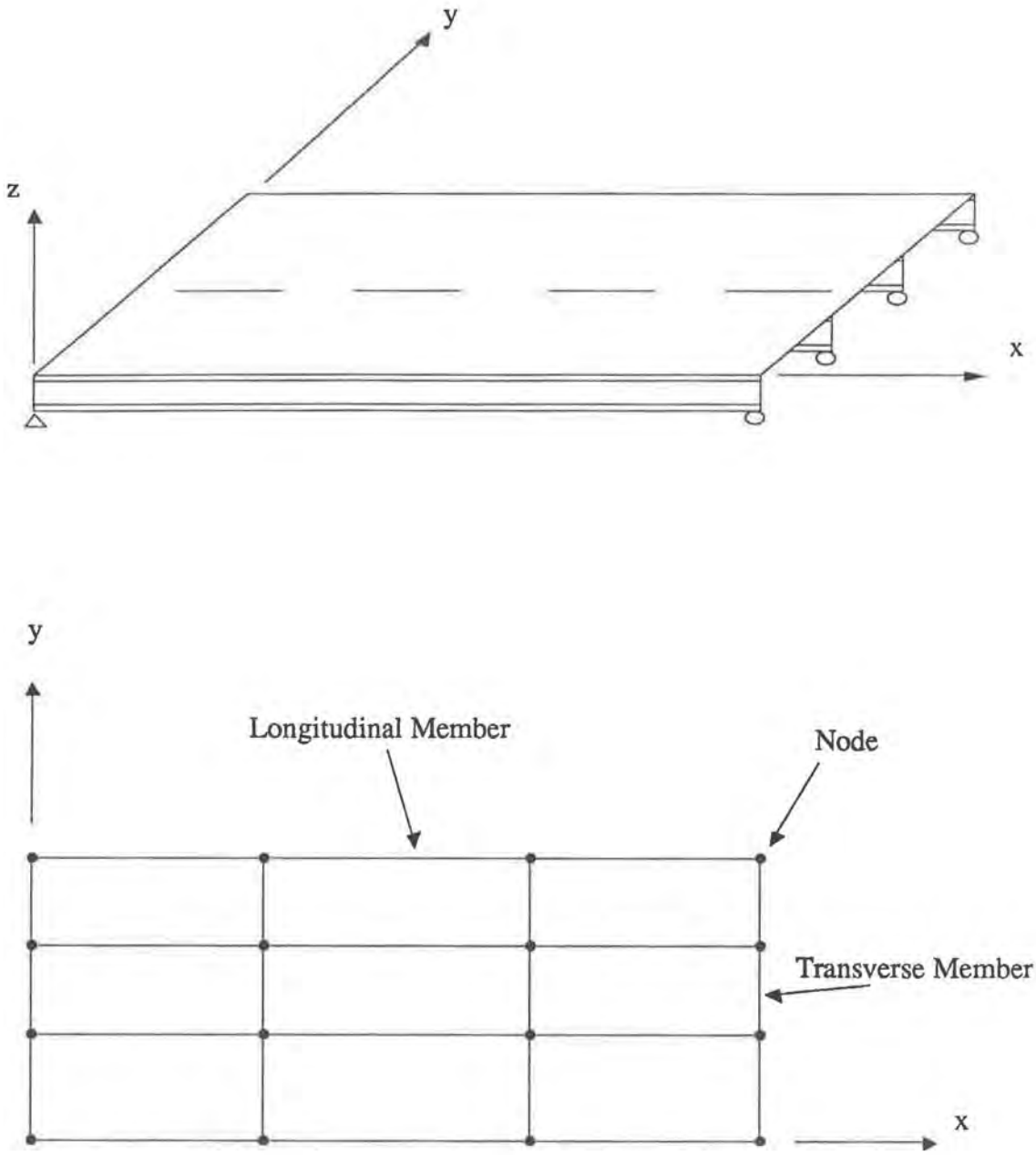

Figure 31. Grid Model of Bridge Deck System

$M_{abs\ max}$ for the standard truck types. The following sections demonstrate how the best grid models were developed.

The Ashville Grid Model

The field tests revealed that the bridge acted in a composite manner. The grid model was developed to act in a composite manner as well.

The concrete deck compressive strength was assumed to be 5000 psi in the analysis. The steel reinforcing in the deck was assumed to be #5 bars spaced 12 inches apart in both the longitudinal and transverse directions. Figure 32 illustrates the cross sections used in the determination of the section properties for the longitudinal and transverse members.

Table 17 presents a comparison of the measured strains and deflections experienced by the bridge, and the strains and deflections calculated with the grid model. The calculated strains are slightly larger than the measured strains. The model closely approximates the observed behavior, and will be used to rate the bridge.

The Vincent Grid Model

It was determined from the field inspection that the 12 in. girders were embedded into the concrete deck 4 in. Therefore, the actual bridge and the best grid model were assumed to act in a composite manner. The girders were also encased in concrete at each support. However, in the grid model the supports were modeled as pins or rollers.

The concrete deck compressive strength was assumed to be 3000 psi in the analysis. The steel reinforcing in the deck was assumed to consist of #4 bars spaced 12 inches apart in both the longitudinal and transverse directions. Figure 33 illustrates the cross sections used in the determination of section properties for the longitudinal and transverse members.

Table 18 presents a comparison of the measured strains and deflections experienced by the bridge deck during the test, and the calculated strains and deflections for the grid model of the bridge deck. The calculated strains and deflections for the grid model are much larger than the measured test strains and deflections. This indicates that the actual bridge deck is stiffer than the grid model.

Table 17. Comparison of Measured and Calculated Strains and Deflections, Ashville Bridge

Test	Location	Girder 1	2	3	4	5
		From Test				
Static	Top	21*	-9	7	-19	
2 trucks	Bot.	82		161	153	
	C.P	88	176	197	157	109
	Defl.	.18"	.13"		.08"	
		From Grid Analysis				
Static	Top	5	5	6	5	5
2 trucks	Bot.	209	223	230	225	206
	C.P.	213	228	235	230	211
	Defl.	.18"	.19"	.19"	.19"	.17"

*units of 10^{-6} in/in

Table 18. Comparison of Measured and Calculated Strains and Deflections, Vincent Bridge

Test	Girder 1	2	3	4	5	6	7	8
From Test, Positive Moment, Two Trucks								
+ Moment Strain	22*	54	25	62		69		
- Moment Strain	-22	-46	-55	-27		-33	-27	-45
+ Moment Deflection	.05"				.07"	.10"		
From Grid Analysis, Positive Moment, Two Trucks								
+ Moment Strain	128	169	136	149	217	166	190	134
Moment Strain	-82	-120	-76	-129	-152	-85	-95	-46
Moment Deflection	.24"	30"	.28"	.33"	.35"	.30"	.31"	.24"

*units of 10^{-6} in/in

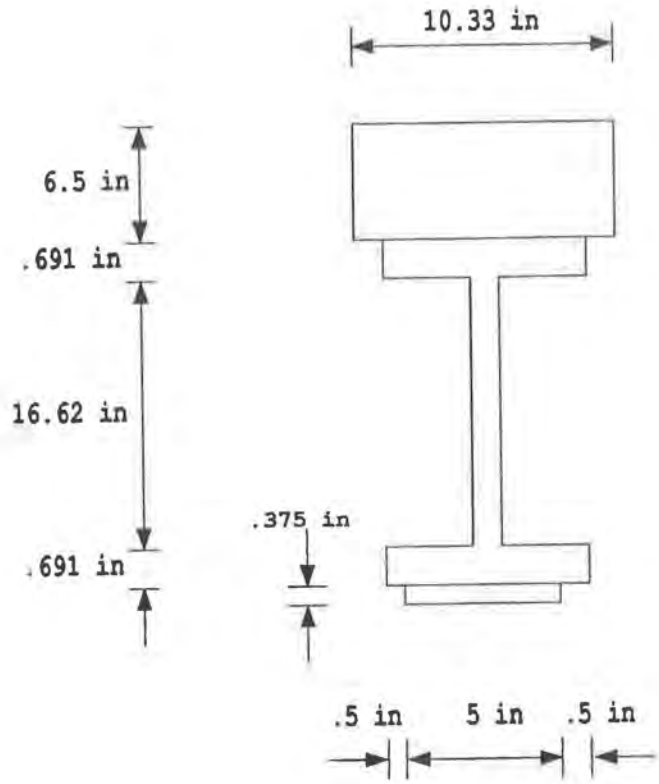

Figure 32. Cross Sections Used for Ashville Section Properties

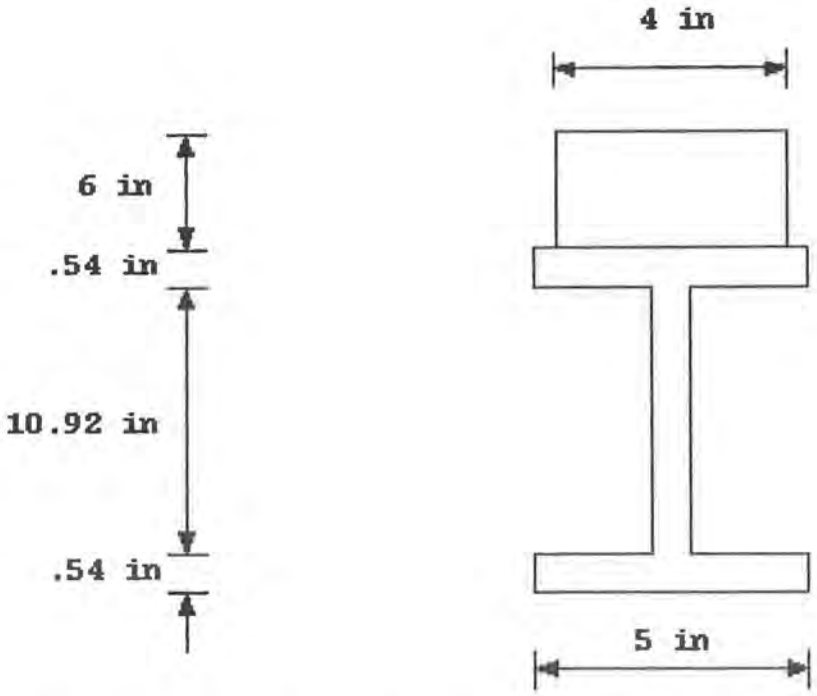

Figure 33. Cross Section Used for Vincent Section Properties

It is obvious that the grid model does not account for all the factors providing stiffness to the bridge. It is impossible to determine what is causing the additional stiffness. One possibility might be added restraint at the support provided by the concrete which encases the girders. At this time the available test data is not sufficient to refine the model any further. The grid model used to calculate the data in Table 18 produced conservative results and will be used to rate the Vincent Bridge.

The Childersburg Grid Model

The field tests revealed that the bridge acted in a composite manner. The grid model was developed by assuming composite action as well.

The concrete deck compressive strength was assumed to be 5000 psi in the analysis. The steel reinforcing in the deck was assumed to be #5 bars spaced 12 inches apart in both the longitudinal and transverse directions. Figure 34 illustrates the cross sections used in the determination of the section properties for the longitudinal and transverse members.

Tables 19 and 20 present a comparison of the measured strains and deflections experienced by the bridge deck during the test, and the calculated strains and deflections for the grid model of the bridge deck. The calculated strains approximate the measured strains closely in both spans.

The Mulberry Fork Grid Model

For the 34 ft span, an analysis of the test data suggests that the interior girders acted in a non-composite manner while the exterior girders behaved compositely. It was assumed that this behavior also occurred in the 44 ft span. This assumption, which seems valid since the spans were constructed with similar details, enables both models to be developed in a consistent manner. Hence, non-composite section properties were used to model the grid members representing the interior girders and composite section properties were used to model the grid members representing exterior girders. Diaphragms were also present near midspan of the 44 ft span. The added stiffness provided by the diaphragms were modeled with transverse beams at the location of the diaphragms.

The concrete deck compressive strength was assumed to be 5000 psi in the analysis. The steel reinforcing in the deck determined from the construction plans. Figure 35 illustrates the cross sections

Table 19. Comparison of Measured and Calculated Strains and Deflections, Childersburg Bridge, 44 ft Span

Test	Location	Girder 1	Girder 2	Girder 3	Girder 4
		From Test			
Stat -	Top	2*	1	-2	
2 trucks	Bot.	91	115	138	82
	Defl.		.16"	.14"	
		From Grid Analysis			
Stat -	Top	-6	-7	-7	-6
2 trucks	Bot.	135	168	169	136
	Defl.	.13"	.16"	.16"	.13"

*units of 10^{-6} in/in

Table 20. Comparison of Measured and Calculated Strains and Deflections, Childersburg Bridge, 77 ft Span

Test	Location	Girder 1	2	3	4
		From Test			
Stat - 2 trucks	Top	-10*	-18	-22	
	Bot.	94	111	104	95
	Defl.		.28"	.18"	
		From Grid Analysis			
Stat - 2 trucks	Top	-24	-29	-28	-23
	Bot.	124	147	145	120
	Defl.	.33"	.38"	.38"	.32"

*units of 10^{-6} in/in

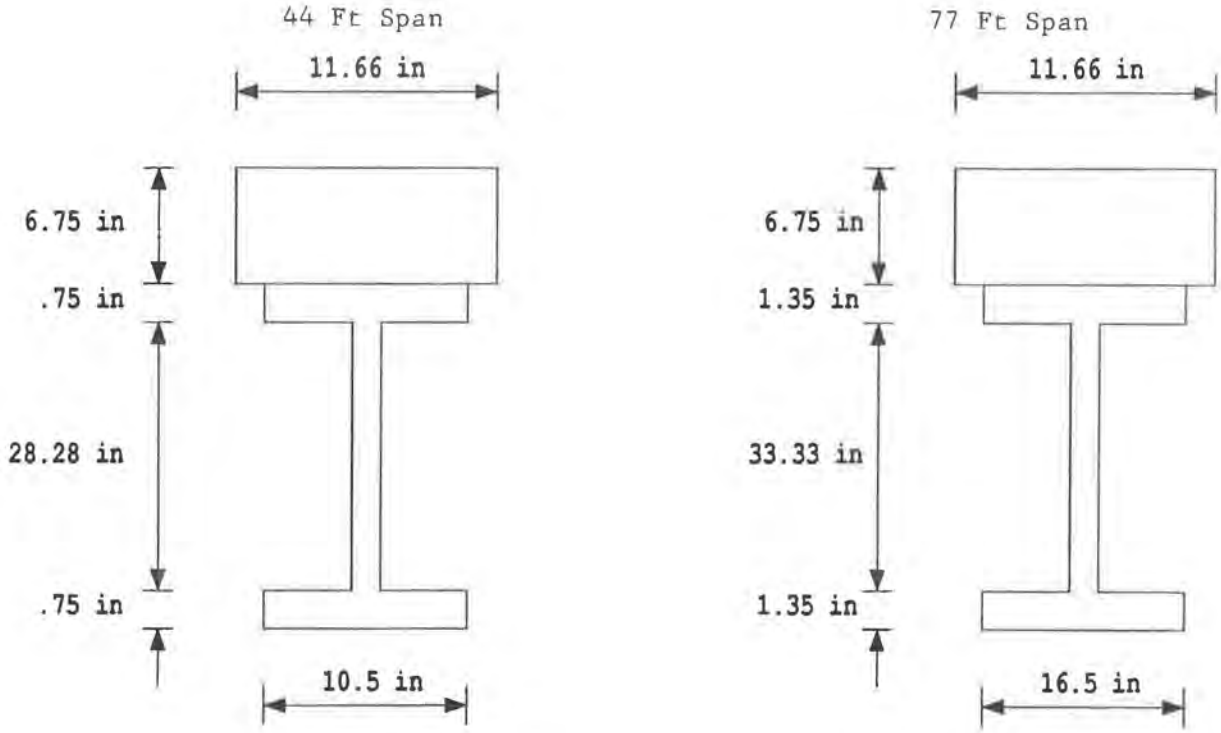

Figure 34. Cross Sections Used for Childersburg Section Properties

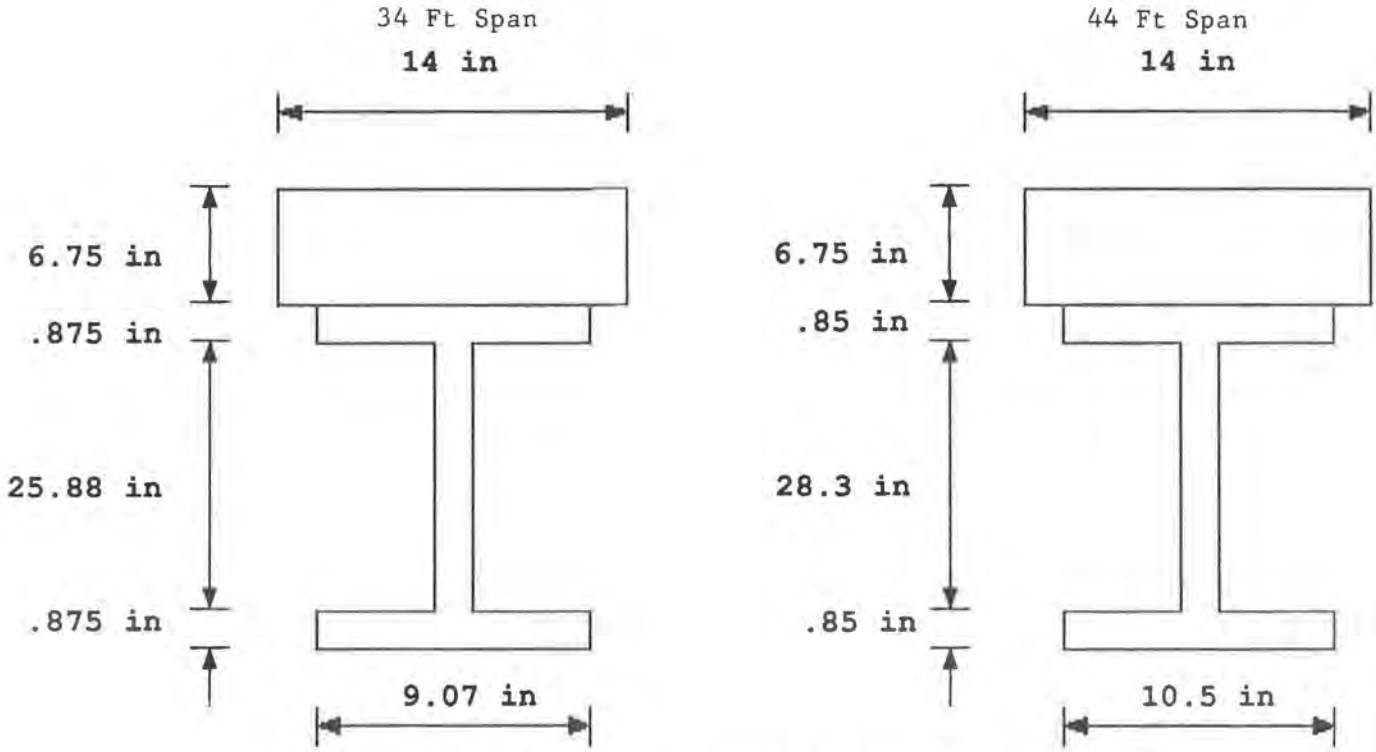

Figure 35. Cross Sections Used for Mulberry Fork Section Properties

used in the determination of section properties for the longitudinal and transverse members of both spans.

Strains computed from the grid analysis of each span are compared to the strains measured during the field tests in Tables 21 and 22. The strains compare favorably for the test loadings. The grid for the 44 ft span appears to represent the actual span better than the grid for the 34 ft span. The grid analysis results do not match the test results exactly. The differences are possibly created by factors such as unintended restraint at the ends, the additional stiffness of the guard rails, and discrepancies associated with modeling the deck as a series of transverse beams. The models do appear sufficiently accurate to be used to determine the absolute maximum moments created by the standard truck loadings. It should be noted that although the grid analysis moments for the exterior girders were the largest for the 44 ft span, the grid analysis results for the interior girders are used in all the rating calculations. The is justified by the bridge behavior observed during the tests.

The Locust Fork Grid Model

For the 49 ft span, an analysis of the test data suggests that all four girders of the span displayed some degree of unintended composite action. The exterior girders displayed a higher degree of composite action than the interior girders. Therefore, a grid model of the 49 ft span was developed using composite section properties for the members representing the exterior girders and non-composite section properties for the members representing the interior girders.

The test data of the continuous span also suggested that the spans were experiencing some degree of composite action. However, it was determined that the negative moment region controled the rating of the bridge. Therefore, it is necessary that the grid model reflect the behavior of the negative moment region, especially at the interior girders where the largest negative strains were experienced. In order to make the grid closely model the bridge behavior in the negative moment region, the bridge deck was assumed to behave in a non-composite manner. Non-composite section properties were used for each longitudinal member.

From the field inspection all supports were either pins or rollers. These supports were reflected in the grid model. Diaphragms were also present on the continuous span. The added stiffness provided by

Table 21. Comparison of Measured and Calculated Strains and Deflections, Mulberry Fork Bridge, 34 ft Span

Test	Location	Girder 1	Girder 2	Girder 3	Girder 4
		From Test			
Stat -	Top	7*	-103	-105	
2 trucks	Bot.	101	124	137	75
Side by Side	Defl.		.20"	.20"	
		From Grid Analysis			
Stat -	Top	-1	-169	-179	-1
2 trucks	Bot.	159	181	192	146
Side by Side	Defl.	.11"	.23"	.23"	.11"

*units of 10^{-6} in/in

Table 22. Comparison of Measured and Calculated Strains and Deflections, Mulberry Fork Bridge, 44 ft Span

Test	Location	Girder 1	Girder 2	Girder 3	Girder 4
		From Test			
Stat -	Top		-121	-133	
2 trucks	Bot.	110	157	160	76
Side by Side	Defl.		.22"	.16"	
		From Grid Analysis			
Stat -	Top	-9	-138	-142	-9
2 trucks	Bot.	173	147	151	167
Side by Side	Defl.	.16"	.27"	.27"	.16"

*units of 10^{-6} in/in

the diaphragms were modeled with transverse beams at the locations of the diaphragms.

The concrete deck compressive strength was assumed to be 5000 psi for both the simple and continuous spans in the analysis. The transverse reinforcing steel in the deck was assumed to be number 5 bars spaced at 12 in. Figure 36 illustrates the cross sections used to determine the section properties for the longitudinal and transverse members of the 49 ft span and the three span continuous section.

Strains computed from the grid analysis of both spans are compared to the strains measured during the field tests in Tables 23 and 24. The grid model results appear sufficiently accurate to be used to determine the absolute maximum moments created by the standard truck loadings.

Grid Analyses Performed for the Rating Process

The grid models developed in the previous section were used to determine the moments created by the test trucks, M_{test}, and the moments created by each standard truck $M_{abs\ max}$. The values calculated for M_{test} and $M_{abs\ max}$ are tabulated in Chapter IV.

M_{test} was determined by positioning the test trucks on the model in the exact same manner they were positioned on the bridge deck during the stationary test which created the largest absolute strain. After analyzing the model, M_{test} was the moment at midspan in the girder that experienced the largest absolute strain.

The type of bridge span determined where on the bridge to position the standard trucks in order to create $M_{abs\ max}$ in each girder. The position of the test trucks used to determine M_{test} was generally different than the position of the standard trucks used to determine $M_{abs\ max}$.

For the Ashville Bridge and the Childersburg Bridges, $M_{abs\ max}$ was determined by positioning the standard truck types along the span in the same manner they would be placed on a simple beam to create the absolute maximum moment. This was also done for the 49 ft simple span of the Locust Fork Bridge.

For the Vincent Bridge, it was determined that the combination of dead load and live load stresses in the negative moment region (at the pier) controled the rating. Therefore the stationary test which produced the largest negative strain will govern M_{test}. To determine $M_{abs\ max}$, two standard trucks, one in each lane, were position so that the center of the trucks were directly over the pier as illustrated in Figure 37.

Table 23. Comparison of Measured and Calculated Strains and Deflections, Locust Fork Bridge, 49 ft Span

Test	Location	Girder 1	Girder 2	Girder 3	Girder 4
		From Test			
Stat -	Top	-13*	-79	-89	
2 trucks	Bot.	130	152	152	119
Side by Side	Defl.		.25"	.24"	
		From Grid Analysis			
Stat -	Top	-4	-176	-175	-4
2 trucks	Bot.	198	189	188	191
Side by Side	Defl.	.23"	.38"	.38"	.23"

*units of 10^{-6} in/in

Table 24. Comparison of Measured and Calculated Strains and Deflections, Locust Fork Bridge, Continuous Spans

Test	Location	Girder 1	2	3	4
		From Test			
Stat -	Top			56*	
2 trucks	Bot.	-115	-185	-148	-76
		From Grid Analysis			
Stat -	Top	141	150	149	138
2 trucks	Bot.	-158	-169	-168	-156

*units of 10^{-6} in/in

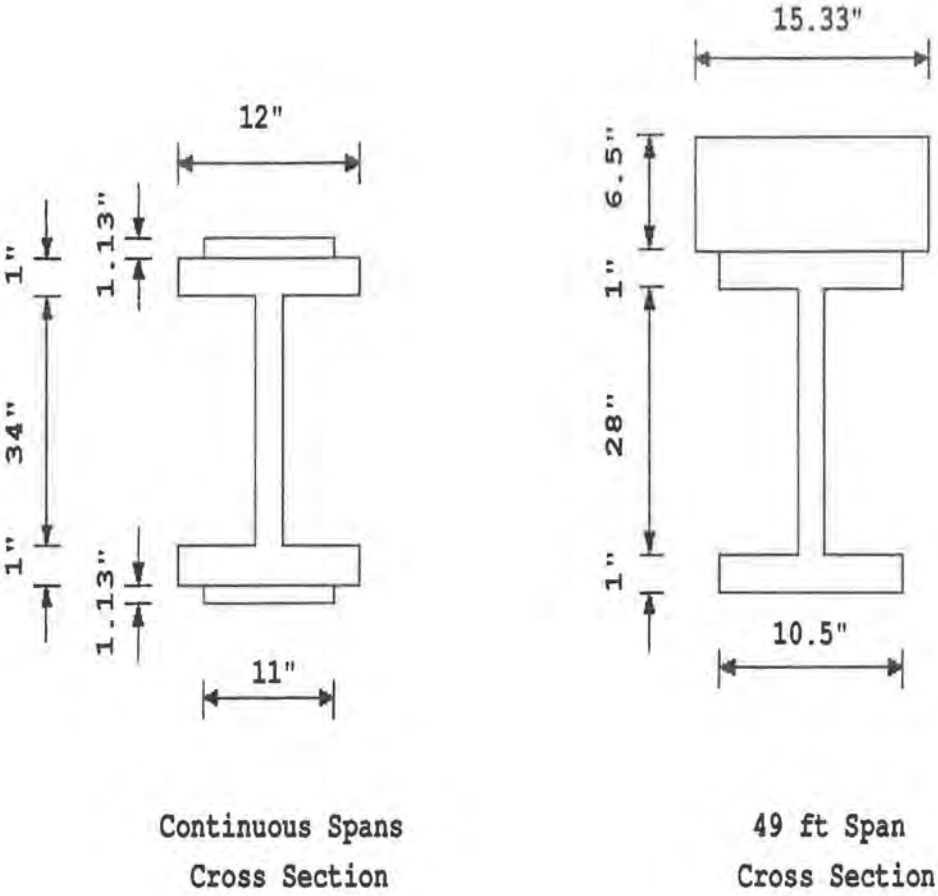

Figure 36. Cross Sections Used for Locust Fork Section Properties

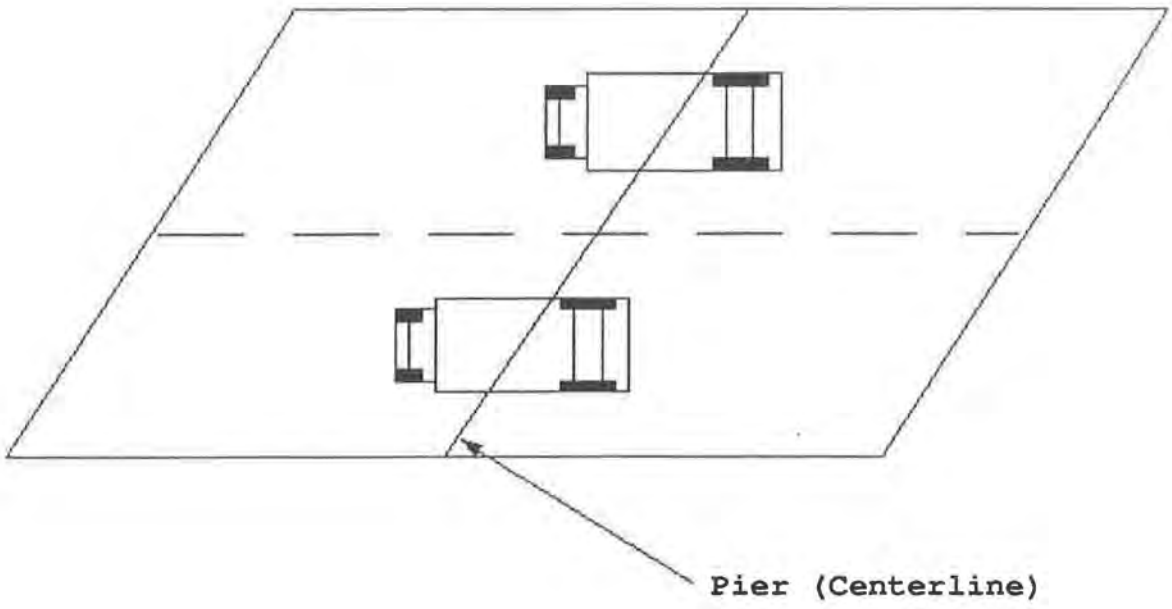

Figure 37. Position of Standard Trucks on Vincent Grid Model

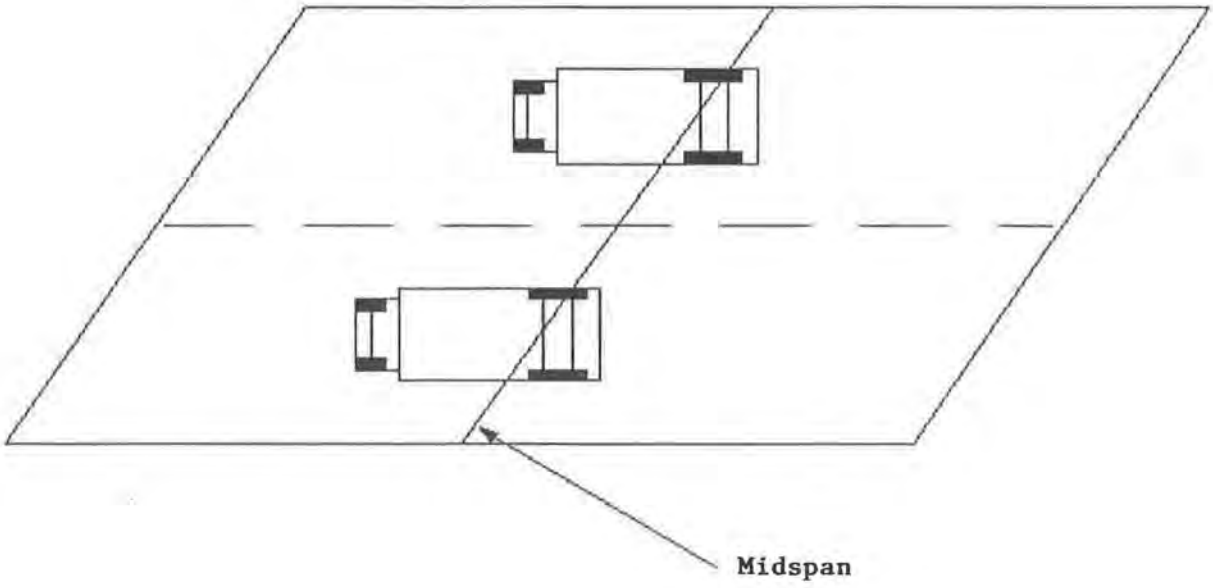

Figure 38. Position of Standard Trucks on Mulberry Fork Grid Model

For the Mulberry Fork Bridge, $M_{abs\ max}$ was determined in both spans by positioning the standard truck types along the span as shown in Figure 38.

For the Locust Fork Bridge, the combination of dead load and live load stresses in the negative moment region (at the pier) controls the rating of the continuous spans. Therefore the stationary test which produced the largest negative strain should be used to determine M_{test}. The negative moment test using four trucks produced the largest negative strain. To determine $M_{abs\ max}$, the standard trucks were positioned at the pier as illustrated in Figure 39 for the continuous spans.

Other Analysis Methods

The test ratings presented in Chapter IV for the Ashville and Childersburg bridges are determined using simple beam moments. The test ratings for the Vincent, Mulberry Fork, and Locust Fork continuous spans are calculated using $M_{abs\ max}$ determined from the grid analyses. To compare results based on the two analysis methods it is convenient to look at the ratios ($M_{test}/M_{abs\ max}$) using moments from a grid analysis and from a simple beam analysis.

These ratios are compared in Table 25 for the Locust Fork Bridge 49 ft simple span. The ratios compare very well for the short multiaxle trucks. The ratios indicate for the long multiaxle trucks, that the test ratings using the grid anlaysis will be somewhat higher. There is no practical difference in the two approaches for the 49 ft span since the ratings are greater than the standard truck weights by either approach.

Since the moment ratios of Table 25 are essentially the same, it is concluded that it is not necessary to use a grid analysis to compute test ratings for simply supported bridges that are not skewed.

Table 25. Comparison of Moment Ratios from Grid and Simple Beam Analysis

Truck Type	Grid Analyses ($M_{test}/M_{abs\ max}$)	Simple Beam ($M_{test}/M_{abs\ max}$)
Two Axle	.96	.94
Tri-Axle	.60	.59
Concrete Truck	.67	.67
Type 3S2 (AL)	1.08	.91
H20-44	1.02	1.00
Schol Bus	2.23	1.96

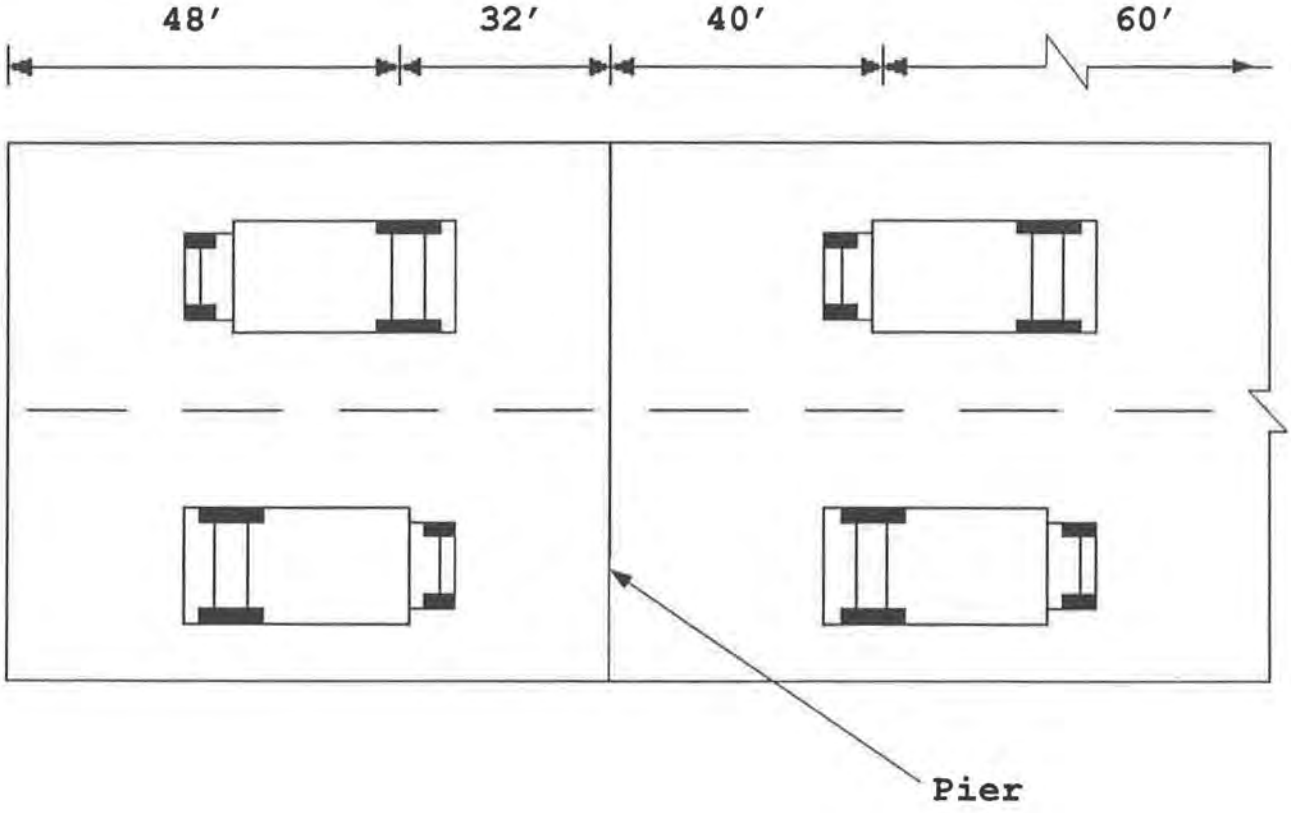

Figure 39. Position of Standard Trucks on Locust Fork Grid Model

IV. BRIDGE RATINGS

Introduction

Bridge ratings determined by three approaches are presented in this chapter. The ratings are referred to simply as the AASHTO rating, grid rating, and test rating. A brief description of each of the rating methods is also given in this chapter. The bridge ratings are based only on the bridge superstructures and not the substructures (piers and abutments). This follows common practice as presented in the AASHTO Manual (1983).

Dead Loads and Allowable Stresses

In order to calculate a bridge rating by each of the rating methods, the allowable stresses and dead load stresses had to be determined for each bridge. Estimated dead loads for each bridge are given in Tables 26 through 30. These dead loads are applicable for a typical interior girder. The dead loads were determined by assuming that the total dead load of the bridge was shared equally by all the bridge girders. Dead load stresses in the girders were calculated from the dead loads by assuming no composite action.

Allowable stresses used in the ratings calculations are listed in Table 31. The allowable stresses for operating ratings were taken from the AASHTO Manual (1983).

Test Ratings

A brief description of the method of calculating bridge ratings from the test results was presented in Chapter II. The fundamental Equations 1 and 2 are repeated here for further illustration. Bridge ratings are determined from

$$\text{Rating} = \frac{M_{cap}}{M_{abs\ max}} W \qquad (1)$$

where M_{cap} = the allowable live load moment capacity

$M_{abs\ max}$ = the absolute maximum moment produced by an applied load

W = the weight of the standard truck

The moment capacity can be determined from the test results as

$$M_{cap} = \frac{\sigma_{all} - \sigma_{dl}}{IF\,\sigma_{ll}} M_{test} \qquad (2)$$

Table 26. Estimated Dead Loads, Ashville

Source	Uniform Load (lb/ft)
Concrete Deck	524
Girder	61
Curbs, Railings	35
Total	620

Table 27. Estimated Dead Loads, Vincent

Source	Uniform Load (lb/ft)
Concrete Deck	225
Girder	32
Curbs, Railings	81
Total	338

Table 28. Estimated Dead Loads, Childersburg

Source	Uniform Load (lb/ft)	
	44 ft Span	77 ft Span
Concrete Deck	451	451
Girder	110	240
Concrete Diaphragms	53	75
Curbs, Railings	125	125
Total	739	891

Table 29. Estimated Dead Loads, Mulberry Fork

Source	Uniform Load (lb/ft)	
	34 ft Span	44 ft Span
Concrete Deck	520	520
Girder	90	116
Curbs, Railings	160	160
Total	770	796

Table 30. Estimated Dead Loads, Locust Fork

Source	Uniform Load (lb/ft)	
	49 ft Span	Continuous Spans
Concrete Deck	528	528
Girder	132	160
Curbs, Railings	160	160
Total	820	848

Table 31. Allowable Operating Stresses

Bridge Name	Allowable Bending Stress for Operating Ratings
Ashville	24.5 ksi
Vincent	22.5 ksi
Childersburg	22.5 ksi
Mulberry Fork	24.5 ksi
Locust Fork	24.5 ksi

where M_{cap} = allowable moment capacity

σ_{all} = allowable stress

σ_{dl} = dead load stress

σ_{ll} = live load stress from tests (see Chapter II)

IF = impact factor (see Chapter II)

M_{test} = moment produced by test truck

The M_{test} values used in Equation 2 for each span are listed in Table 32. Ratings were determined for each standard truck illustrated in Figure 40. Test ratings and $M_{abs\ max}$ values for each bridge are listed in Tables 33 through 40. Note that the moments for the Ashville Bridge and both spans of the Childersburg bridge were determined from a simple beam analysis. The M_{test} values for those spans are the moments induced at midspan of a simple beam by one test truck. In a like manner the $M_{abs\ max}$ values listed under the "Test Ratings" heading in Tables 33, 34 and 35 were determined from a simple beam analysis with one standard truck. The test ratings determined from Equation 1 are for the fully loaded case of trucks in each lane.

The M_{test} and $M_{abs\ max}$ moments for bridges other than the Ashville and Childersburg spans were determined by grid analysis. The moments from grid analyses listed in Tables 32 through 40 are the bending moments in the most critically loaded girder of the bridge.

AASHTO Ratings

The AASHTO ratings given in Tables 33 through 40 were determined from hand calculations following the procedures given in the AASHTO Manual (1983). A complete example of the AASHTO rating calculations are given in Appendix C.

Equation 1 applies to the AASHTO rating procedure. However, the moment capacity is determined for the most critically loaded girder of the bridge from the following

$$M_{cap} = M_{all} - M_{dl} \qquad (3)$$

where M_{dl} = dead load moment

M_{all} = $S\sigma_{all}$

S = girder section modulus

Table 32. M_{test} Values

Bridge Span	M_{test}
Ashville	270 kip-ft*
Vincent	9 kip-ft
Childersburg, 44 ft	375 kip-ft*
Childersburg, 77 ft	731 kip-ft*
Mulberry Fork, 34 ft	100 kip-ft
Mulberry Fork, 44 ft	120 kip-ft
Locust Fork, 49 ft	176 kip-ft
Locust Fork, Continuous	390 kip-ft

Values for $M_{abs\ max}$ in Equation 1 are based on a simple beam analysis of the bridge. One wheel line of the standard truck is positioned on the bridge to create the absolute maximum moment. This maximum moment is then multiplied by an impact factor and a wheel load distribution factor to obtain $M_{abs\ max}$.

Grid Ratings

The fundamental Equation 1 applies to the grid rating method as well. The moment capacity of the critical girder in each bridge was determined from Equation 2. The moments, $M_{abs\ max}$, were then determined from a grid analysis as discussed in Chapter III.

Grid ratings for each of the bridges are listed in Tables 33 through 40. An example of the grid rating calculations is given in Appendix D.

Comparison of the Bridge Ratings

Inspection of the ratings of Tables 33 through 40 indicates that the test and grid ratings are greater than the AASHTO ratings in all cases. This illustrates the inherent conservatism of the AASHTO method. The test ratings are higher than the grid ratings in all cases except for the Mulberry Fork 44 ft span and the Locust Fork continuous spans. It should be expected that the grid ratings would be lower since the grid models generally overestimated the strains recorded in the bridge tests.

Comparisons of AASHTO and BARS Ratings

A study of the documentation for the BARS program was carried out as a part of the project reported here. Based on the program documentation, it is concluded that BARS is a computer program that carries out rating calculations by the methods outlines in the AASHTO Manual (1983). To illustrate this, AASHTO and BARS ratings for three bridge spans are given in Tables 41, 42 and 43. The BARS ratings were provided by the AHD. It is seen from Tables 41, 42 and 43 that the AASHTO and BARS ratings are essentially the same.

Table 33. Ashville Operating Ratings

Truck Type	Std. Wt.	Test Ratings		Grid Ratings		AASHTO Ratings (tons)
		$M_{abs\ max}$ (kip-ft)	Rating (tons)	$M_{abs\ max}$ (kip-ft)	Rating (tons)	
Two Axle	25	275	53	110	55	21
Tri-Axle	37.5	474	48	182	50	21
Conc. Trk.	33	401	48	159	50	21
3S2 (AL)	40	293	63	146	67	35
H20-44	20	286	42	110	44	18
Sch. Bus	12.5	145	70	42	73	22

Table 34. Childersburg Operating Ratings, 44 ft Span

Truck Type	Std. Wt.	Test Ratings		Grid Ratings		AASHTO Ratings (tons)
		$M_{abs\ max}$ (kip-ft)	Rating (tons)	$M_{abs\ max}$ (kip-ft)	Rating (tons)	
Two Axle	25	399	64	213	61	39
Tri-Axle	37.5	640	60	343	57	36
Conc. Trk.	33	565	59	303	57	36
3S2 (AL)	40	405	106	206	101	63
H20-44	20	386	53	206	50	32
Sch. Bus	12.5	191	65	105	62	41

Table 35. Childersburg Operating Ratings, 77 ft Span

Truck Type	Std. Wt.	Test Ratings		Grid Ratings		AASHTO Ratings (tons)
		$M_{abs\ max}$ (kip-ft)	Rating (tons)	$M_{abs\ max}$ (kip-ft)	Rating (tons)	
Two Axle	25	810	76	430	65	46
Tri-Axle	37.5	1258	73	670	63	45
Conc. Trk.	33	1109	73	594	62	44
3S2 (AL)	40	1021	96	523	85	57
H20-44	20	394	69	380	59	41
Sch. Bus	12.5	715	78	202	69	47

Table 36. Vincent Operating Ratings

Truck Type	Std. Wt.	$M_{abs\ max}$ * (kip-ft)	Grid (tons)	Test (tons)	AASHTO (tons)
Two Axle	25	34	32	37	23
Tri-Axle	37.5	54	30	35	23
Conc. Trk.	33	46	31	36	24
3S2 (AL)	40	49	35	41	23
H20-44	20	30	29	34	22
Sch. Bus	12.5	20	27	31	20

*from grid analysis

Table 37. Mulberry Fork Operating Ratings, 34 ft Span

Truck Type	Std. Wt.	$M_{abs\ max}$ * (kip-ft)	Grid (tons)	Test (tons)	AASHTO (tons)
Two Axle	25	115	56	77	37
Tri-Axle	37.5	171	57	78	34
Conc. Trk.	33	166	51	70	33
3S2 (AL)	40	131	79	108	56
H20-44	20	120	43	59	28
Sch. Bus	12.5	54	60	82	37

*from grid analysis

Table 38. Mulberry Fork Operating Ratings, 44 ft Span

Truck Type	Std. Wt.	$M_{abs\ max}$ * (kip-ft)	Grid (tons)	Test (tons)	AASHTO (tons)
Two Axle	25	139	65	63	36
Tri-Axle	37.5	220	62	59	34
Conc. Trk.	33	190	60	60	33
3S2 (AL)	40	147	99	95	59
H20-44	20	130	56	54	30
Sch. Bus	12.5	61	75	71	37

*from grid analysis

Table 39. Locust Fork Operating Ratings, 49 ft Span

Truck Type	Std. Wt.	$M_{abs\ max}$ * (kip-ft)	Grid (tons)	Test (tons)	AASHTO (tons)
Two Axle	25	184	56	70	32
Tri-Axle	37.5	293	57	66	30
Conc. Trk.	33	261	51	66	30
3S2 (AL)	40	163	79	128	49
H20-44	20	172	43	60	27
Sch. Bus	12.5	79	60	82	33

*from grid analysis

Table 40. Locust Fork Operating Ratings, Continuous Spans

Truck Type	Std. Wt.	$M_{abs\ max}$ * (kip-ft)	Grid (tons)	Test (tons)	AASHTO (tons)
Two Axle	25	441	59	53	40
Tri-Axle	37.5	671	58	52	40
Conc. Trk.	33	589	58	52	39
3S2 (AL)	40	629	66	60	46
H20-44	20	361	57	52	39
Sch. Bus	12.5	213	61	55	41

*from grid analysis

Table 41. BARS and AASHTO Ratings, Childersburg, 44 ft Span

Truck Type	Std. Wt.	BARS (tons)	AASHTO (tons)
Two Axle	25	—	39
Tri-Axle	37.5	36	36
Conc. Trk.	33	36	36
3S2 (AL)	40	60	63
H20-44	20	32	32
Sch. Bus	12.5	41	41

Table 42. BARS and AASHTO Ratings, Mulberry Fork, 34 ft Span

Truck Type	Std. Wt.	BARS (tons)	AASHTO (tons)
Two Axle	25	—	37
Tri-Axle	37.5	33	34
Conc. Trk.	33	33	33
3S2 (AL)	40	55	56
H20-44	20	28	28
Sch. Bus	12.5	35	37

Table 43. BARS and AASHTO Ratings, Mulberry Fork, 44 ft Span

Truck Type	Std. Wt.	BARS (tons)	AASHTO (tons)
Two Axle	25	—	36
Tri-Axle	37.5	33	34
Conc. Trk.	33	33	33
3S2 (AL)	40	56	59
H20-44	20	29	30
Sch. Bus	12.5	38	37

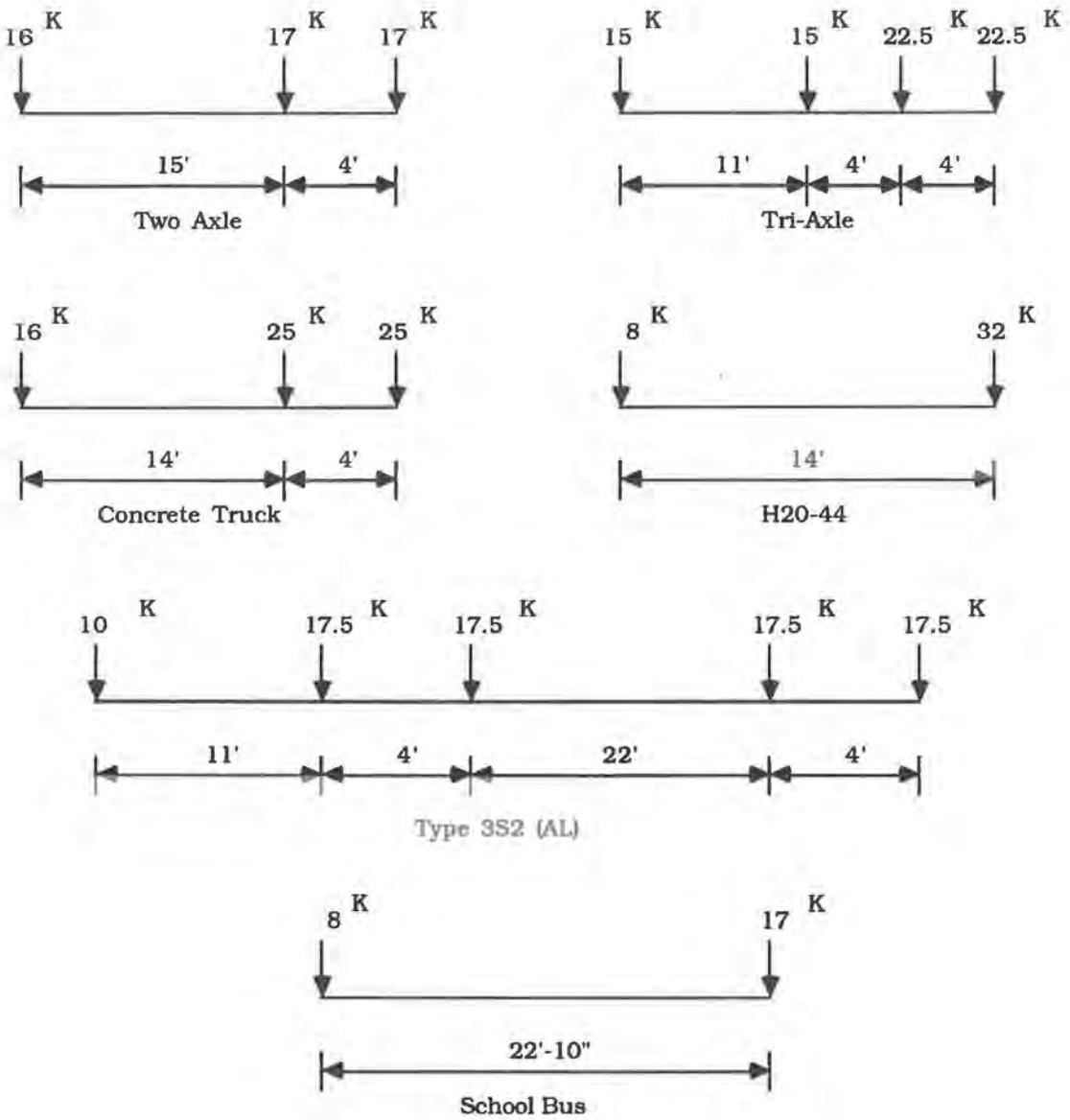

Figure 40. Standard Truck Types.

V. CONCLUSIONS

The results of the bridge testing clearly show that each bridge that has been selected in this project is capable of load limits larger than those determined by the AASHTO rating method. The girder strains measured during the bridge tests were smaller than those which would be predicted by the AASHTO simplified method of analysis. Evidence of this can be seen from comparisons of the AASHTO and test ratings. Based on the test ratings presented in Chapter IV, it is suggested that no posting of load limits below the standard truck weights is necessary for the Ashville, Childersburg, Locust Fork, and Mulberry Fork bridges. The Vincent bridge is currently posted because of substructure conditions at the bridge. It is suggested that the test ratings of the Vincent bridge not be utilized until the substructure deficiencies are corrected.

The AASHTO ratings, calculated using the procedures described in the AASHTO Manual (1983), were essentially the same as the BARS ratings. Comparisons of the ratings as well as study of the BARS documentation indicate that BARS is an automated version of the AASHTO method.

Grid analyses were performed to determine test ratings and grid ratings. However, it was found that simple beam analyses were as effective in determining the test ratings as the grid analyses.

Grid analysis results are dependent on the assumptions made in modeling a bridge. It was found that models developed without test data were not able to accurately represent the observed bridge behavior. Test data was used to refine the grid models through assumptions about effective cross section properties, material properties, and support restraint. Comparisons of measured strains and results from the refined grid models showed improvement. It is expected that with further refinement of the modeling techniques grid analyses can produce very accurate results.

VI. REFERENCES

American Association of State Highway and Transportation Officials (1983). Manual for Maintenance Inspection of Bridges, Washington, D.C.

American Association of State Highway and Transportation Officials (1989). Standard Specifications for Highway Bridges, 14th Edition, Washington, D.C.

American Institute of Steel Construction (1947). Steel Construction. A Manual for Architects, Engineers and Fabricators of Buildings and Other Steel Structures, 5th Edition, New York, N.Y.

Bakht, B. and Jaeger, L.G. (1985). Bridge Analysis Simplified, McGraw-Hill, Inc., New York, N.Y., 294 p.

Bakht, B. and Jaeger, Bridge Analysis by Microcomputer, McGraw-Hill, Inc., New York, N.Y., 330 p.

Bakht, B. and Csagoly, P.F. (1980). "Diagnostic Testing of a Bridge," ASCE Journal of Structural Engineering, 106(7).

Burdette, E.G. and Goodpasture (1988). Correlation of Bridge Load Capacity Estimates with Test Data. NCHRP Report 306, NCHRP 12-28(8) Final Report, Transportation Research Board, Washington, D.C.

Gere, J.M. and W. Weaver, Jr. (1985). Analysis of Framed Structures, D. Van Nostrand Company, Inc., New York, N.Y., 475 p.

Mores, F. (1990). "Bridge Capacity Assessment and Control of Posting, Permit and Legal Vehicle Loads," Presented at the First International Conference on Bridge Management, Guildford, UK, March 1990. Published in Bridge Management: Inspection, Maintenance, Assessment and Repair, New York, N.Y.

Przemieniecki, J.S. (1968). Theory of Matrix Structural Analysis, McGraw-Hill, Inc., New York, N.Y., 468 p.

APPENDIX A

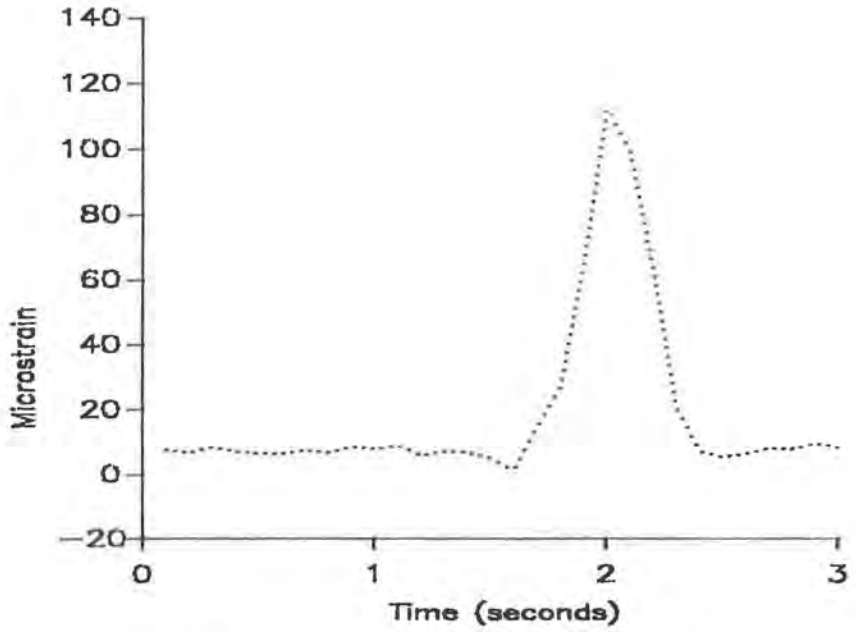

Figure A1. Dynamic Strain from Ashville Bridge, One Truck at 55 mph, Cover Plate, Girder 2

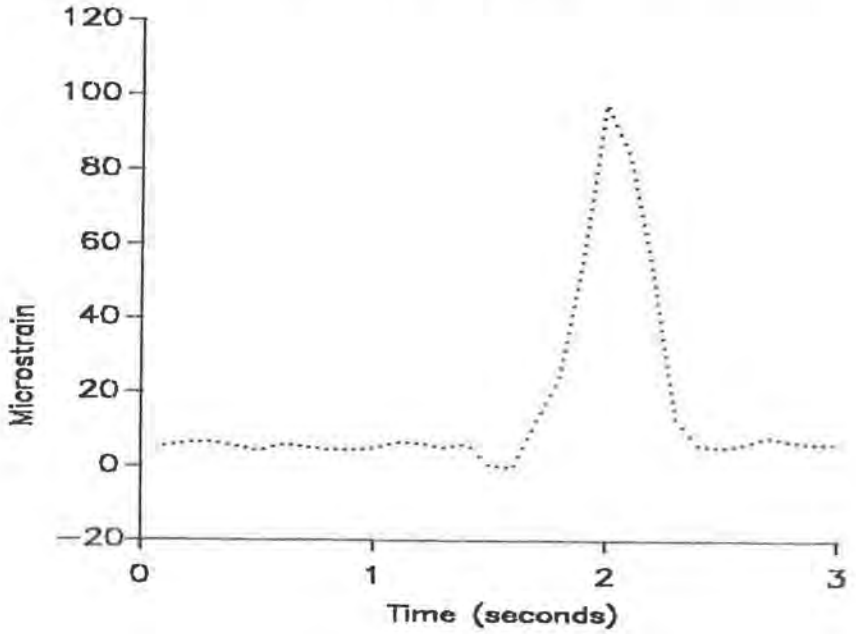

Figure A2. Dynamic Strain from Ashville Bridge, One Truck at 55 mph, Cover Plate, Girder 3

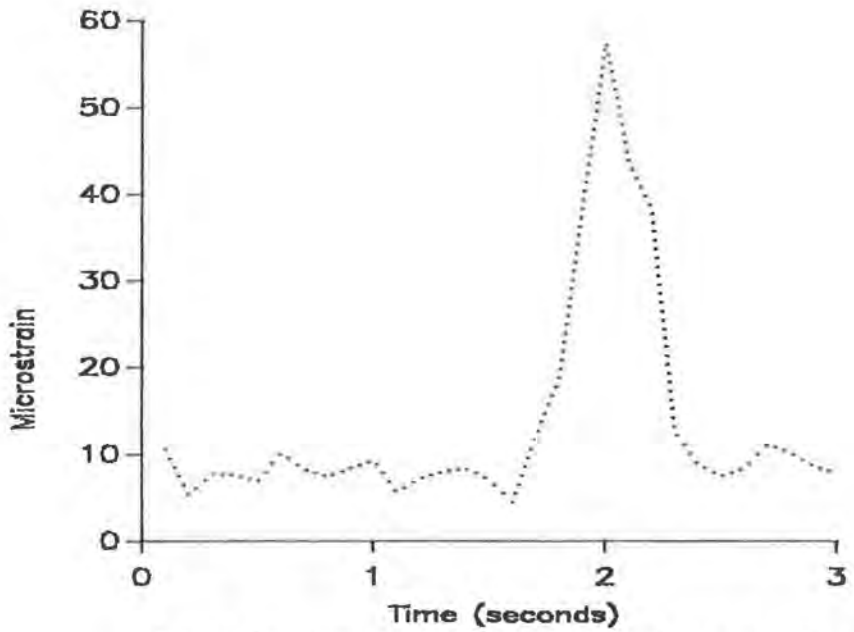

Figure A3. Dynamic Strain from Ashville Bridge, One Truck at 55 mph, Cover Plate, Girder 4

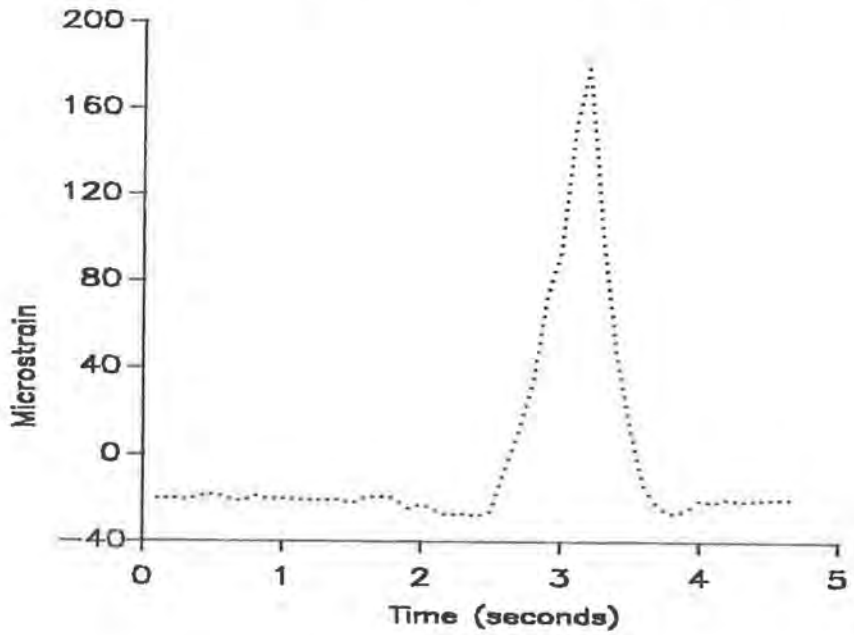

Figure A4. Dynamic Strain from Ashville Bridge, Two Trucks at 40 mph, Cover Plate, Girder 2

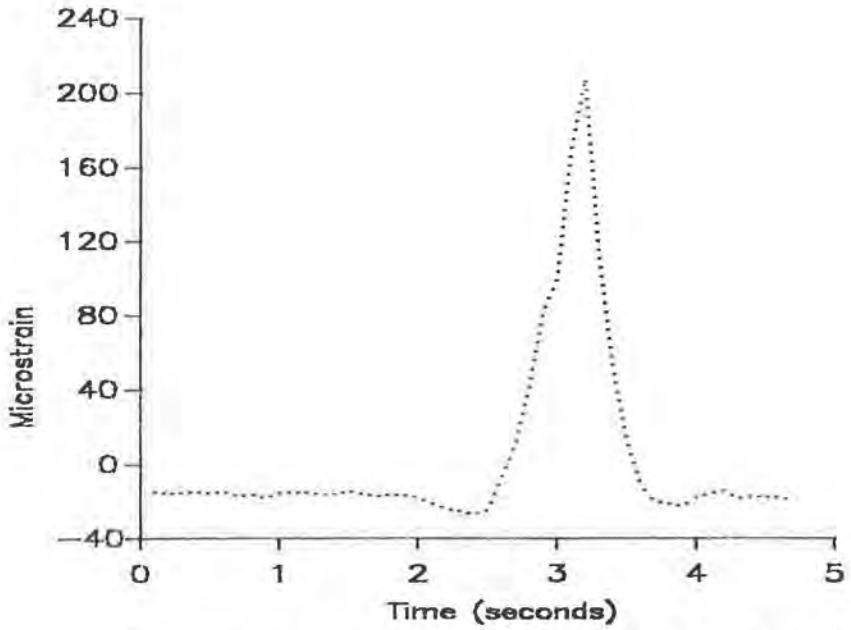

Figure A5. Dynamic Strain from Ashville Bridge, Two Trucks at 40 mph, Cover Plate, Girder 3

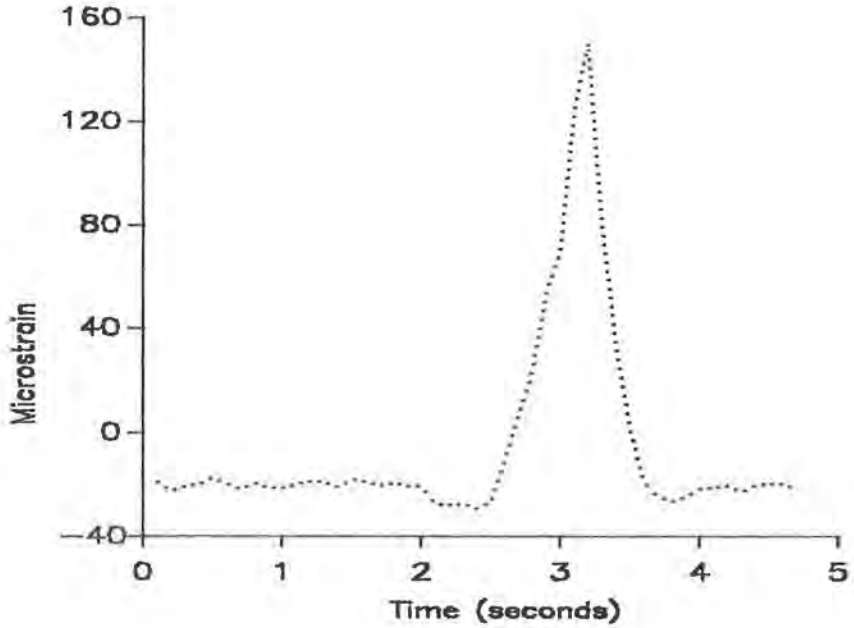

Figure A6. Dynamic Strain from Ashville Bridge, Two Trucks at 40 mph, Cover Plate, Girder 4

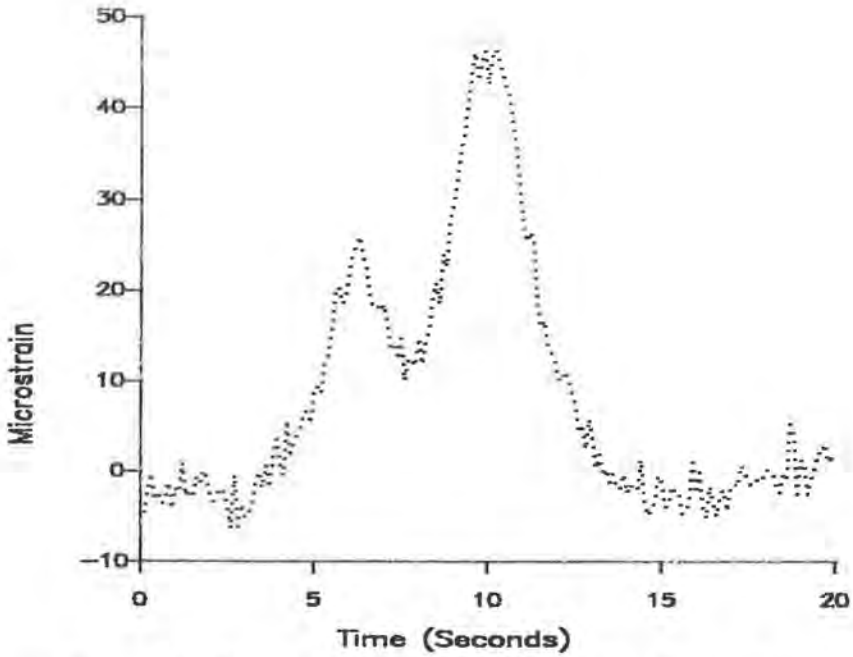

Figure A7. Dynamic Strain from Vincent Bridge, One Truck, Crawl Speed, Positive Moment Region, Girder 2

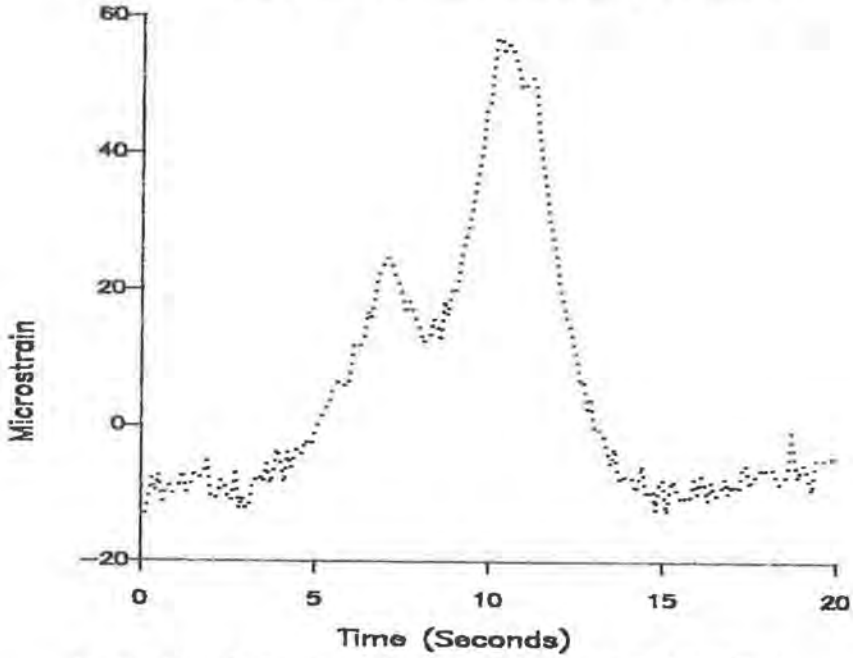

Figure A8. Dynamic Strain from Vincent Bridge, One Truck, Crawl Speed, Positive Moment Region, Girder 4

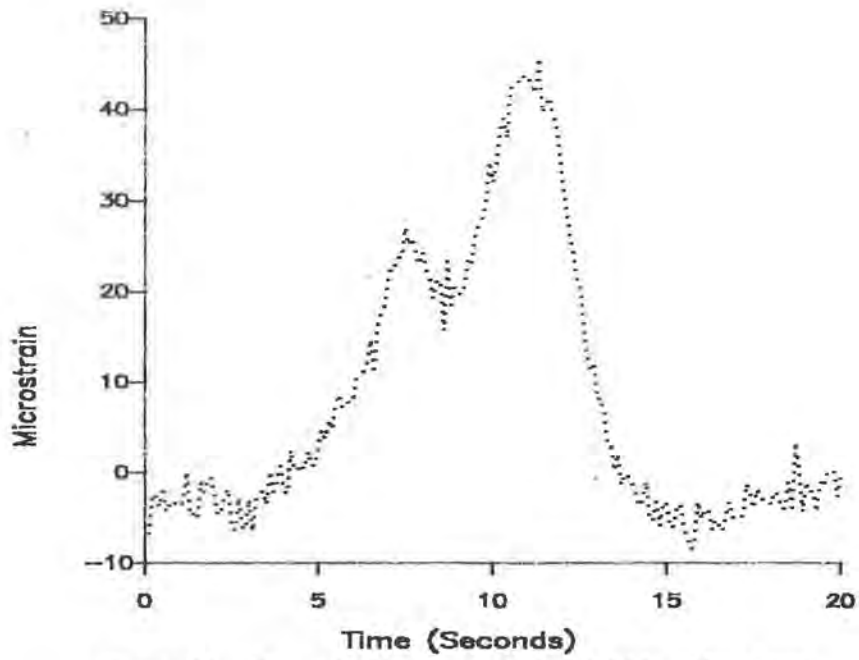

Figure A9. Dynamic Strain from Vincent Bridge, One Truck, Crawl Speed, Positive Moment Region, Girder 5

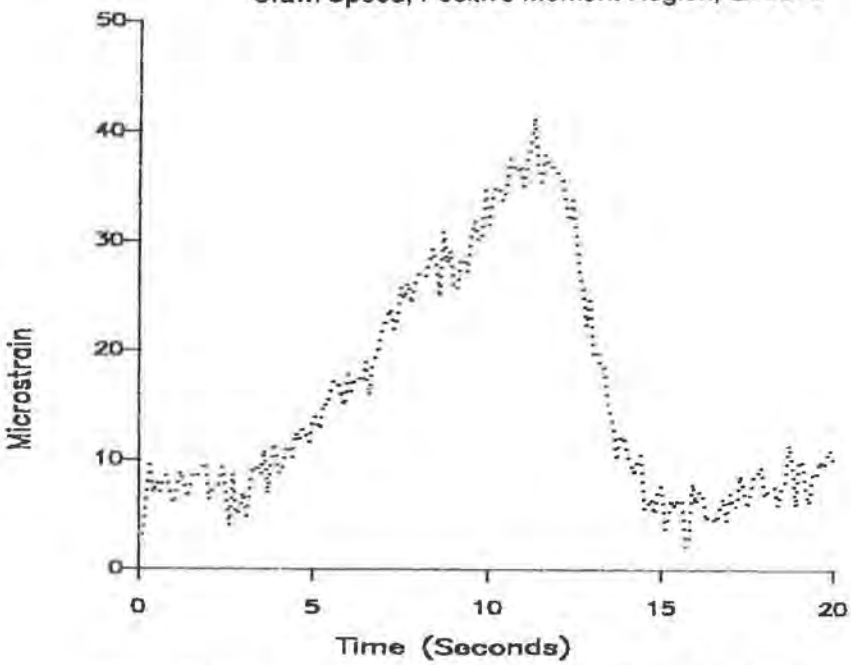

Figure A10. Dynamic Strain from Vincent Bridge, One Truck, Crawl Speed, Positive Moment Region, Girder 6

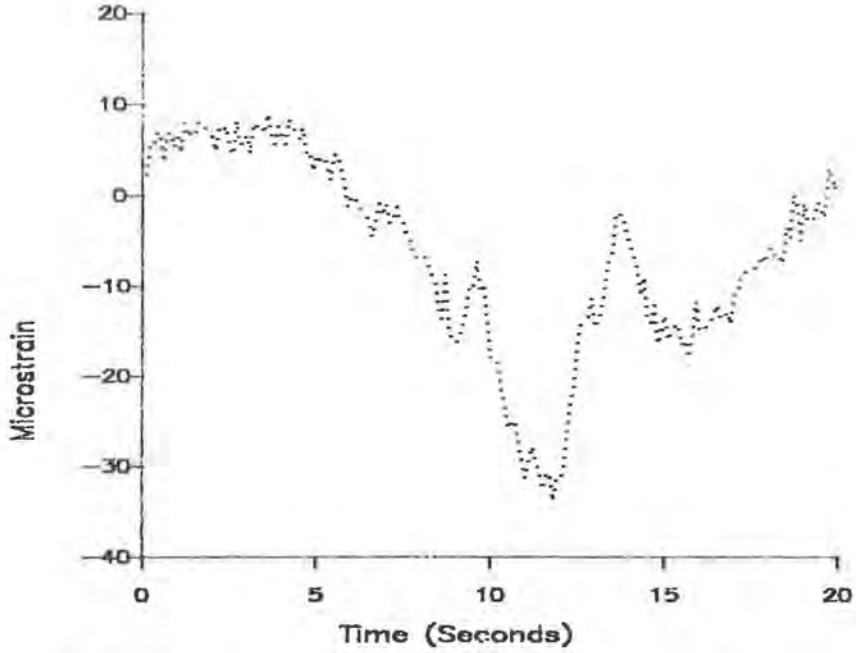

Figure A11. Dynamic Strain from Vincent Bridge, One Truck, Crawl Speed, Negative Moment Region, Girder 2

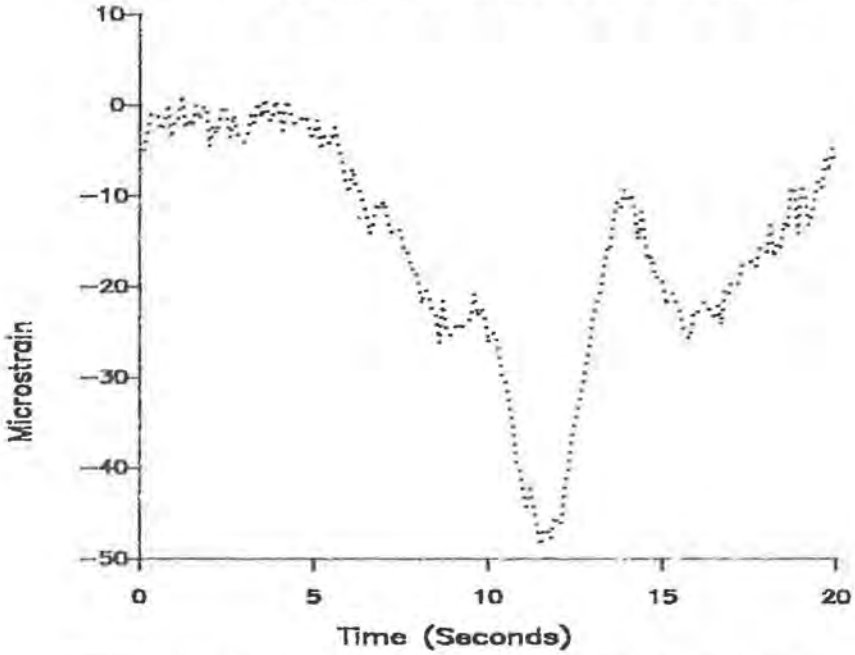

Figure A12. Dynamic Strain from Vincent Bridge, One Truck, Crawl Speed, Negative Moment Region, Girder 3

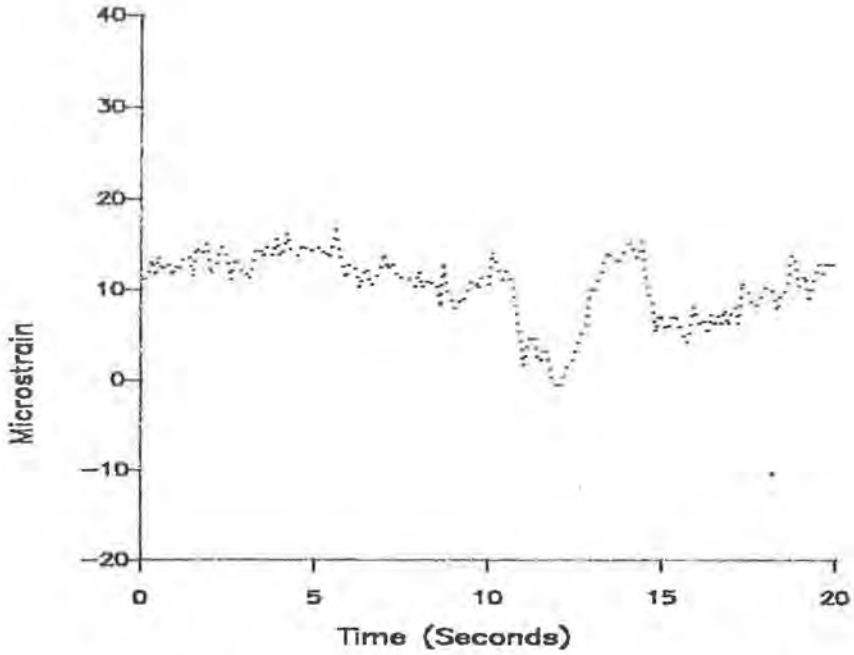

Figure A13. Dynamic Strain from Vincent Bridge, One Truck, Crawl Speed, Negative Moment Region, Girder 4

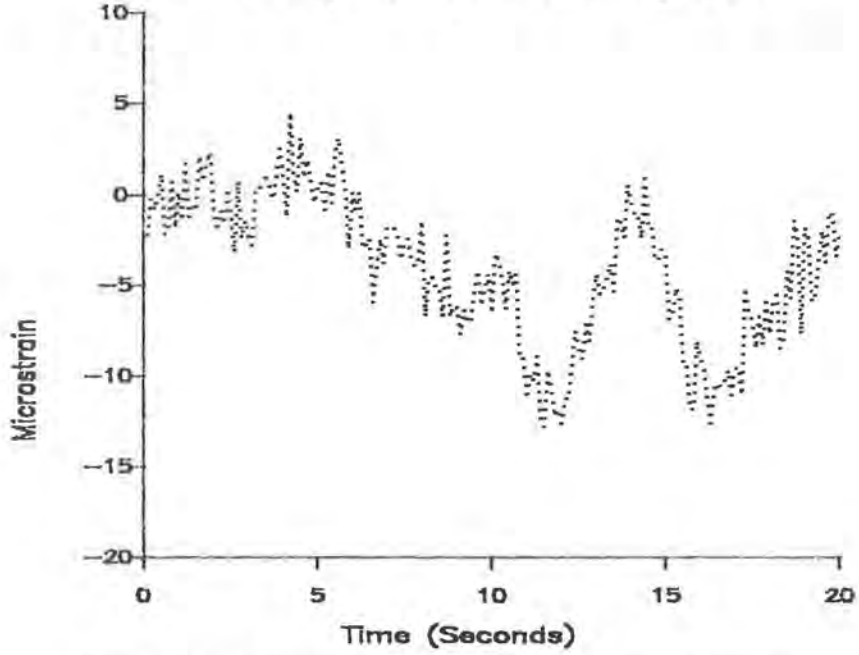

Figure A14. Dynamic Strain from Vincent Bridge, One Truck, Crawl Speed, Negative Moment Region, Girder 5

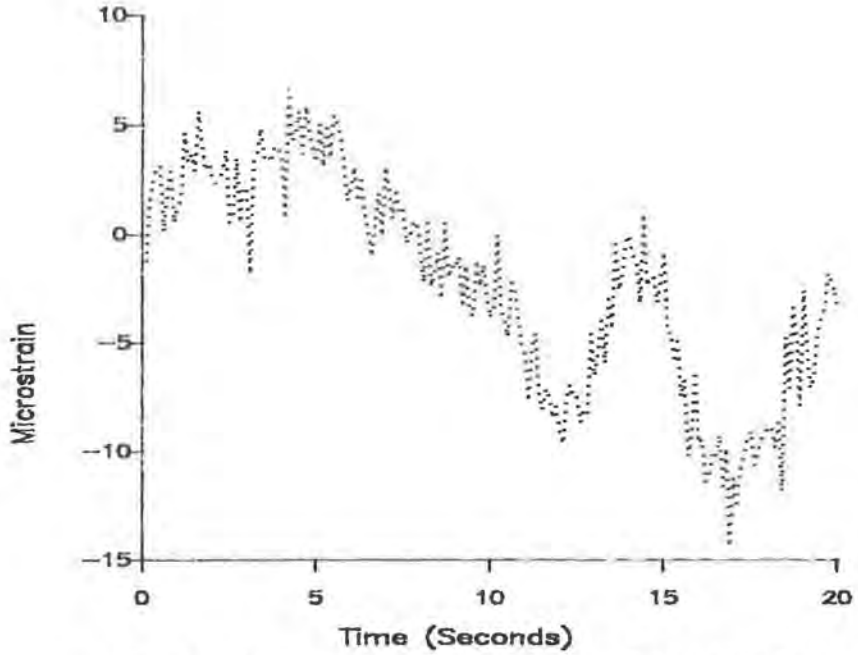

Figure A15. Dynamic Strain from Vincent Bridge, One Truck, Crawl Speed, Negative Moment Region, Girder 6

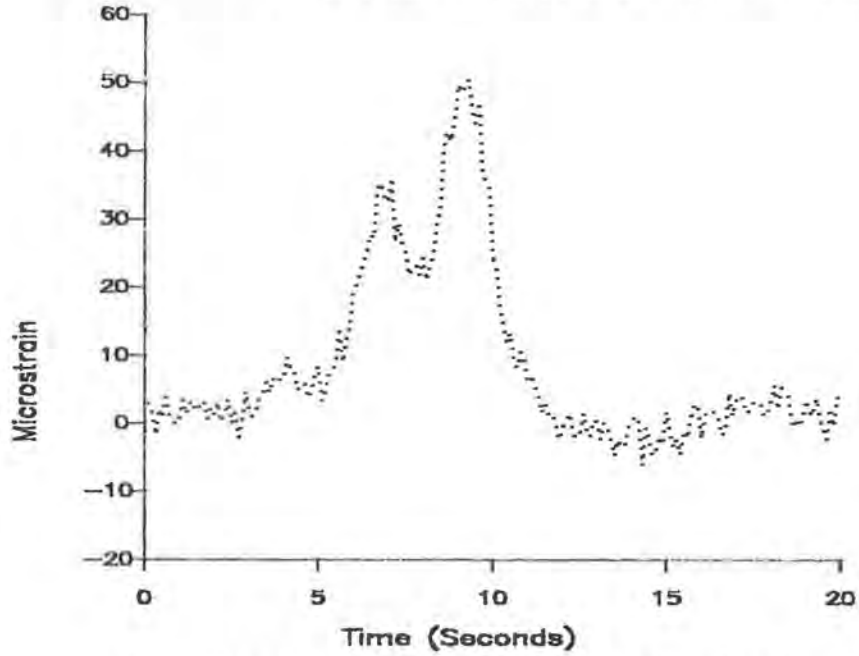

Figure A16. Dynamic Strain from Vincent Bridge, Two Trucks, Crawl Speed, Positive Moment Region, Girder 2

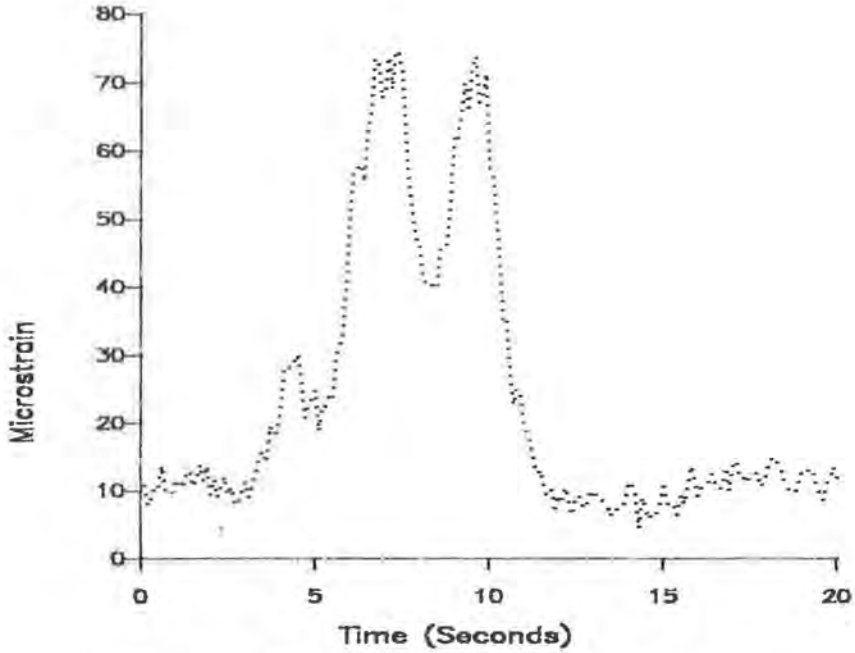

Figure A17. Dynamic Strain from Vincent Bridge, Two Trucks, Crawl Speed, Positive Moment Region, Girder 4

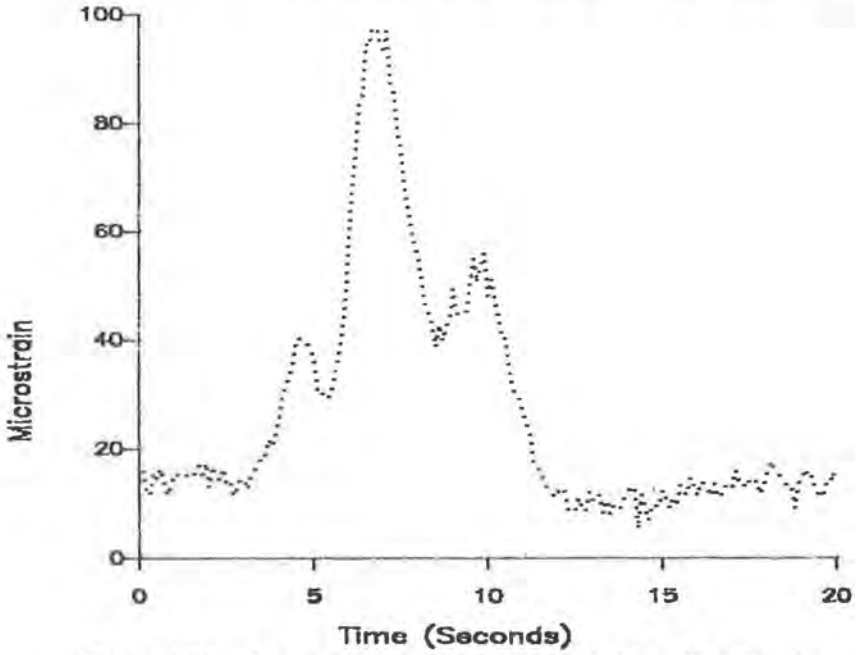

Figure A18. Dynamic Strain from Vincent Bridge, Two Trucks, Crawl Speed, Positive Moment Region, Girder 5

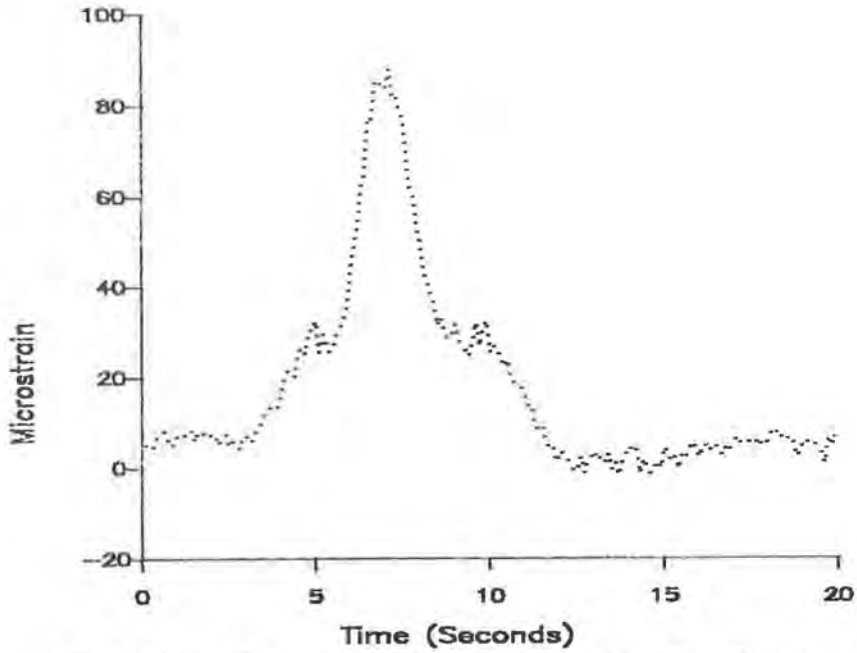

Figure A19. Dynamic Strain from Vincent Bridge, Two Trucks, Crawl Speed, Positive Moment Region, Girder 6

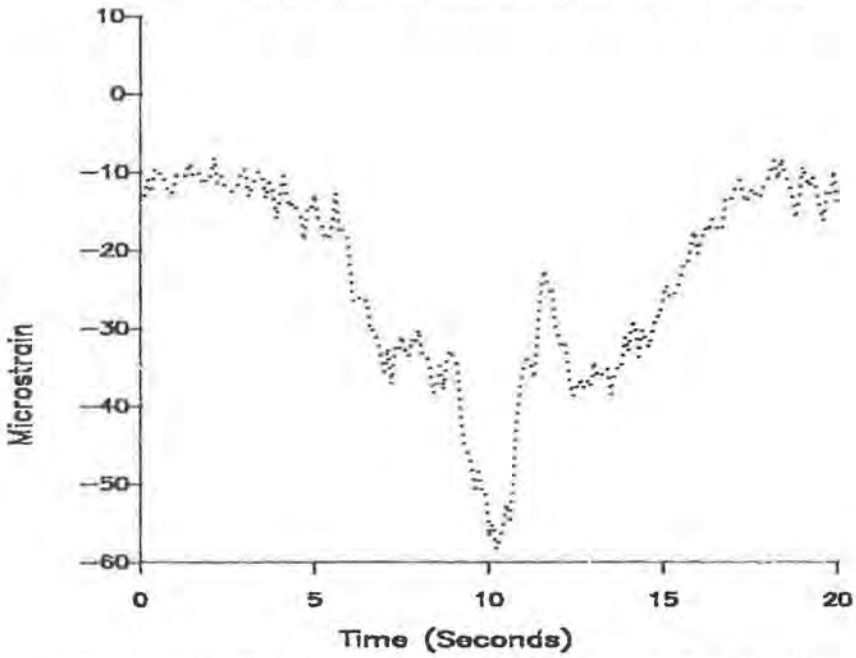

Figure A20. Dynamic Strain from Vincent Bridge, Two Trucks, Crawl Speed, Negative Moment Region, Girder 2

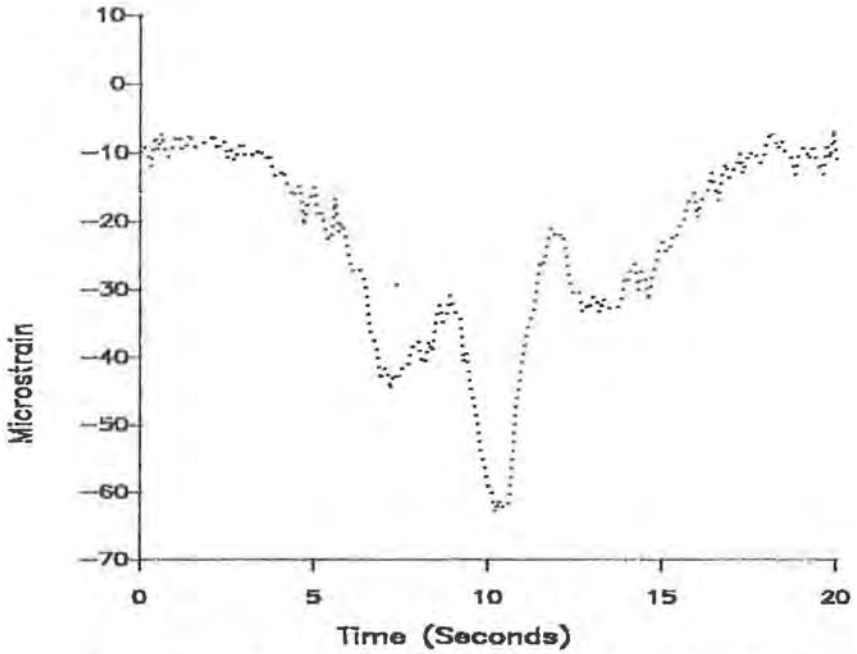

Figure A21. Dynamic Strain from Vincent Bridge, Two Trucks, Crawl Speed, Negative Moment Region, Girder 3

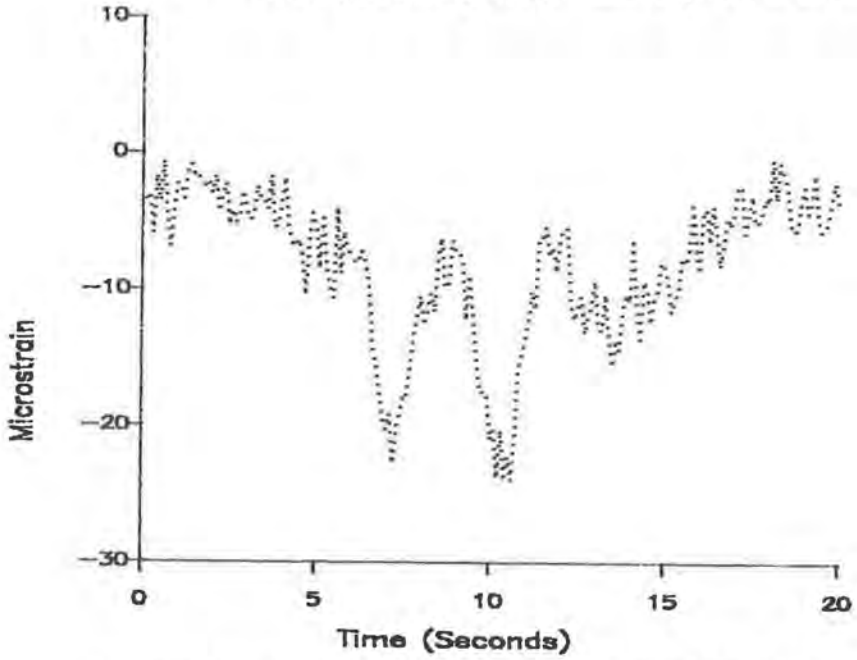

Figure A22. Dynamic Strain from Vincent Bridge, Two Trucks, Crawl Speed, Negative Moment Region, Girder 4

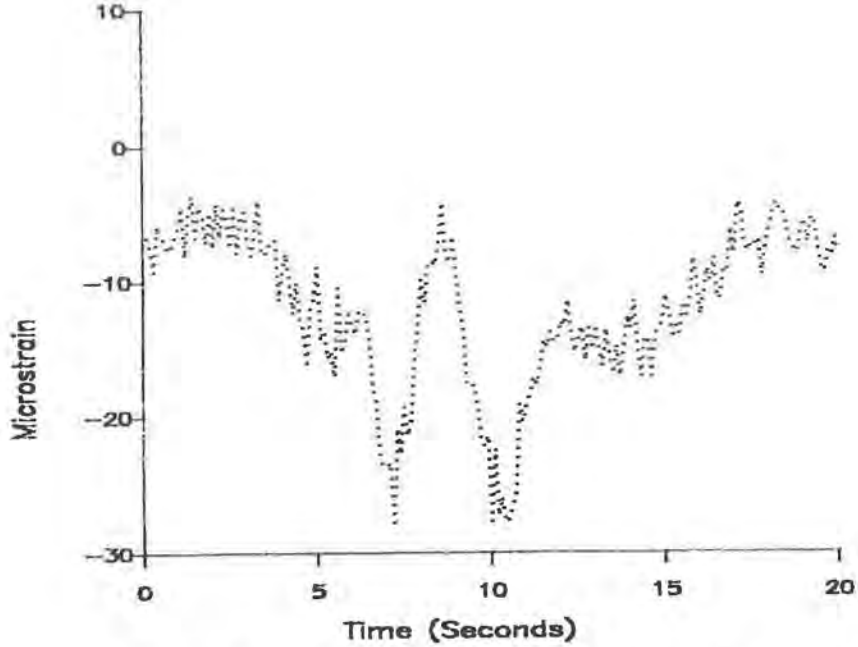

Figure A23. Dynamic Strain from Vincent Bridge, Two Trucks, Crawl Speed, Negative Moment Region, Girder 5

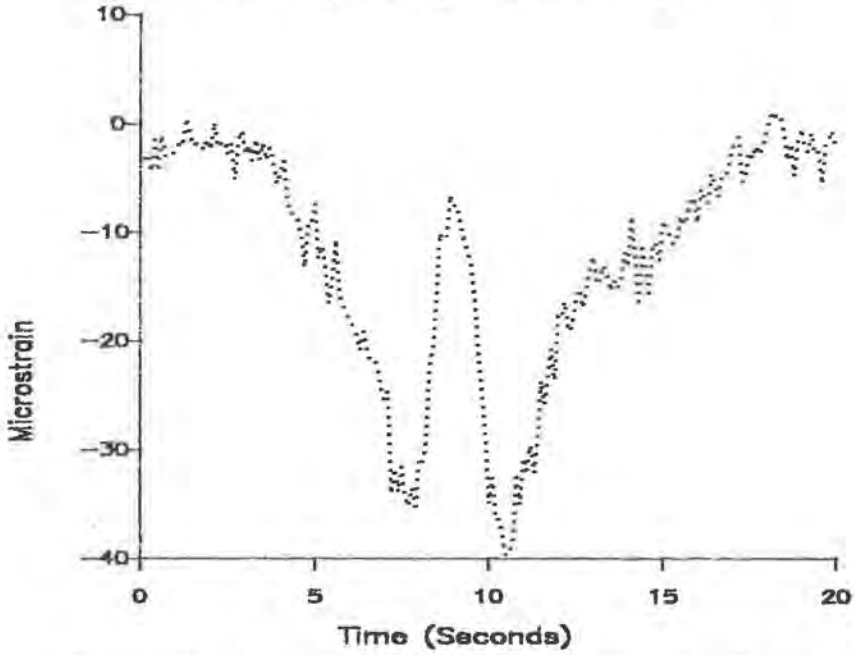

Figure A24. Dynamic Strain from Vincent Bridge, Two Trucks, Crawl Speed, Negative Moment Region, Girder 6

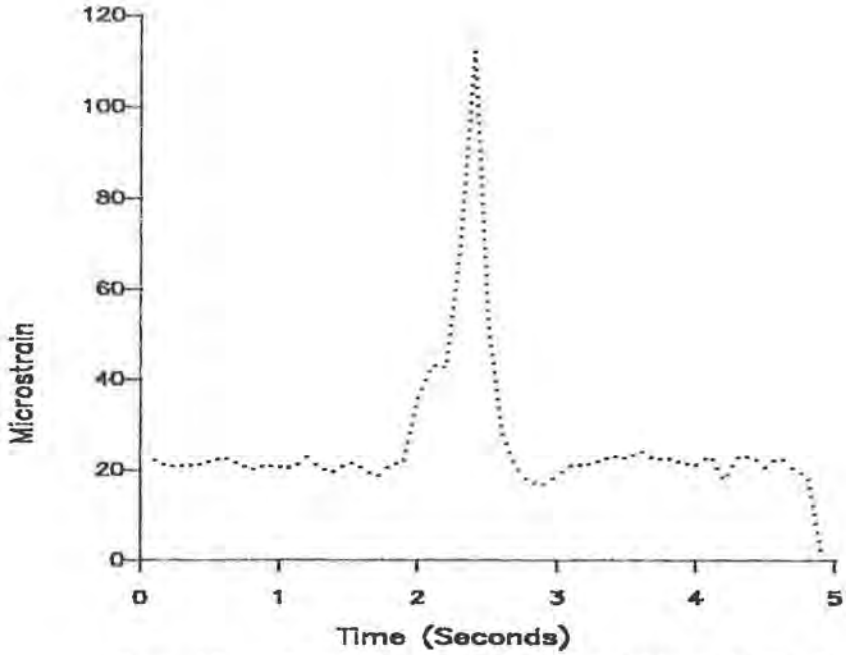

Figure A25. Dynamic Strain from Vincent Bridge, One Truck at 40 mph, Positive Moment Region, Girder 4

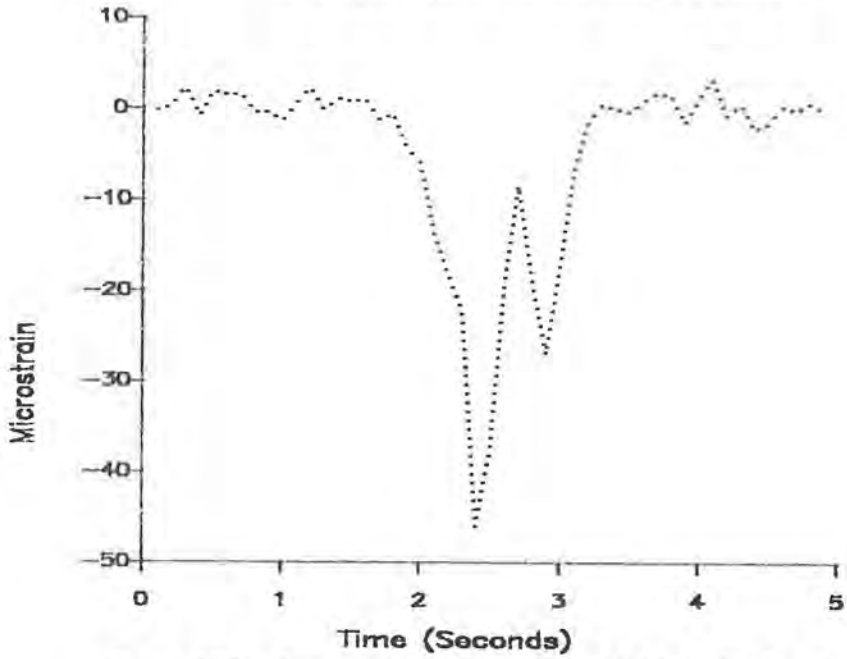

Figure A26. Dynamic Strain from Vincent Bridge, One Truck at 40 mph, Negative Moment Region, Girder 3

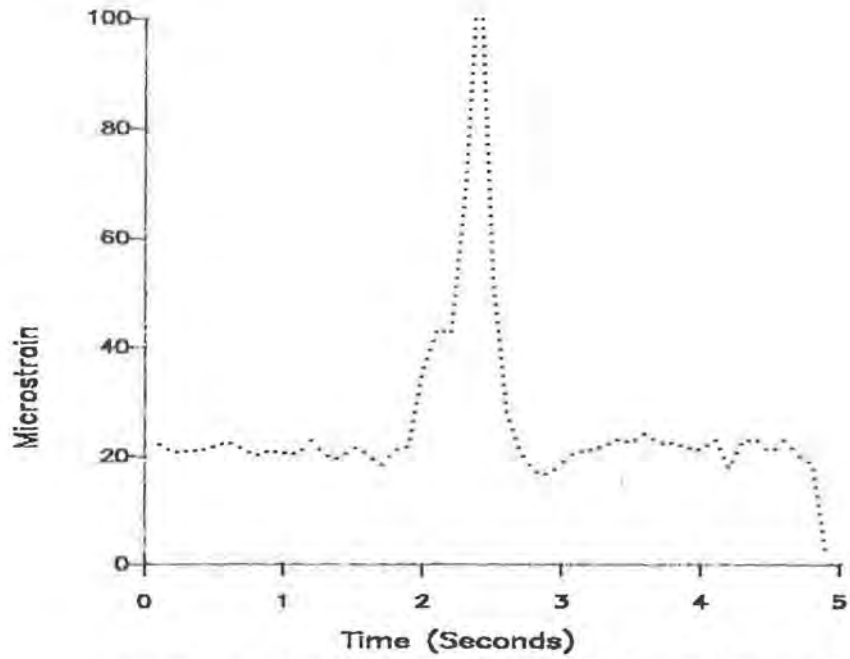

Figure A27. Dynamic Strain from Vincent Bridge, Two Trucks at 40 mph, Positive Moment Region, Girder 4

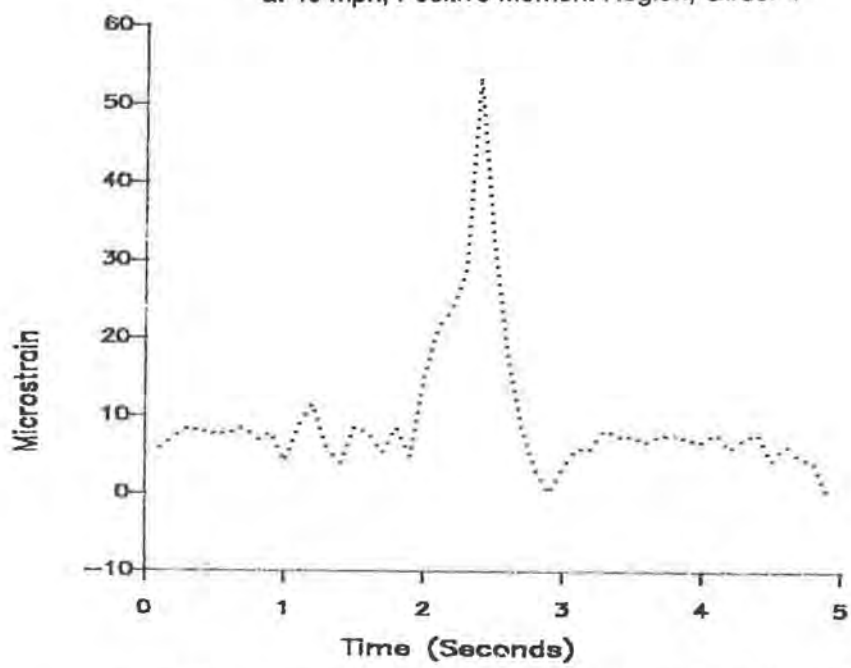

Figure A28. Dynamic Strain from Vincent Bridge, Two Trucks at 40 mph, Positive Moment Region, Girder 6

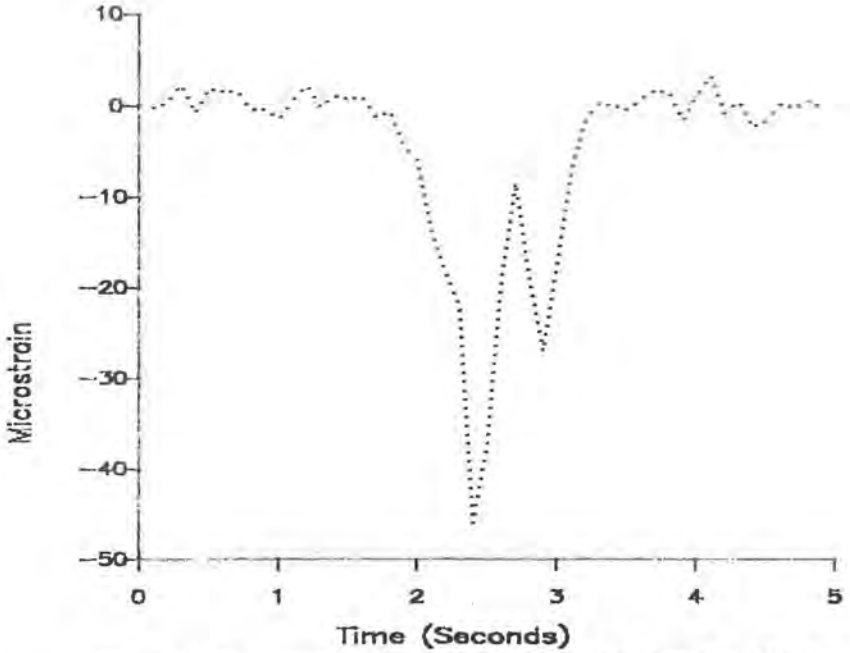

Figure A29. Dynamic Strain from Vincent Bridge, Two Trucks at 40 mph, Negative Moment Region, Girder 3

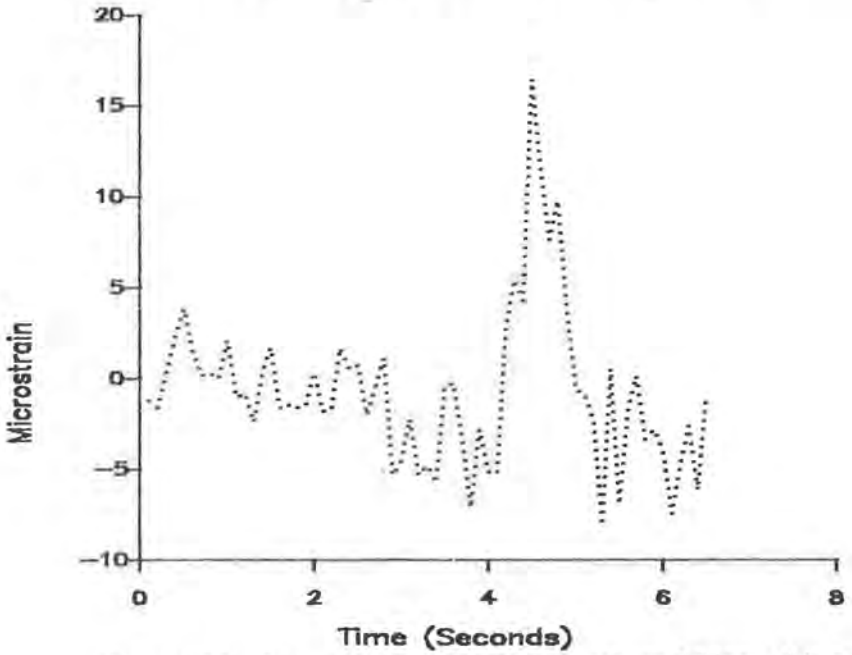

Figure A30. Dynamic Strain from Childersburg Bridge, 44 ft. span, One Truck at 60 mph, Bottom Flange, Girder 1

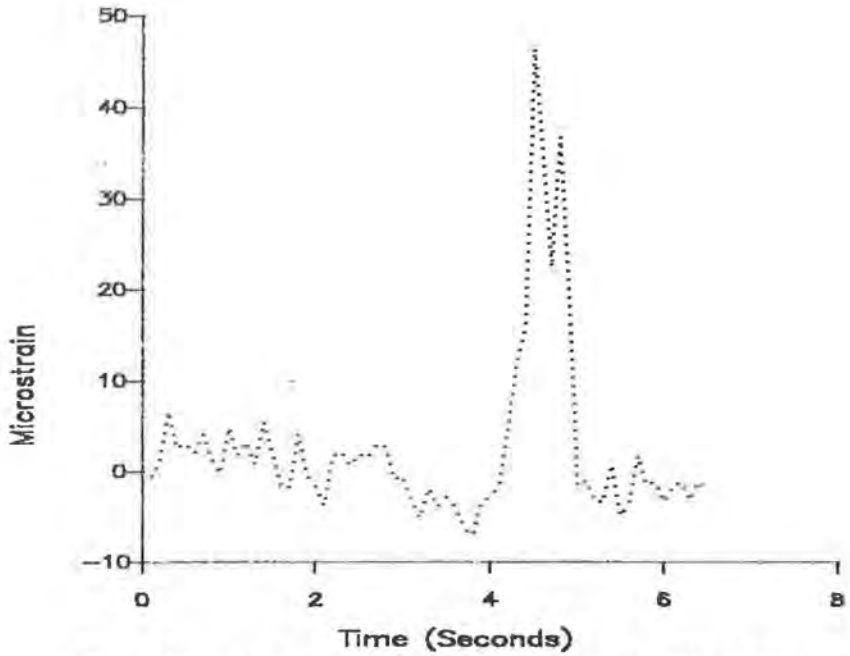

Figure A31. Dynamic Strain from Childersburg Bridge, 44 ft. span, One Truck at 60 mph, Bottom Flange, Girder 2

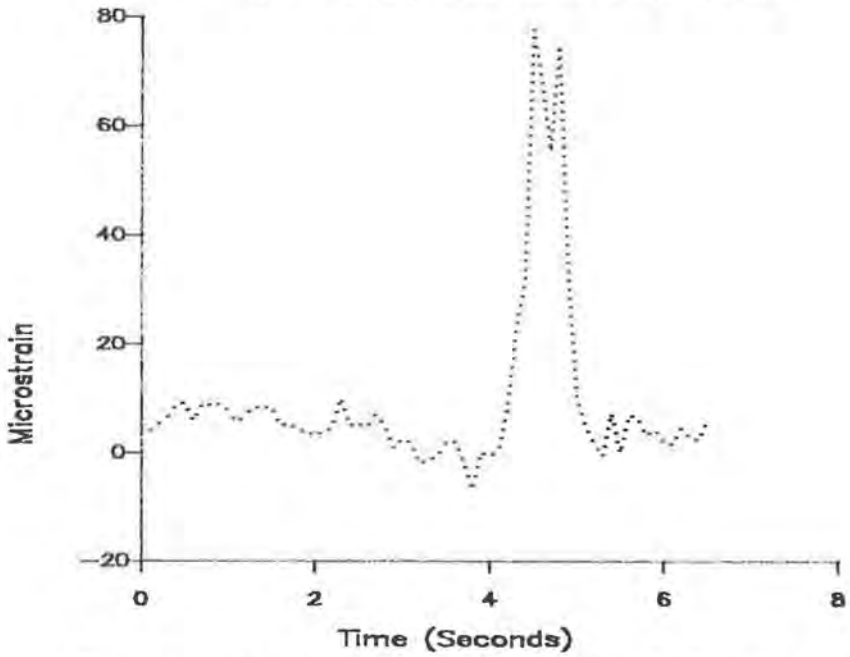

Figure A32. Dynamic Strain from Childersburg Bridge, 44 ft. span, One Truck at 60 mph, Bottom Flange, Girder 3

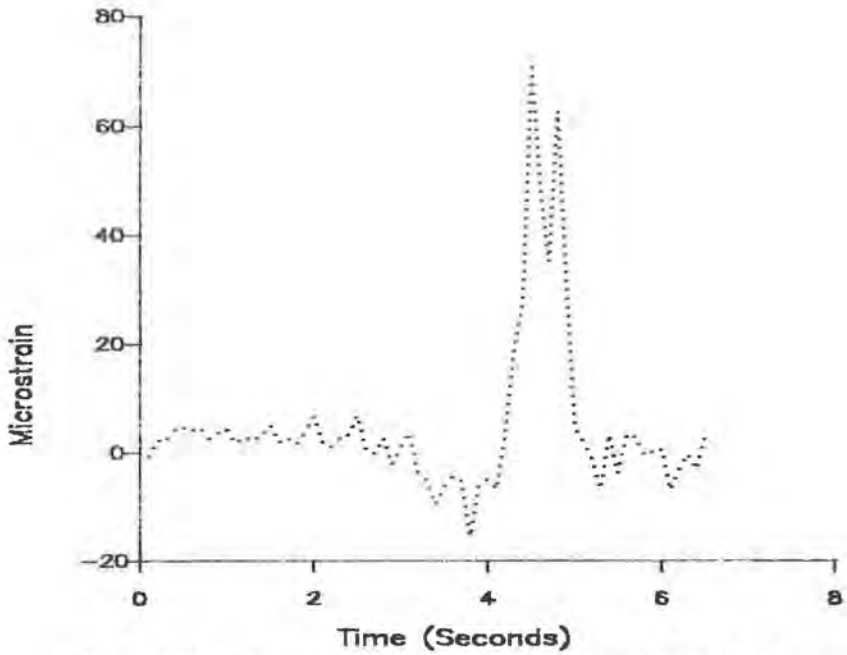

Figure A33. Dynamic Strain from Childersburg Bridge, 44 ft. span, One Truck at 60 mph, Bottom Flange, Girder 4

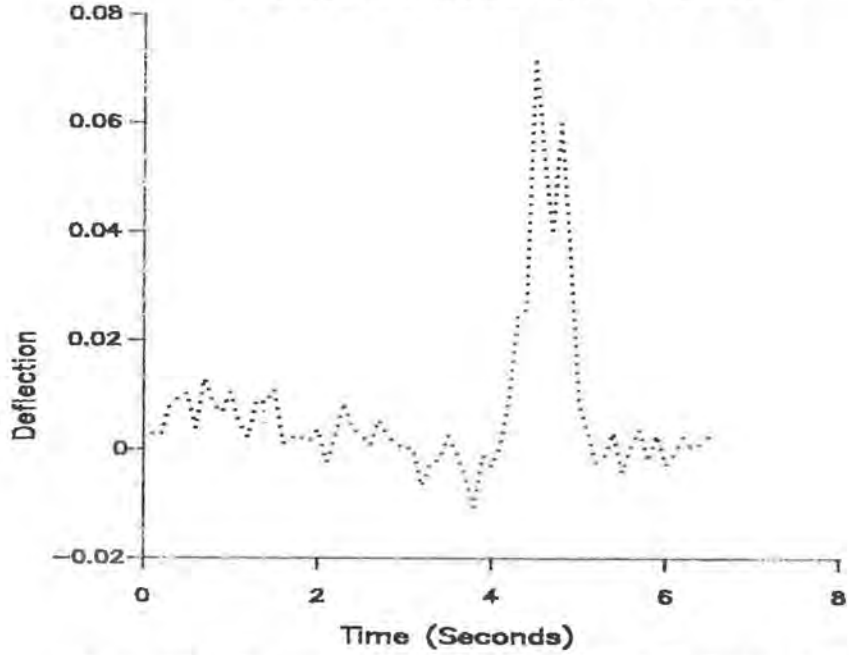

Figure A34. Dynamic Deflection from Childersburg Bridge, 44 ft. span, One Truck at 60 mph, Bottom Flange, Girder 2

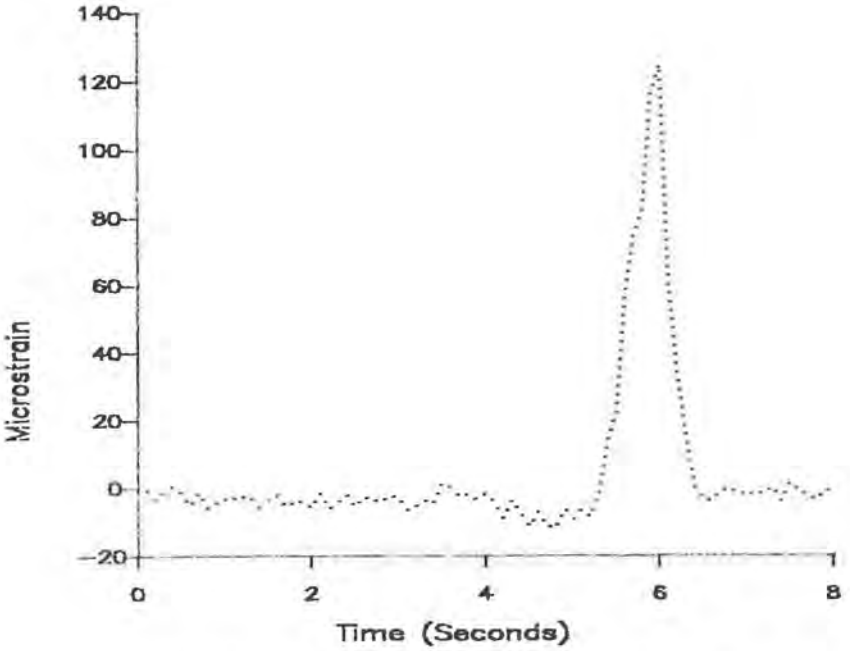

Figure A35. Dynamic Strain from Childersburg Bridge, 44 ft. span, Two Trucks at 40 mph, Bottom Flange, Girder 2

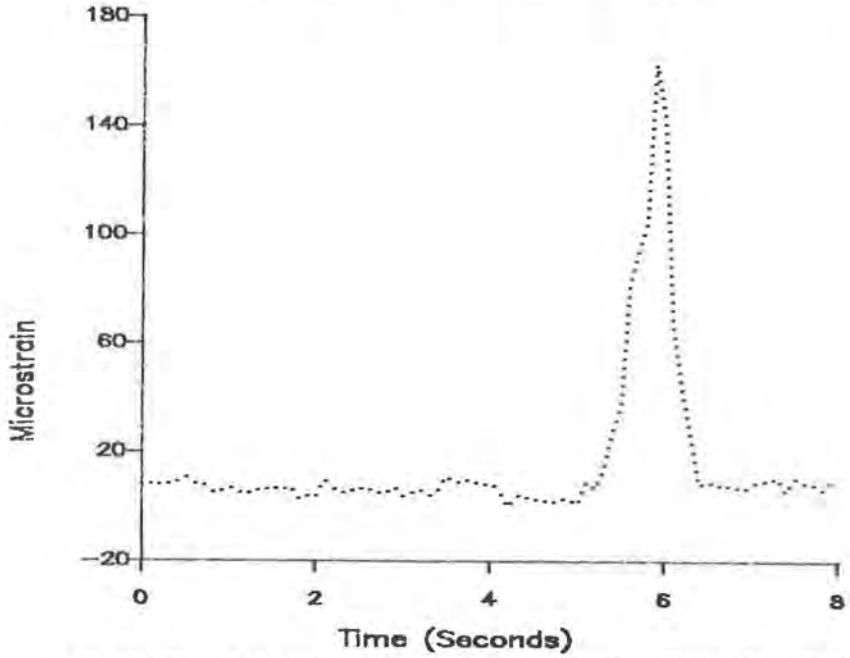

Figure A36. Dynamic Strain from Childersburg Bridge, 44 ft. span, Two Trucks at 40 mph, Bottom Flange, Girder 3

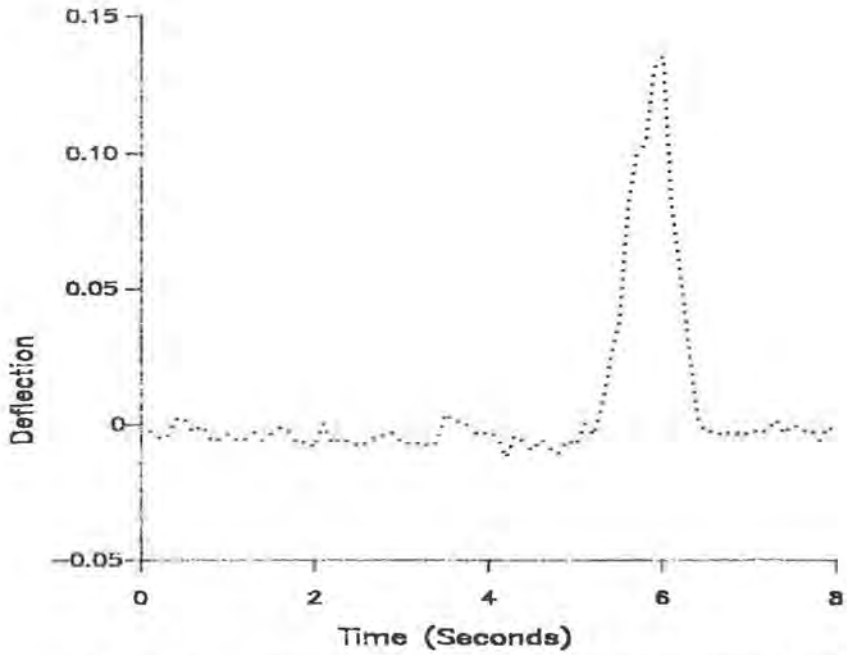

Figure A37. Dynamic Deflection from Childersburg Bridge, 44 ft. span, Two Trucks at 40 mph, Bottom Flange, Girder 2

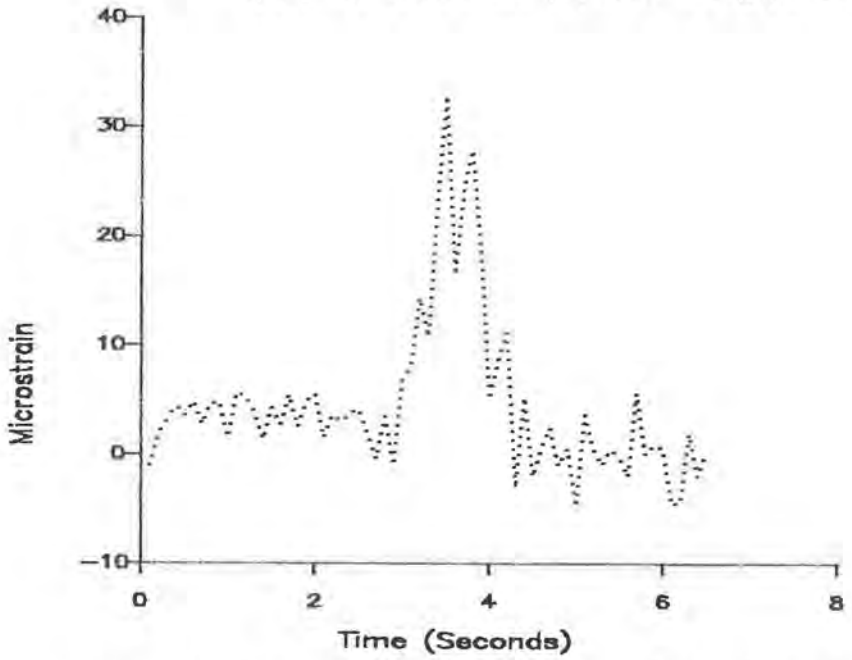

Figure A38. Dynamic Strain from Childersburg Bridge, 77 ft. span, One Truck at 60 mph, Bottom Flange, Girder 1

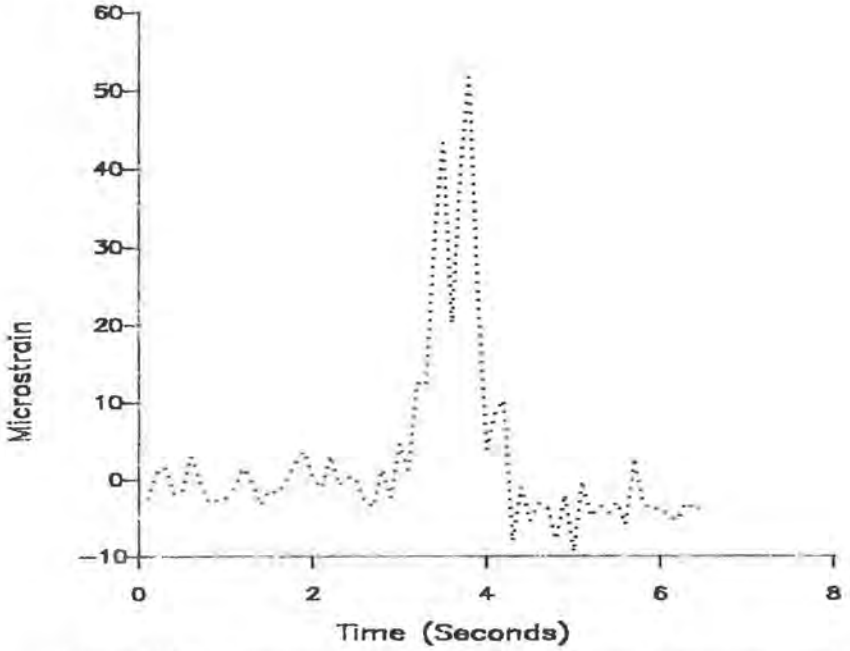

Figure A39. Dynamic Strain from Childersburg Bridge, 77 ft. span, One Truck at 60 mph, Bottom Flange, Girder 2

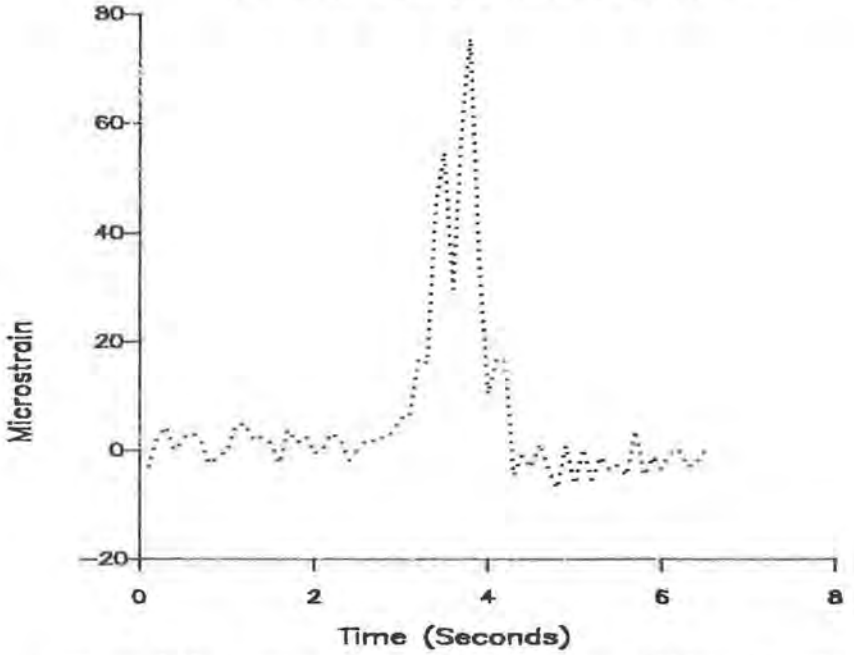

Figure A40. Dynamic Strain from Childersburg Bridge, 77 ft. span, One Truck at 60 mph, Bottom Flange, Girder 3

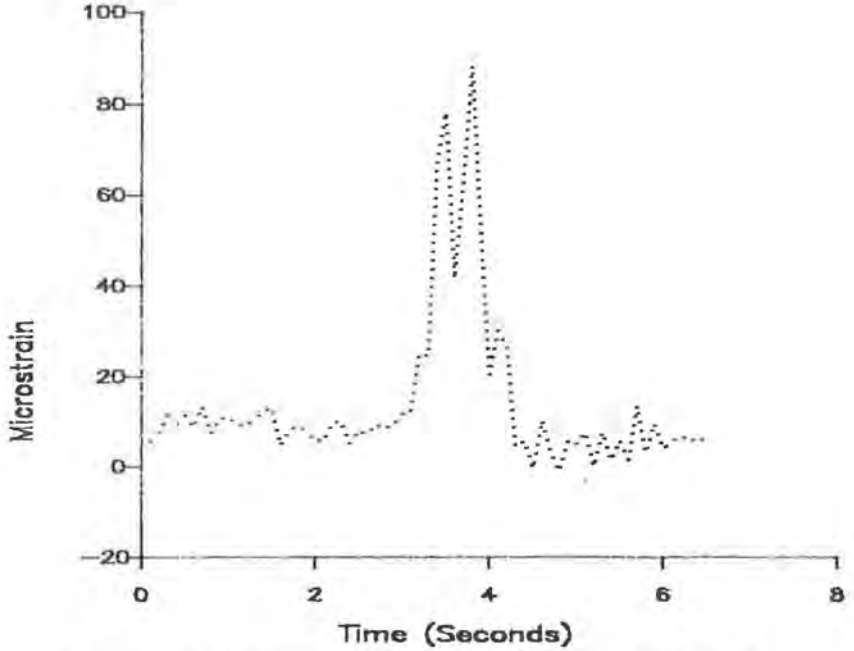

Figure A41. Dynamic Strain from Childersburg Bridge, 77 ft. span, One Truck at 60 mph, Bottom Flange, Girder 4

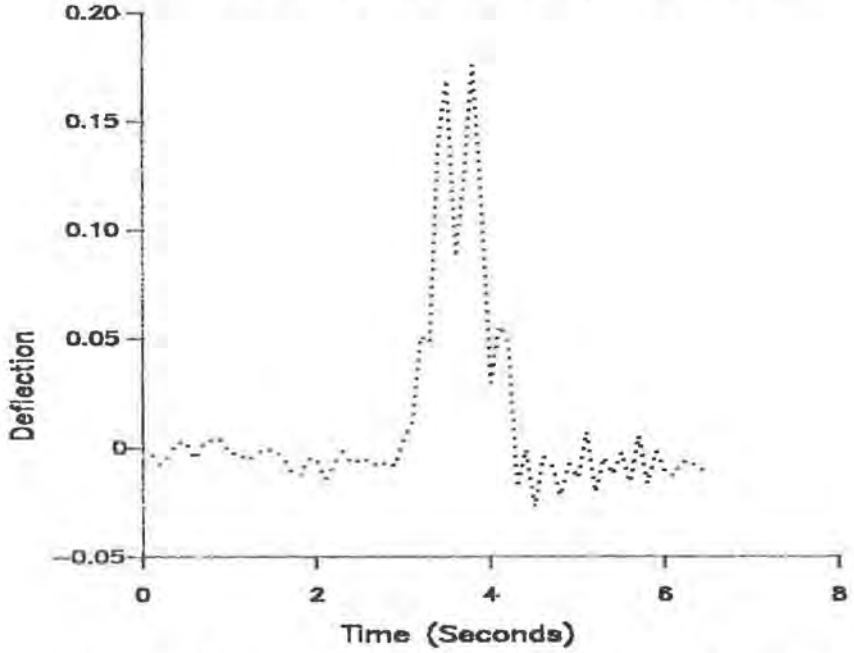

Figure A42. Dynamic Deflection from Childersburg Bridge, 77 ft. span, One Truck at 60 mph, Bottom Flange, Girder 2

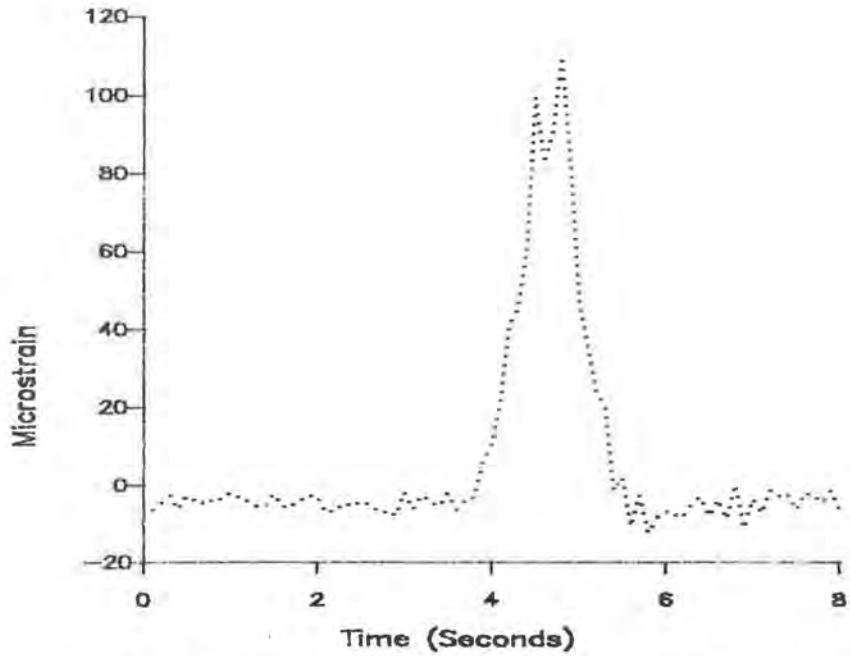

Figure A43. Dynamic Strain from Childersburg Bridge, 77 ft. span, Two Trucks at 40 mph, Bottom Flange, Girder 2

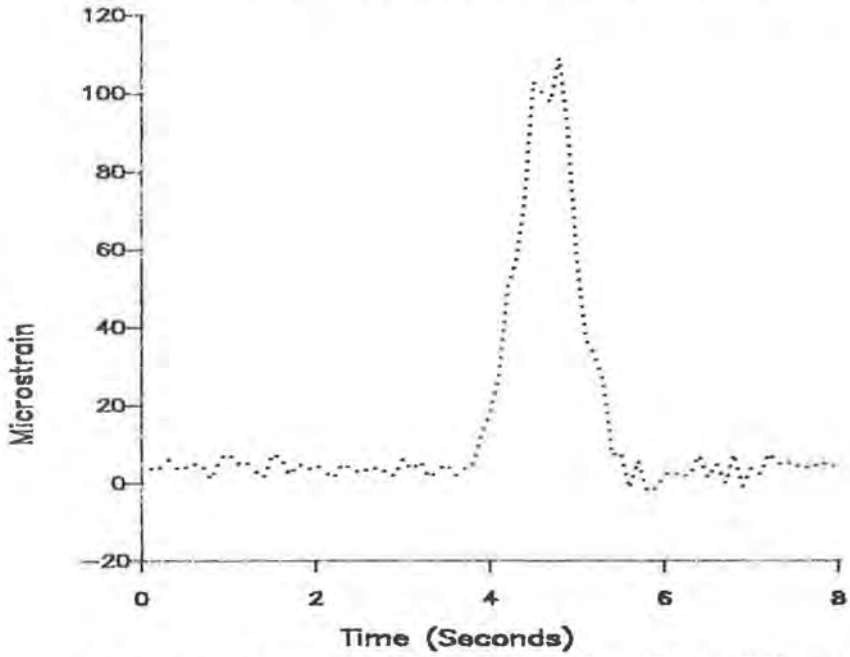

Figure A44. Dynamic Strain from Childersburg Bridge, 77 ft. span, Two Trucks at 40 mph, Bottom Flange, Girder 3

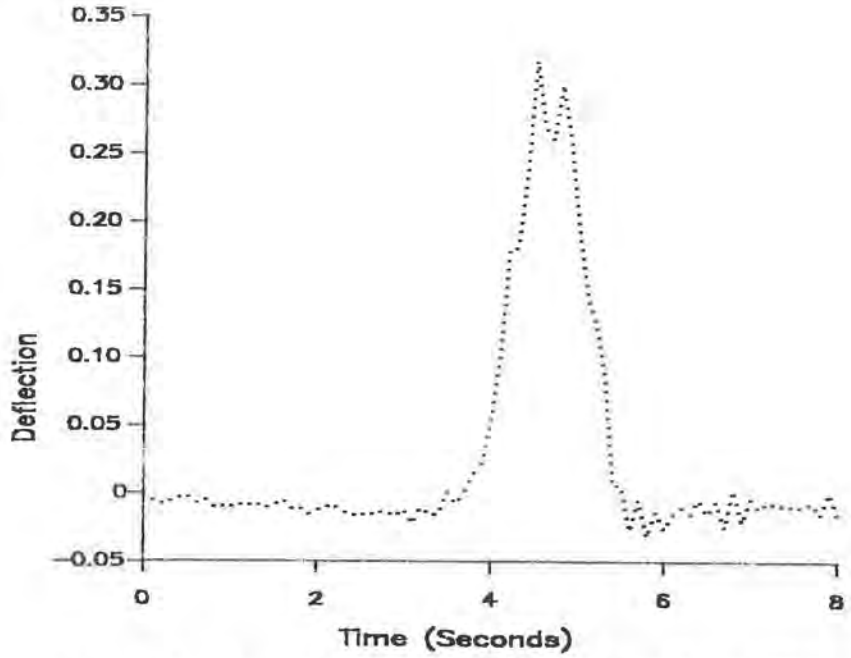

Figure A45. Dynamic Deflection from Childersburg Bridge, 77 ft. span, Two Trucks at 40 mph, Bottom Flange, Girder 2

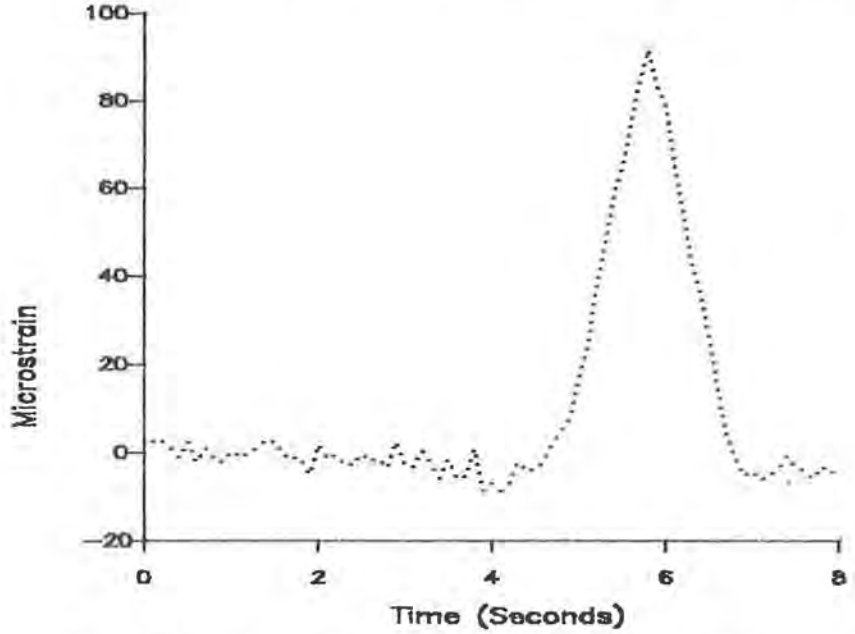

Figure A46. Dynamic Strain from Locust Fork Bridge, 49 ft. span, One Truck at 50 mph, Bottom Flange, Girder 1

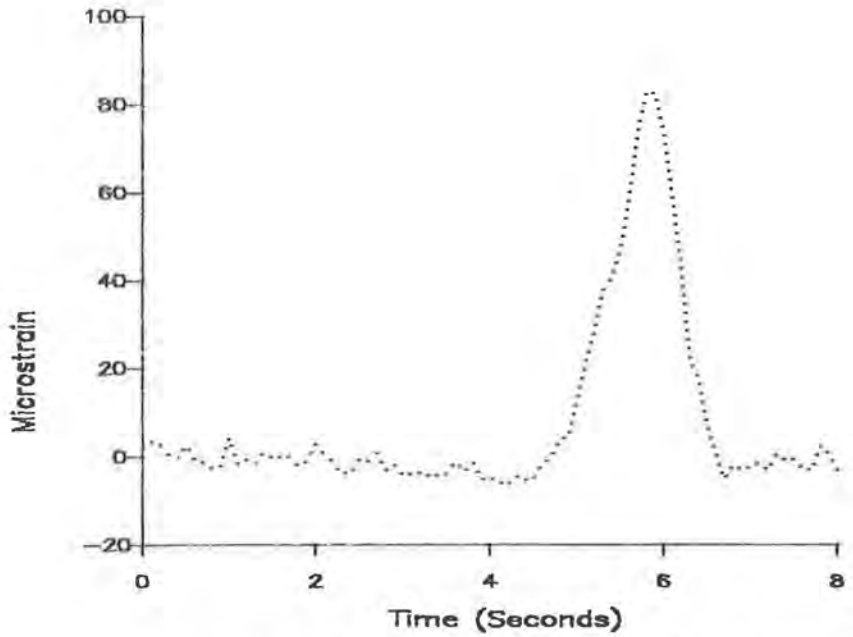

Figure A47. Dynamic Deflection from Locust Fork Bridge, 49 ft. span, One Truck at 50 mph, Bottom Flange, Girder 2

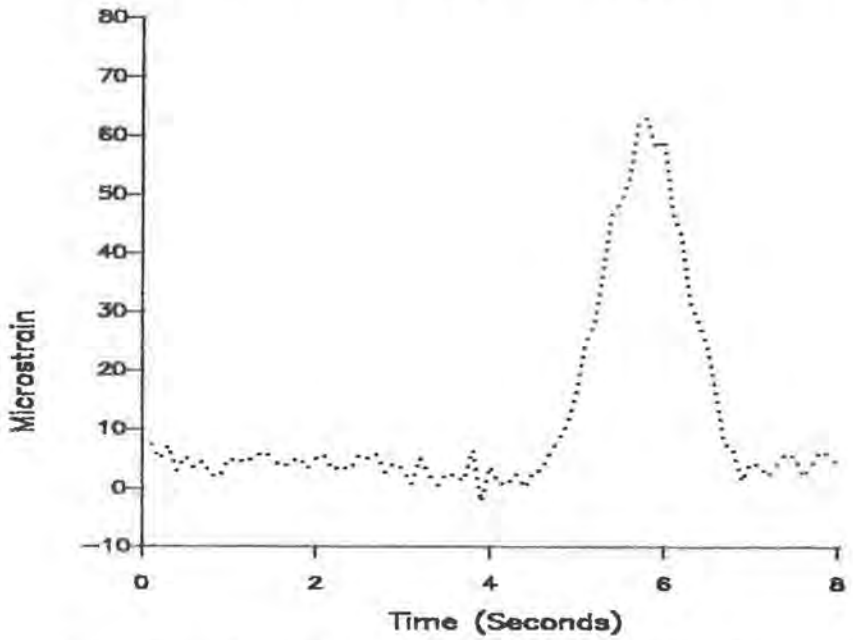

Figure A48. Dynamic Strain from Locust Fork Bridge, 49 ft. span, One Truck at 50 mph, Bottom Flange, Girder 3

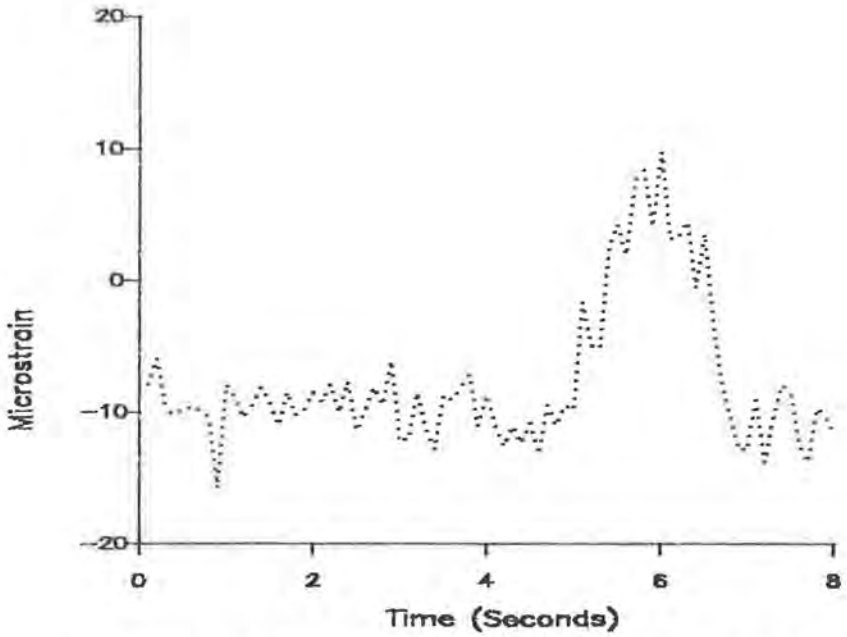

Figure A49. Dynamic Strain from Locust Fork Bridge, 49 ft. span, One Truck at 50 mph, Bottom Flange, Girder 4

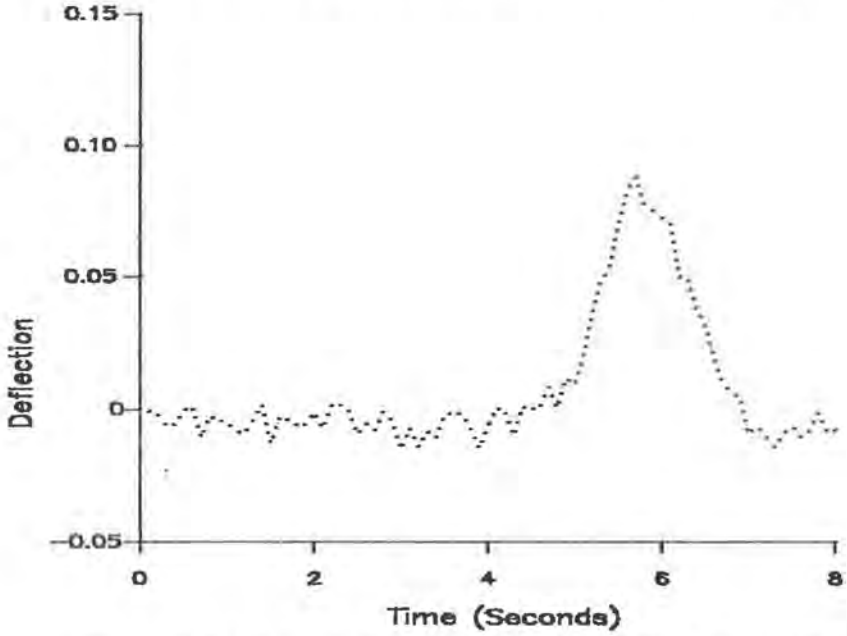

Figure A50. Dynamic Deflection from Locust Fork Bridge, 49 ft. span, One Truck at 50 mph, Bottom Flange, Girder 3

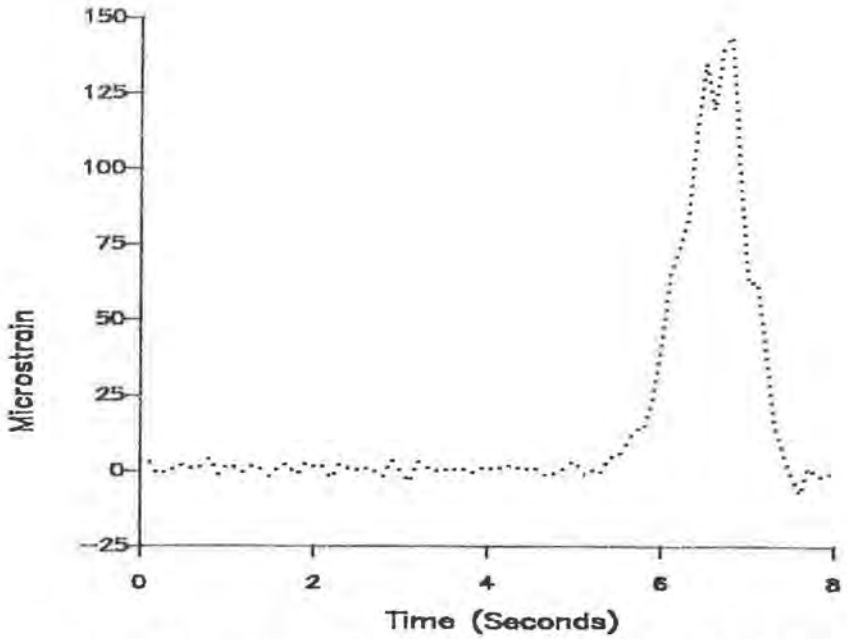

Figure A51. Dynamic Strain from Locust Fork Bridge, 49 ft. span, Two Trucks at 20 mph, Bottom Flange, Girder 2

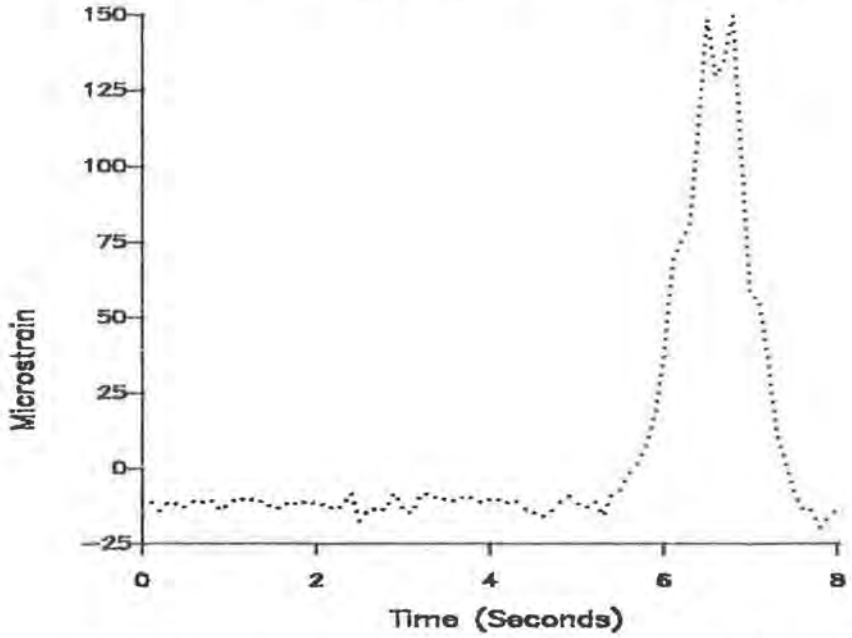

Figure A50. Dynamic Strain from Locust Fork Bridge, 49 ft. span, Two Trucks at 20 mph, Bottom Flange, Girder 3

APPENDIX B

APPENDIX B

Details of Modeling Bridges as Grids

The grid analyses were carried out using a computer program developed by the Principal Investigator, Chai H. Yoo, based on the stiffness method. The grid program follows closely the discussion of grid analysis presented by Weaver and Gere (1990). A listing of the FORTRAN code is given in Appendix E. The grid program requires an input file for each bridge to be anlyzed. The input file contains information about the deck geometry, support conditions, material properties, section properties, and applied loads. Unknown information about the material properties and member details was either assumed or determined from the AASHTO Manual (1983). The following sections outline how the information needed for the grid analyses was determined. Much of the discussion refers to specific requirements of the program listed in Appendix E.

Bridge Deck Geometry

In order to analyze the deck system as a grid, a coordinate system must be defined such that the bridge deck lies in the x-y plane. The deck is then broken up into longitudinal and transverse members. Each row of longitudinal members represents a girder, while each row of transverse members represents a portion of the concrete deck and/or diaphragms.

Jaeger and Bakht (1989) recommend that the decking be represented by at least seven rows of transverse members. Figure B1 depicts a slab on girder bridge with 4 girders and a span length of 120 ft. This model has 4 rows of longitudinal members and 11 rows of transverse members. Each interior transverse member represents a 12 ft. wide strip of the concrete deck, while each exterior transverse member represents a 6 ft. wide strip of the deck.

A skewed bridge should also have transverse members connected to girder. Figure B2 illustrates the suggested model for a skewed bridge with 4 girders and a span length of 150 ft. Notice that it is not possible to connect a transverse member to node 1. The width of concrete deck represented by each transverse member for a skewed bridge is dependent on the location of the transverse member.

Each member in a grid has two nodes. Nodes occur wherever longitudinal members and transverse members end or intersect. All output generated by the grid program, such as member end moments and

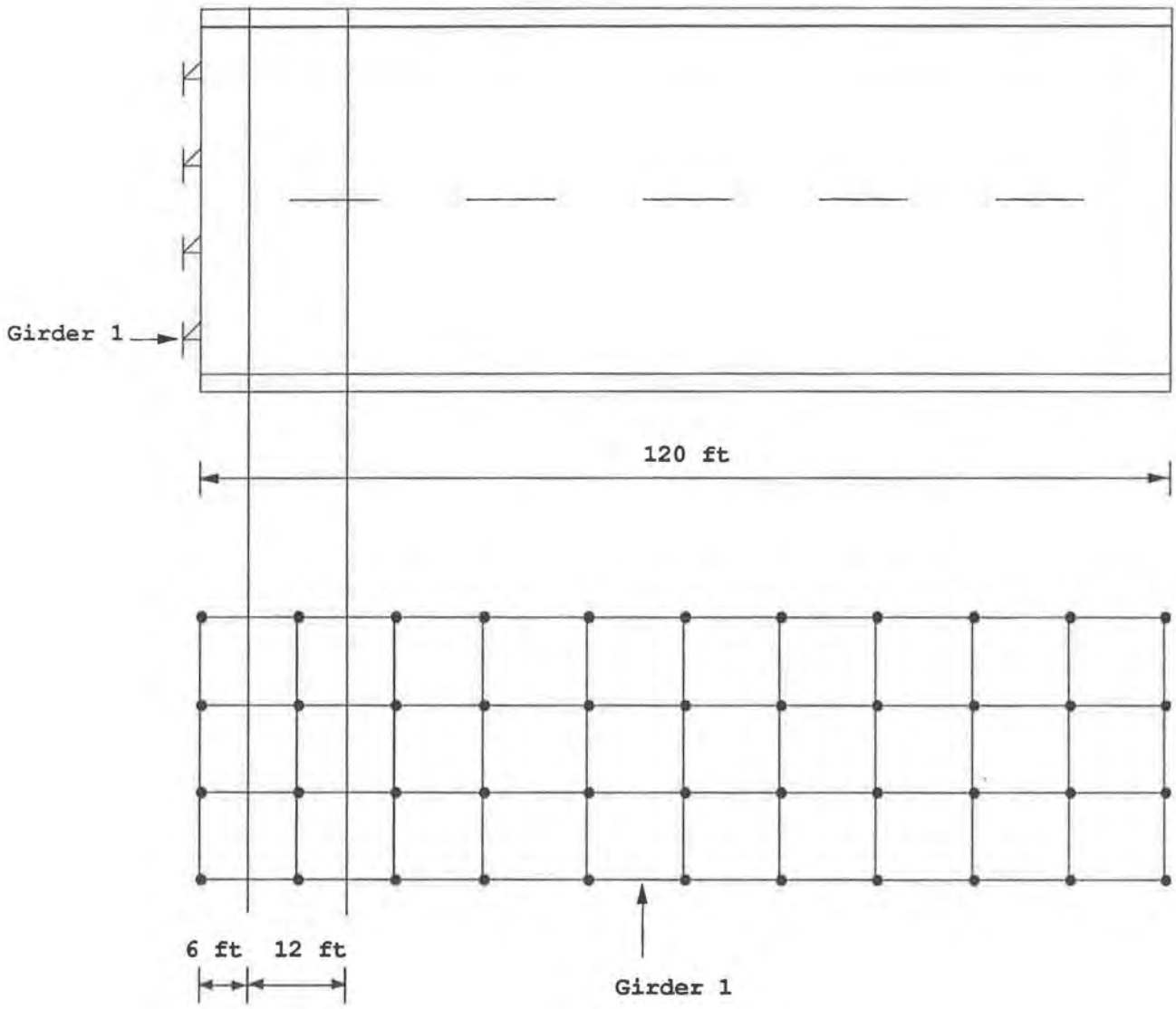

Figure B1. Grid Model for 120 ft Bridge Span

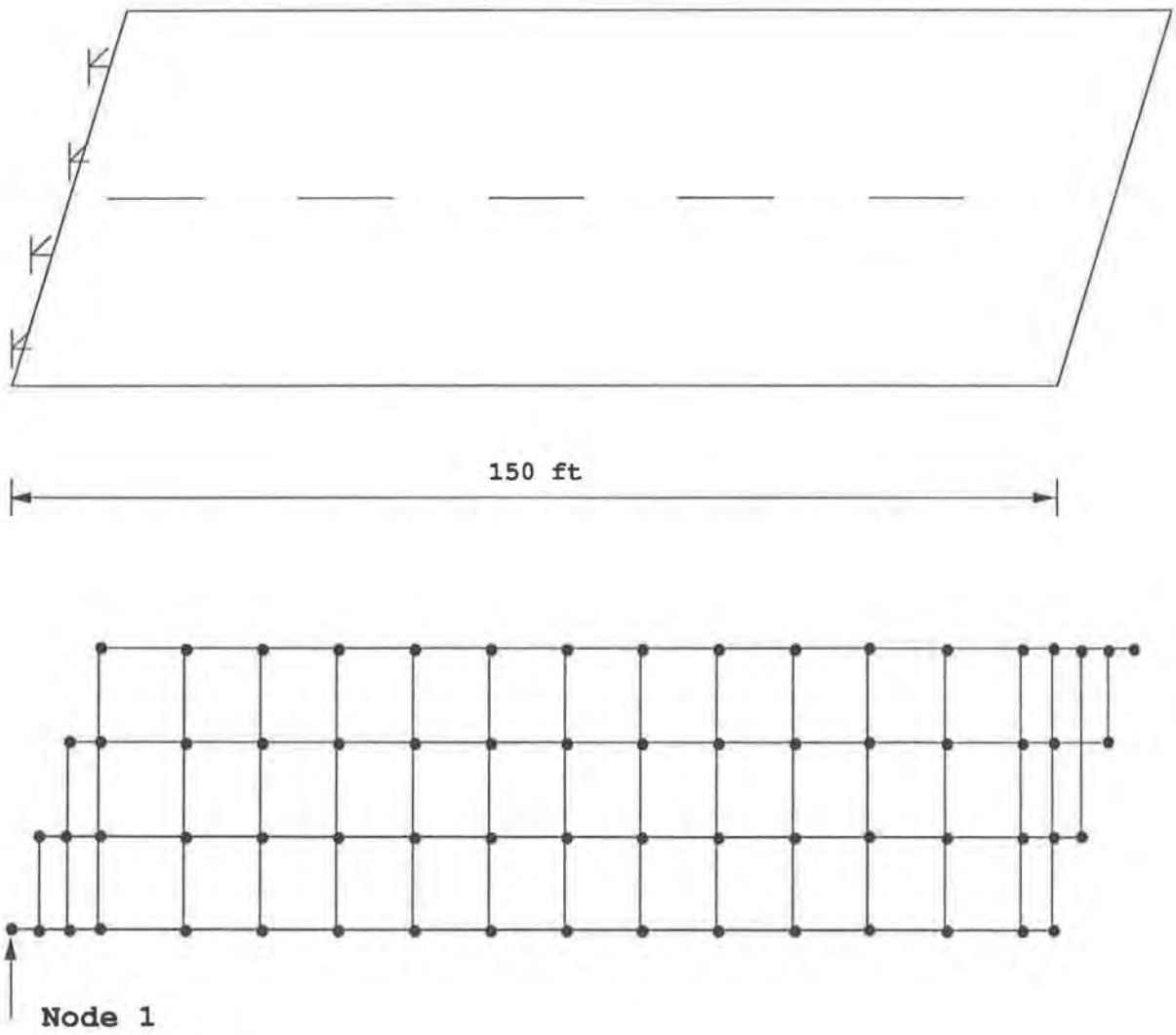

Figure B2. Grid Model for 150 ft Skewed Bridge Span

deflections, is for the nodal locations only. If output is desired at a location other than the intersection of a longitudinal and transverse membr, an extra node must be created. Extra nodes can be placed along a member wherever necessary. Each extra node creates an extra member. Figure B3 illustrates node locations and extra node locations.

The location and number of each node must be provided as input to the grid program. To reduce the computational effort required by the grid analysis, the nodes should be numbered so that the node numbers increase in the direction of the smallest dimension. This numbering scheme will minimize the band width of (or the number of nonzero terms in) the stiffness matrix. An example of proper node numbering is illustrated in Figure B4.

An estimate of the semi-band width, BW, is required input for the grid program. A suitable estimate can be made from

$$BW = 3(ND + 1) \qquad \text{(B1)}$$

where ND is the maximum difference between the node numbers for the ends of any member.

The number and connectivity of each member must be entered into the input file. Member numbering is arbitrary, however, it is desirable to number in a systematic way so that determining the location of each member does not present a problem. Member connectivity refers to the nodes at the end of each member. An example of member numbering is given in Figure B5.

Restrained Degrees of Freedom

As mentioned earlier, each node has a certain number of DOF depending on the type of framed structure. For a grid, each node has 3 DOF. They are translation along the z-axis, rotation about the x-axis, and rotation about the y-axis. These 3 DOF characterize the flexural and torsional deformations experienced by the grid to the applied loads.

A restrained DOF refers to a displacement which is prevented from occurring by restraint. For example consider the idealized roller support used to model the beams resting on the bearings in Figure B6. For the grid, these roller supports restrict translation along the z-axis and rotation about the x-axis, and allow rotation about the y-axis. Therefore the translation along the z-axis and rotation about the x-axis for

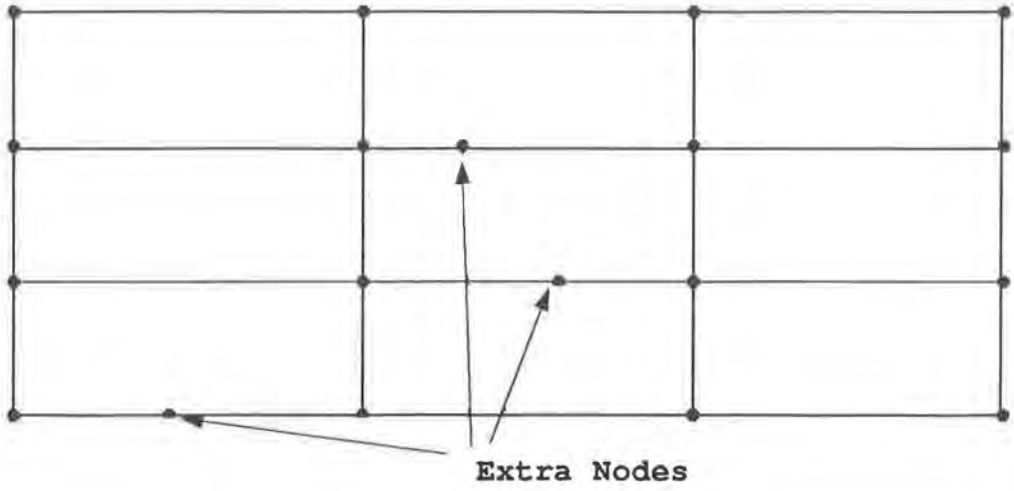

Figure B3. Extra Nodes

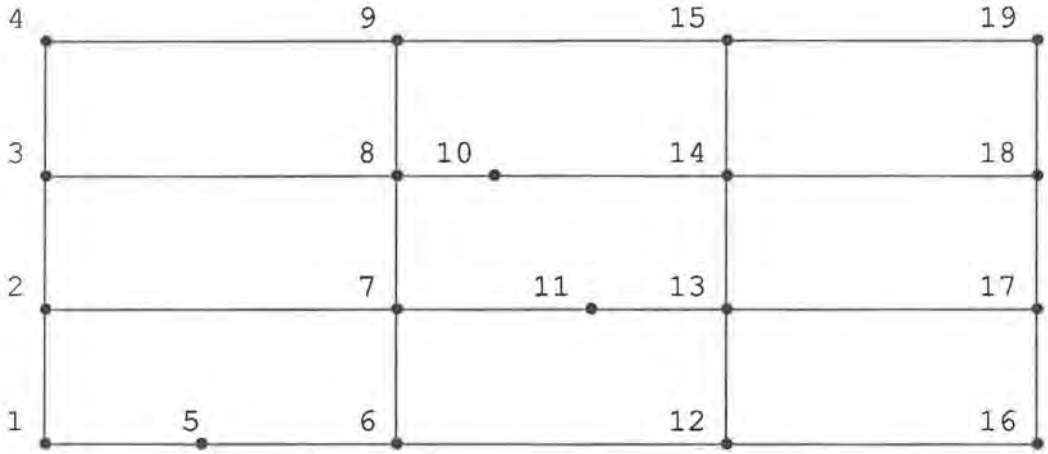

Figure B4. Node Numbering

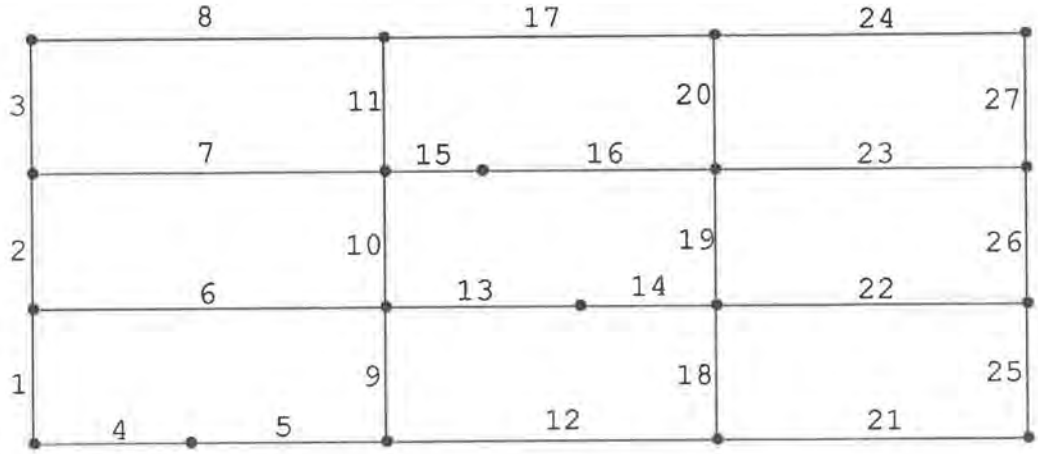

Figure B5. Member Numbering

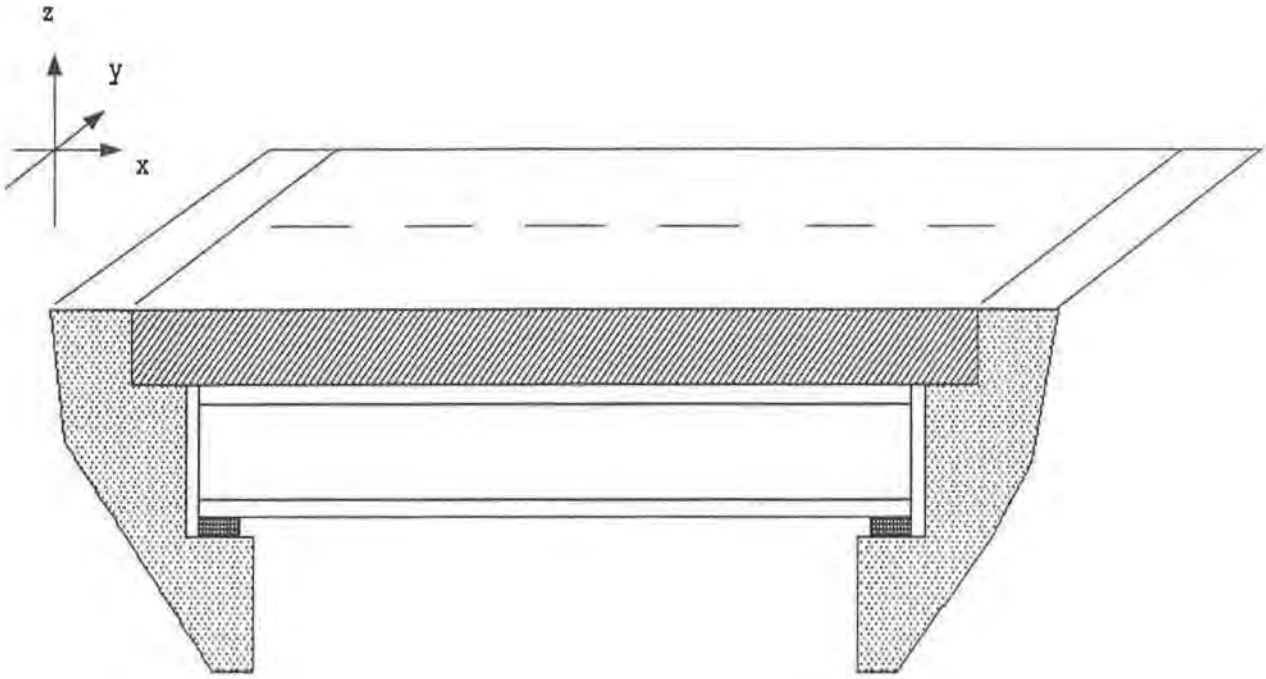

Figure B6. Typical Bridge Girder Supports

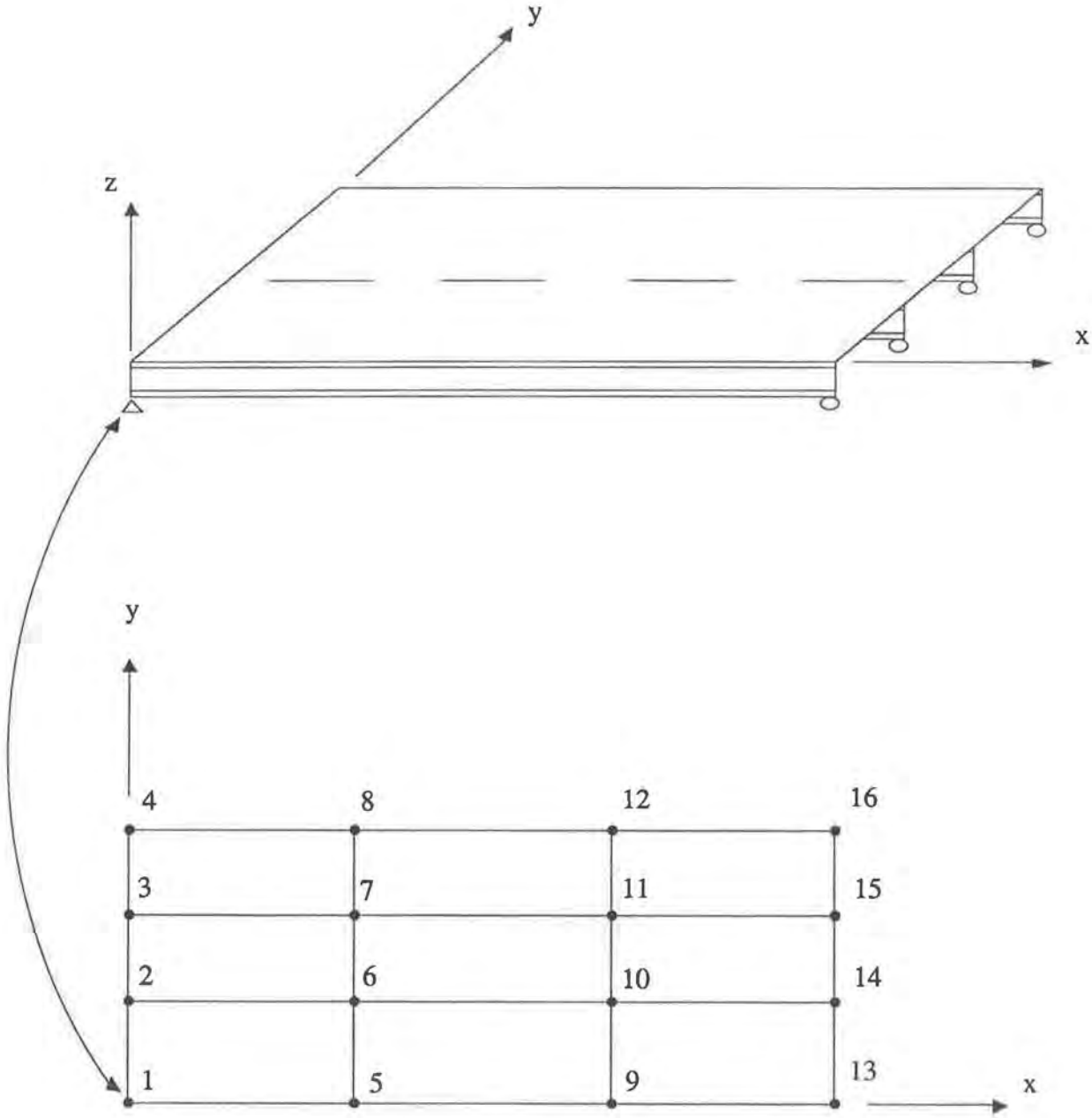

Figure B7. Illustration of the Restrained Nodes and Restrained DOF's

each roller support are assumed to be restrained. The rotation about the y-axis for each roller support is assumed to be unrestrained.

The number of nodes at which DOF are restrained and the total number of DOF restrained for all nodes must be entered into the input file. An example of how to determine these quantities is presented in Figure B7. The grid has a total of 16 nodes and 48 DOF. The eight nodes at the supports have restrained DOF. The x-axis rotation and z-axis translation are restrained at each support. Hence a total of 16 DOF are restrained.

Material Properties

The material properties are either specified in the plans, determined from the AASHTO Manual (1983), or assumed. Material properties are not only needed for the grid program input file, but also for determining section properties.

The analysis of the bridge deck by the grid program requires that the structure consist of only one material. Therefore, the concrete deck area was transformed into an equivalent area of steel using the modular ratio, n, for each bridge. The modular ratio is a function of the concrete strength. Values of n were taken from the AASHTO Specifications (1989). The compressive strength of concrete, f'c is either assumed or determined from the construction details. Once transformed, the section properties in terms of steel are calculated for the longitudinal and transverse members.

Young's Modulus, E, and the shear modulus, G, must be entered into the input file. These were assumed to be 29,000 ksi and 11,540 ksi respectively for steel.

Properties for Longitudinal Members

The moment of inertia and the torsional constant must be input into the program for each longitudinal and transverse member.

The effective width of the concrete deck in the longitudinal direction can be determined using the AASHTO Specifications (1989). For bridges which behave in a non-composite manner, the moment of inertia of the member is simply found by summing the girder moment of inertia and the moment of inertia of the transformed deck area.

For bridges which act in a composite manner, the moment of inertia of the composite section must be calculated. An example of this calculation is presented in Appendix G.

The torsional constant is found by summing the torsional constants of the girder, $k_{t\ girder}$, and the deck, $k_{t\ deck}$. The torsional constant of the deck is calculated after transforming the concrete to steel. An example of this calculation is presented in Appendix G.

Section Properties for Transverse Members

The width of concrete deck used to determine the transverse section properties depends on the length of the bridge and the number of rows of transverse members used. Jaeger and Bakht (1990) suggest using at least seven rows of trnasverse members. Each grid model developed as part of this project was developed using 10 or more rows of transverse members. Before calculating the moment of inertia, the width of the transverse member must be transformed to steel using the modular ratio. An example of this calculation is presented in Appendix G.

The torsional constant was determined by calculating the torsional constant of a rectangular cross section for the transformed area. An example of this calculation is presented in Appendix G.

Applied Nodal Forces

In the development of the model for each bridge, the applied live loads were assumed to be concentrated forces. Each model assumes that the concentrated forces are applied only at the nodes. Therefore these forces must be distributed to the adjacent nodes. The distribution is accomplished using a double interpolation scheme. The effects of twisting moments in the deck were neglected. An example of the distribution of forces to adjacent nodes is illustrated in Figure B8. The total force at each node resulting from multiple applied loads is determined by simply adding the nodal forces resulting from each load.

Example Input File for Grid Program

An example input file for the bridge shown in Figure B9 is shown in Figure B10. The example bridge shown in Figure B9 is used to generate the input file for the grid program in Figure B10. The example bridge deck system is assumed to act in a non-composite manner. The bridge is broken up into a total of 17 members connected by 12 nodes. The exterior transverse members (1, 2, 16, 17) are parallel to

F1 = (((P X b) / l) X d) / w

F2 = (((P X a) / l) X d) / w

F3 = (((P X a) / l) X c) / w

F4 = (((P X b) / l) X c) / w

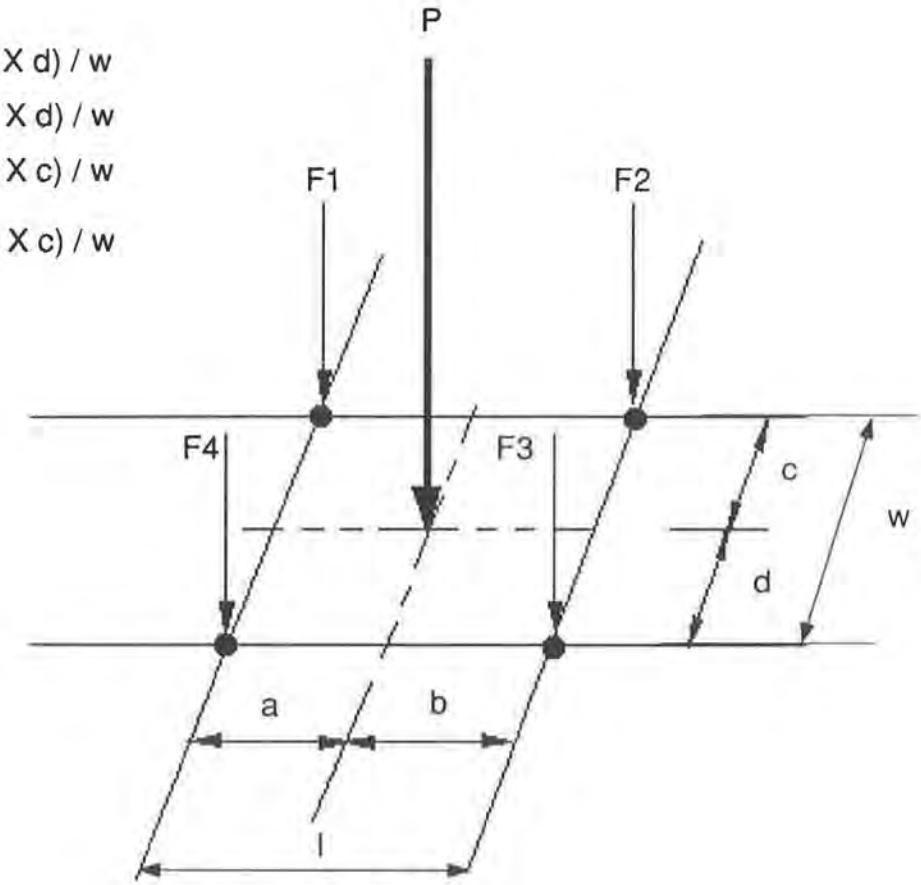

Figure B8. Distribution of an Applied Force to Adjacent Nodes

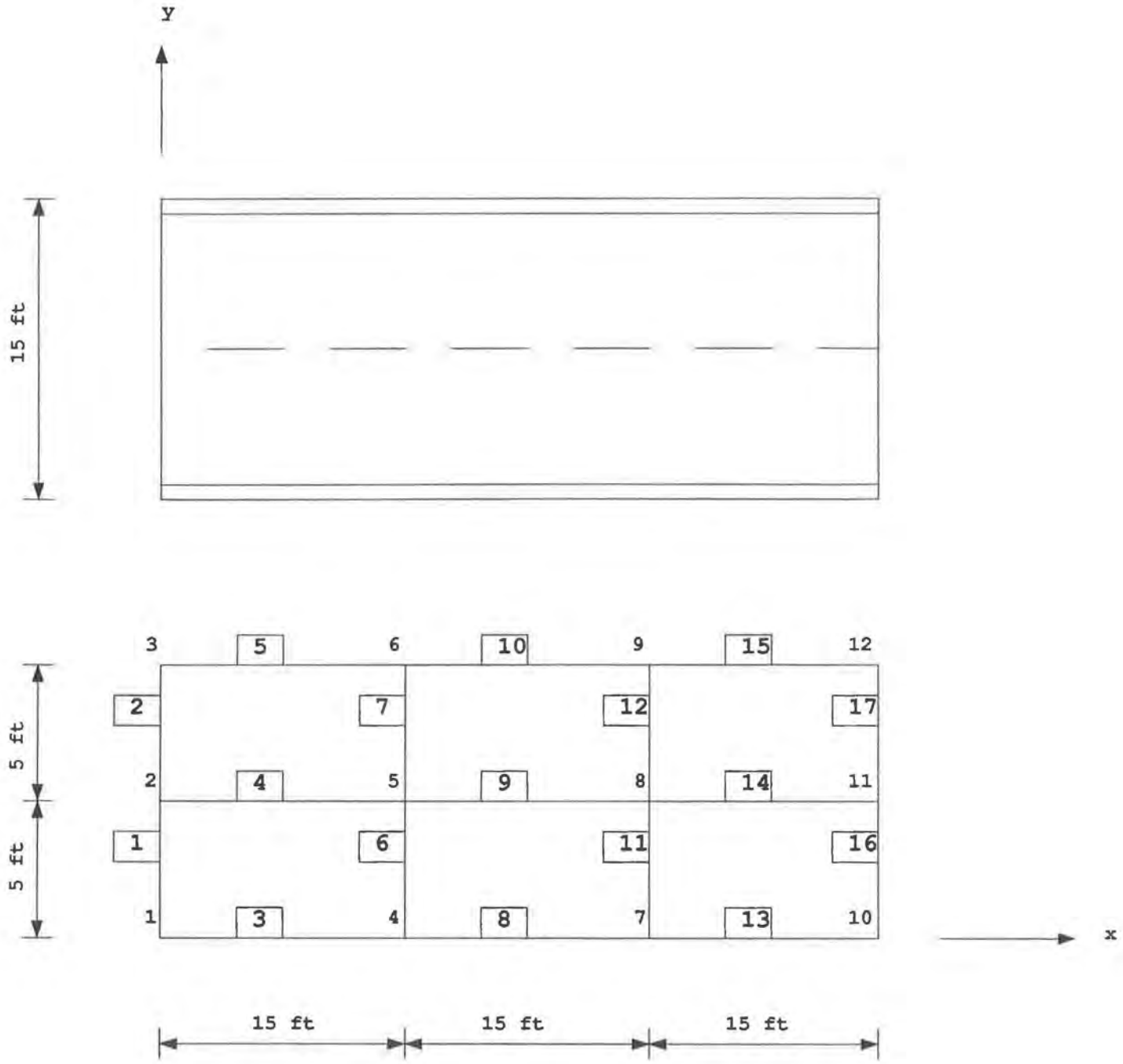

Figure B9. Example Bridge for Grid Program Input.

```
Line 1     Example Bridge (Band Width = (12-9+1) X 3 = 12)
Line 2     17,12,12,6,29000.,11540.,12
Line 3     1,0.0,0.0,
Line 4     2,0.0,60.0,
Line 5     3,0.0,120.0,
Line 6     4,180.0,0.0,
Line 7     5,180.0,60.0,
Line 8     6,180.0,120.0,
Line 9     7,360.0,0.0,
Line 10    8,360.0,60.0,
Line 11    9,360.0,120.0,
Line 12    10,540.0,0.0,
Line 13    11,540.0,60.0,
Line 14    12,540.0,120.0,
Line 15    1,1,2,140.0,12.5,
Line 16    2,2,3,140.0,12.5,
Line 17    3,1,4,220.0,450.0,
Line 18    4,2,5,220.0,450.0,
Line 19    5,3,6,220.0,450.0,
Line 20    6,4,5,280.0,25.0,
Line 21    7,5,6,280.0,25.0,
Line 22    8,4,7,220.0,450.0,
Line 23    9,5,8,220.0,450.0,
Line 24    10,6,9,220.0,450.0,
Line 25    11,7,8,280.0,25.0,
Line 26    12,8,9,280.0,25.0
Line 27    13,7,10,220.0,450.0,
Line 28    14,8,11,220.0,450.0,
Line 29    15,9,12,220.0,450.0,
Line 30    16,10,11,140.0,12.5,
Line 31    17,11,12,140.0,12.5,
Line 32    1,1,0,1,
Line 33    2,1,0,1,
Line 34    3,1,0,1,
Line 35    10,1,0,1,
Line 36    11,1,0,1,
Line 37    12,1,0,1,
Line 38    1,
Line 39    9,0,
Line 40    4,0.,0.,-6.4,
Line 41    5,0.,0.,-8.5,
Line 42    6,0.,0.,-6.4,
Line 43    7,0.,0.,-7.4,
Line 44    8,0.,0.,-9.8,
Line 45    9,0.,0.,-7.4,
Line 46    10,0.,0.,-0.6,
Line 47    11,0.,0.,-0.9,
Line 48    12,0.,0.,-0.6,
```

Figure B10. Grid Program Input File for Example Bridge

the y-axis and represent a 7.5 ft portion of concrete deck. These members have a moment of inertia of 12.5 in^4 and a torsional constant of 140 in^4. The interior transverse members (6, 7, 11, 12) are also parallel to the y-axis and represent a 15 ft portion of concrete deck. These members have a moment of inertia of 25 in^4 and a torsional constant of 280 in^4. The longitudinal members parallel to the x-axis represent the girders. Each girder has a moment of inertia of 450 in^4 and a torsional constant of 10 in^4. The grid has six restrained nodes (1, 2, 3, 10, 11, 12). The DOF restrained at each restrained node are rotation about the x-axis and translation along the z-axis. Therefore, there are 12 DOF restrained.

Preceding each line of input data in Figure B10 is a line number. This line number will be used to refer to a specific line of data in order to explain that line of data. This line number is not part of the grid program input file, and should not be included in any generated input file for the grid program.

Line 1 displays the title of the problem, which can be sixty characters long. Line 2 indicates the number of members, the number of nodes, the number of restrained DOF's, the number of nodes with restrained DOF, Young's Modulus in ksi, the shear modulus in ksi, and the semi-band width.

Lines 3 through 17 display nodal information. Each of these lines contains the assigned node number, the x-axis coordinate in inches and the y-axis coordinate in inches. Notice that lines 9 through 11 represent nodes which are not connected to transverse members. These extra nodes can be used to read information at each node's location. Each extra node, however, creates an extra member.

Lines 18 through 37 display member information. Each of these lines contains the assigned member number, the beginning node number, the ending node number, the torsional constant, and the moment of inertia.

Lines 38 through 43 display information regarding the nodes with restrained DOF. Each of these lines contains the number of the node, whether or not rotation about the x-axis is restrained, whether or not rotation about the y-axis is restrained, and whether or not translation along the z-axis is restrained. A restrained DOF is indicated with a 1, and an unrestrained DOF is indicated by a 0.

Lines 44 through 54 display information regarding loading information. Line 44 determines the number of loading cases. Line 45 informs the program of the number of loaded joints, and the number of loaded members. Loads were applied only to the nodes using the double interpolation scheme.

Therefore the number of loaded members was always zero. Lines 46 through 54 contain information about the number of the loaded nodes, the magnitude and direction of the moment about the x-axis, the magnitude and direction of the moment about the y-axis, and the magnitude and direction of the force along the z-axis. Since the transfer of moments was neglected, the magnitude of the applied moments at each node was always zero.

APPENDIX C

APPENDIX C

EXAMPLE AASHTO RATING

The following steps outline the procedure for rating the 34 ft. span of the Mulberry Fork Bridge based on the method described in the AASHTO manual (1983).

1. Establish allowable stresses.

Inventory	Operating	
F_y = 33,000 psi	F_y = 33,000 psi	MMIB 5.4.2
F_b = 18,000 psi	F_b = 24,500 psi	MMIB 5.4.2A

2. Establish section properties.

Girder: W 24 X 90

Concrete Slab: d = 6.75"

Neutral Axis: y = 12.125"

Inertia: I = 2700 in^4

Section Modulus: S = 220.9 in^3

3. Calculate dead loads.

Weight of slab: 2080.7 lbs/ft

Weight of curbs and railings: 639.1 lbs/ft

Weight per girder: (2080.7 lbs/ft + 639.1 lbs/ft) / 4 = 680 lbs/ft

Weight of girder: 90 lbs/ft

Total weight per girder: 770 lbs/ft — AASHTO 3.3.6

AASHTO 3.23.2.3.1.1

4. Calculate moment due to dead loads.

Note that this dead load moment is slightly larger than the moments at the actual locations of the various maximum live load moments.

M_{DL} = 111 kip-ft ($wL^2/8$)

5. Calculate Impact Factor.

I = 50 / (34 + 125) = .31 --> .3 AASHTO 3.8.2.1

IF = 1 + I = 1.3

6. Calculate live load Distribution Factor.

S = 7 / 5.5 = 1.27 AASHTO 3.23.2.3.1.5

7. Calculate live load moments for standard trucks.

Live load moments were calculated using statics. M_{LL} is the moment caused by the one wheel line of the standard truck. M_{AL} is the AASHTO live load moment. MMIB 5.2.3

AASHTO 3.23.2

AASHTO 3.11

M_{AL} = M_{LL} X Impact Factor X Distribution Factor

Two Axle: M_{AL} = 137.7 kip-ft X 1.3 X 1.27 = 227.3 kip-ft

Tri Axle: M_{AL} = 371.5 kip-ft

Concrete Truck: M_{AL} = 330.8 kip-ft

Type 3S2 (AL): M_{AL} = 241.5 kip-ft

H20-44: M_{AL} = 234.4 kip-ft

School Bus: M_{AL} = 112.3 kip-ft

8. Calculate live load member capacity.

$M_{cap} = (F_b \times S) / 12 - M_{DL} = (24.5 \text{ ksi} \times 220.9 \text{ in}^3) / 12 - 111.8 \text{ kip-ft} = 339 \text{ kip-ft}$

9. Calculate AASHTO Operating ratings.

Truck Rating: $M_{cap} / M_{AL} \times$ (Std Truck Wt)

Two Axle: 339 kip-ft / 227.3 kip-ft X 25 tons = 37 tons

Tri Axle: 34 tons

Concrete Truck: 33 tons

Type 3S2(AL): 56 tons

H20-44: 28 tons

School Bus: 37 tons

APPENDIX D

APPENDIX D

EXAMPLE GRID RATING

The following steps outline the procedure used to rate the Mulberry Fork Bridge 34 ft span by the Grid analysis. Included in Appendix B is an example input and the source code for the grid analysis program, GRIDDBL.FORT is included in Appendix F.

1. Define a coordinate system such that the bridge deck is located in the x-y plane.

2. Break the bridge up into longitudinal members and transverse members.

3. Define the coordinates of each node (a node is located at each end of every member), and assign a number to each node.

4. Define each member by specifying the member number, a beginning node and ending node.

5. Calculate section properties needed for each member type.

   a) Longitudinal members

      Interior Girders - non composite

      $I = I_{deck} + I_{girder} = 34.4\ in^4 + 2683\ in^4 = 2717.4\ in^4$

      $k_t = k_{t\ deck} + k_{t\ girder} = 956.5\ in^4 + 5.3\ in^4 = 961.8\ in^4$

      Exterior Girders - composite

      $I = 8205.2\ in^4$

      $k_t = 1441.6\ in^4$

   b) Transverse members

      The width of most transverse members for the Mulberry Fork Bridge 34 ft. span is 4.4 ft. or 52.8 in. and the depth of each transverse member was 6.75 in.

$I = 29.3\ in^4$

$k_t = 820.0\ in^4$

6. Determine the restrained Degrees of Freedom (DOF)

The 34 ft. span is simply supported. The four girders are represented by four rows of longitudinal members. There are eight restrained nodes in the model, one at the end of each girder. Each node has two DOF restrained for a total of 16 DOF restrained.

7. Determine applied loads on each node.

8. Create an input file based on the grid model of the bridge for the grid program.

9. With the output from the grid program establish the inventory and operating ratings based on the moment capacity of the bridge.

$M_{abs\ max}$ is the absolute maximum moment which occurs in each girder. $M_{abs\ max}$ is calculated for each truck loading by the grid program and presented in the output.

10. Grid Operating Ratings:

M_{cap} (interior grider) = f_{all} X S - M_{DL}

M_{cap} = [(24.5 ksi X 220.9 in^3) - 1335 kip-in] / 12 = 340 kip-ft

Rating = M_{cap} / (1.3 X M_{grid}) X (Standard Truck Weight)

Two Axle = 340 kip-ft / (1.3 X 115 kip-ft) X 25 tons = 56 tons

Tri Axle: 57 tons

Concrete Truck: 52 tons

Type 3S2(AL): 79 tons

H20-44: 43 tons

School Bus: 60 tons

APPENDIX E

APPENDIX E

EXAMPLE TEST RATING

The following steps outline the procedure used to rate the Mulberry Fork 34 ft span using the test data and grid analyses.

1. Determine s_{all} from AASHTO Manual (1983)

$$s_{all} = 24.5 \text{ ksi}$$

2. Determine s_{dl} from estimated dead loads. Assume the girders carry the total dead load. If the bridge span is continuously supported, determine where the combination of live load and dead load stresses are greatest.

Estimated Dead Load = 770 lbs/ft

M_{dl} = 111 kip-ft ($wL^2/8$)

$s_{dl} = M_{dl} \times 12 \text{ in/ft} / S = 111 \text{ kip-ft} * 12 \text{ in/ft} / 220.9 \text{ in}^3 = 6.0 \text{ ksi}$

3. Determine s_{ll} from the table of measured stationary strains. The girder with the largest σ_{ll} is the controlling girder.

$s_{ll} = 137 \times 10^{-6}$ (Girder 3)

4. Compare the measured impact factor of the controlling girder with the calculated AASHTO impact factor, IF. Use the larger of the two.

AASHTO IF = 1.30 <-- Use in Eq. 2

5. Using the best grid model, determine M_{test} in the controlling girder positioning the test trucks on the model in the exact same manner they were placed on the bridge during the stationary test which produced the largest live load stress.

Stationary test = two trucks side by side

M_{test} = 100 kip-ft (Girder 3)

6. Using equation 2, calculate M_{cap} for the bridge span.

$$M_{cap} = \frac{24.5 \text{ ksi} - 6.0 \text{ ksi}}{1.3 \times 4.0} \times 100 \text{ kip-ft} = 356 \text{ kip-ft}$$

7. Using the best grid model, determine $M_{abs\ max}$ by positioning the standard trucks on the bridge to create the absolute maximum moment in the bridge.

Two Axle ($M_{abs\ max}$) = 115 kip-ft

Tri-Axle = 171 kip-ft

Concrete Truck = 166 kip-ft

3S2 (AL) = 131 kip-ft

H20-44 = 120 kip-ft

School Bus = 54 kip-ft

8. Using equation 1, calculate the rating of the bridge span.

Two Axle = kip-ft / 115 kip-ft X 25 tons = 77 tons

Tri-Axle = 78 tons

Concrete Truck = 70 tons

3S2 (AL = 108 tons

H20-44 = 59 tons

School Bus = 82 tons

APPENDIX F

APPENDIX F

GRIDDBL.FORT SOURCE CODE

```
      IMPLICIT REAL*8 (A-H,O-Z)
      REAL TIT(20),AA(140000)
      DIMENSION A(1),K(1)
C
C     TIT=ALPHNUMERIC CHARACTER STRING OF 80
C     M=NUMBER OF MEMBERS
C     NJ=NUMBER OF JOINTS
C     NR=NUMBER OF SUPRESSED KINEMATIC DOF
C     NRJ=NUMBER OF RESTRICTED JOINTS (SUPPORTS)
C     E=MODULUS OF ELASTICITY
C     G=SHEAR MODULUS
C     IBW=BANDWIDTH OF ASSEMBLED STRUCTURAL STIFFNESS MATRIX
C     X=X-COORDINATE
C     Y=Y-COORDINATE
C     JJ=NEAR END JOINT NUMBER
C     JK=FAR END JOINT NUMBER
C     KT=ST. VENANT TORSIONAL CONSTANT
C     FIY=MOMENT OF INERTIA
C     JRL=INDICATOR OF RESTRAINT. IF RESTRAINED, =1, OTHERWISE, =0
C     NLCASE=NUMBER OF LOADING CASES
C     NLJ=NUMBER OF LOADED JOINTS
C     NLM=NUMBER OF LOADED MEMBERS
C     A(3*K-2)=VERTICAL LOAD APPLIED AT A JOINT
C     A(3*K-1)=TORQUE
C     A(3*K)=BENDING MOMENT
C     AML(I,1)=EQ. VERTICAL LOAD AT JJ DUE TO LOAD IN A MEMBER
C     AML(I,2)=EQ. TORQUE
C     AML(I,3)=EQ. BENDING MOMENT
C     AML(I,4)=EQ.VERTICAL LOAD AT JK DUE TO LOAD IN A MEMBER
C     AML(I,5)=EQ. TORQUE
C     AML(I,6)=EQ. BENDING MOMENT
```

```
C
C
C       FOR MORE INFORMATION ABOUT THIS PROGRAM, SEE "ANALYSIS OF
C       FRAMAED STRUCTURES' BY GERE AND WEAVER, VAN NOSTRAND, 1965
C
C
      COMMON AA
      COMMON/SETUP/N,M,NJ,NR,NRJ,E,G,IBW,NTDF
      EQUIVALENCE (AA(1),A(1)),(AA(1),K(1))
 9999 READ(5,501,END=9997) (TIT(I), I=1,20)
  501 FORMAT(20A4)
      WRITE(6,601) (TIT(I), I=1,20)
  601 FORMAT(1H1,20A4)
C 500 FORMAT(2I5)
      READ (5,*) M,NJ,NR,NRJ,E,G,IBW
C 502 FORMAT (4I5,2G10.0,I5)
      NDJ=3
      N=NDJ*NJ-NR
      NDF=3*NJ-NR
      NTDF=3*NJ
      N1=1
      N2=N1+NDF
      N3=N2+IBW*NDF
      N4=N3+NJ
      N5=N4+NJ
      N6=N5+M
      N7=N6+M*9
      N8=N7+M
      N9=N8+M
      N10=N9+NTDF
      N11=N10+NTDF
      N12=N11+NTDF
      N13=N12+M*6
      N14=N13+NTDF
      N15=(N14+NTDF)*2-1
      N16=N15+M
      N17=N16+M
      N18=N17+NTDF
      N19=N18+NTDF
```

```
      NSIZE=N19+M
      WRITE(6,610) NSIZE
  610 FORMAT(//5X,'TOTAL BLANK COMMON ARRAY',I6//)
      IF(NSIZE.GT.140000) GO TO 999
      CALL MAINN (A(N1),A(N2),A(N3),A(N4),A(N5),A(N6),A(N7),A(N8),
     *A(N9),A(N10),A(N11),A(N12),A(N13),A(N14),K(N15),K(N16),K(N17),
     *K(N18),K(N19))
      GO TO 9999
  999 WRITE(6,600)
  600 FORMAT(///' TOTAL CORE EXCEEDS BLANK COMMON'//)
 9997 END
      SUBROUTINE MAINN (D,S,X,Y,AL,R,KT,FIY,A,AE,AR,AML,AC,DJ,JJ,JK,
     *JCRL,JRL,LML)
      IMPLICIT REAL*8 (A-H,O-Z)
      DOUBLE PRECISION KT
      DIMENSION SMD(6,6),SMR(6,6),AAA(6),SM(6,6),AMD(6)
      DIMENSION D(N),S(N,IBW),JJ(M),JK(M),X(NJ),Y(NJ),AL(M),R(M,9),
     * JCRL(NTDF),JRL(NTDF),KT(M),FIY(M),LML(M),A(NTDF),AE(NTDF),
     *AR(NTDF),AML(M,6),AC(NTDF),DJ(NTDF)
      COMMON/SETUP/N,M,NJ,NR,NRJ,E,G,IBW,NTDF
C ANALYSIS OF FRAMED STRUCTURES
      IW=0
      NDJ=3
      WRITE (6,503)
      WRITE (6,504)
      WRITE (6,505)M,NJ,NR,NRJ,E,G
  505 FORMAT (4I5,2F10.1)
      WRITE (6,511)
      WRITE (6,512)
      DO 25  K=1,NJ
      READ (5,*) J,X(J),Y(J)
   25 WRITE (6,514) J,X(J),Y(J)
      WRITE (6,515)
      WRITE (6,516)
      DO 30 K=1,M
      READ (5,*) I,JJ(I),JK(I),KT(I) ,FIY(I)
      IF (JJ(I).LE.JK(I)) GO TO 26
      J=JJ(I)
      JJ(I)=JK(I)
```

```
      JK(I)=J
   26 JJI=JJ(I)
      JKI=JK(I)
      XCL=X(JKI)-X(JJI)
      YCL=Y(JKI)-Y(JJI)
      AL(I)=DSQRT(XCL**2+YCL**2)
      CX=XCL/AL(I)
      CY=YCL/AL(I)
      WRITE (6,518) I,JJ(I),JK(I),KT(I) ,FIY(I),AL(I)
      R(I,3)=0.0
      R(I,6)=0.0
      R(I,7)=0.0
      R(I,8)=0.0
      R(I,1)=CX
      R(I,5)=CX
      R(I,9)=1.0
      R(I,2)=CY
   30 R(I,4)=-CY
      DO 11 I=1,N
      DO 11 J=1,IBW
   11 S(I,J)=0.
      DO 12 I=1,NTDF
      JCRL(I)=0
   12 JRL(I)=0
      WRITE (6,519)
      WRITE (6,520)
      DO 40 J=1,NRJ
      READ (5,*) K,JRL(3*K-2),JRL(3*K-1),JRL(3*K)
   40 WRITE (6,522) K,JRL(3*K-2),JRL(3*K-1),JRL(3*K)
      JCRL(1)=JRL(1)
      NNR=N+NR
      DO 50 K=2,NNR
   50 JCRL(K)=JCRL(K-1)+JRL(K)
C PART 2  STRUCTURE STIFFNESS MATRIX
      I=0
      JUBW=0
   60 I=I+1
      IF (I.GT.M) GO TO 260
      J1=3*JJ(I)-2
```

```
      J2=3*JJ(I)-1
      J3=3*JJ(I)
      K1=3*JK(I)-2
      K2=3*JK(I)-1
      K3=3*JK(I)
      SCM1B=G*KT(I)/AL(I)
      SCM2Y=4.0*E*FIY(I)/AL(I)
      SCM3Y=1.5*SCM2Y/AL(I)
      SCM4Y=2.0*SCM3Y/AL(I)
      SM(1,1)= SCM1B
      SM(4,4)= SCM1B
      SM(1,4)=-SCM1B
      SM(4,1)=-SCM1B
      SM(2,2)= SCM2Y
      SM(5,5)= SCM2Y
      SM(2,5)= SCM2Y/2.0
      SM(5,2)= SCM2Y/2.0
      SM(2,6)= SCM3Y
      SM(6,2)= SCM3Y
      SM(5,6)= SCM3Y
      SM(6,5)= SCM3Y
      SM(3,3)= SCM4Y
      SM(6,6)= SCM4Y
      SM(3,6)=-SCM4Y
      SM(6,3)=-SCM4Y
      SM(2,3)=-SCM3Y
      SM(3,2)=-SCM3Y
      SM(3,5)=-SCM3Y
      SM(5,3)=-SCM3Y
      JOO=2*NDJ/3
      JEO=2*NDJ
  110 DO 120 K=1,JOO
      DO 120 J=1,JEO
      SMR(J,3*K-2)=SM(J,3*K-2)*R(I,1)+SM(J,3*K-1)*R(I,4)+SM(J,3*K)*R(I,7
     *)
      SMR(J,3*K-1)=SM(J,3*K-2)*R(I,2)+SM(J,3*K-1)*R(I,5)+SM(J,3*K)*R(I,8
     *)
  120 SMR(J,3*K)=SM(J,3*K-2)*R(I,3)+SM(J,3*K-1)*R(I,6)+SM(J,3*K)*R(I,9)
  125 DO 130 J=1,JOO
```

```
      DO 130 K=1,JEO
      SMD(3*J-2,K)=R(I,1)*SMR(3*J-2,K)+R(I,4)*SMR(3*J-1,K)+R(I,7)*
     *SMR(3*J,K)
      SMD(3*J-1,K)=R(I,2)*SMR(3*J-2,K)+R(I,5)*SMR(3*J-1,K)+R(I,8)*
     *SMR(3*J,K)
130   SMD(3*J,K)=R(I,3)*SMR(3*J-2,K)+R(I,6)*SMR(3*J-1,K)+R(I,9)*
     *SMR(3*J,K)
150   IF  (JRL(J1).NE.0) GO TO 180
      JROW=J1-JCRL(J1)
      S(JROW,1)=S(JROW,1)+SMD(1,1)
      IF (JRL(J2).NE.0) GO TO 155
      S(JROW,2)=S(JROW,2)+SMD(1,2)
155   IF (JRL(J3).NE.0) GO TO 160
      JCOL=J3-JCRL(J3)-JROW+1
      S(JROW,JCOL)=S(JROW,JCOL)+SMD(1,3)
160   IF (JRL(K1).NE.0) GO TO 165
      JCOL=K1-JCRL(K1)-JROW+1
      S(JROW,JCOL)=SMD(1,4)
165   IF (JRL(K2).NE.0) GO TO 170
      JCOL=K2-JCRL(K2)-JROW+1
      S(JROW,JCOL)=SMD(1,5)
170   IF (JRL(K3).NE.0) GO TO 175
      JCOL=K3-JCRL(K3)-JROW+1
      S(JROW,JCOL)=SMD(1,6)
175   IF (JCOL.LE.JUBW) GO TO 180
      JUBW=JCOL
180   IF (JRL(J2).NE.0) GO TO 210
      JROW=J2-JCRL(J2)
      S(JROW,1)=S(JROW,1)+SMD(2,2)
      IF (JRL(J3).NE.0) GO TO 185
      S(JROW,2)=S(JROW,2)+SMD(2,3)
185   IF (JRL(K1).NE.0) GO TO 190
      JCOL=K1-JCRL(K1)-JROW+1
      S(JROW,JCOL)=SMD(2,4)
190   IF (JRL(K2).NE.0) GO TO 195
      JCOL=K2-JCRL(K2)-JROW+1
      S(JROW,JCOL)=SMD(2,5)
195   IF (JRL(K3).NE.0) GO TO 200
      JCOL=K3-JCRL(K3)-JROW+1
```

```
      S(JROW,JCOL)=SMD(2,6)
200   IF (JCOL.LE.JUBW) GO TO 210
      JUBW=JCOL
210   IF (JRL(J3).NE.0) GO TO 230
      JROW=J3-JCRL(J3)
      S(JROW,1)=S(JROW,1)+SMD(3,3)
      IF (JRL(K1).NE.0) GO TO 215
      JCOL=K1-JCRL(K1)-JROW+1
      S(JROW,JCOL)=SMD(3,4)
215   IF (JRL(K2).NE.0) GO TO 220
      JCOL=K2-JCRL(K2)-JROW+1
      S(JROW,JCOL)=SMD(3,5)
220   IF (JRL(K3).NE.0) GO TO 225
      JCOL=K3-JCRL(K3)-JROW+1
      S(JROW,JCOL)=SMD(3,6)
225   IF (JCOL.LE.JUBW) GO TO 230
      JUBW=JCOL
230   IF (JRL(K1).NE.0) GO TO 240
      JROW=K1-JCRL(K1)
      S(JROW,1)=S(JROW,1)+SMD(4,4)
      IF (JRL(K2).NE.0) GO TO 235
      S(JROW,2)=S(JROW,2)+SMD(4,5)
235   IF (JRL(K3).NE.0) GO TO 240
      JCOL=K3-JCRL(K3)-JROW+1
      S(JROW,JCOL)=S(JROW,JCOL)+SMD(4,6)
240   IF (JRL(K2).NE.0) GO TO 250
      JROW=K2-JCRL(K2)
      S(JROW,1)=S(JROW,1)+SMD(5,5)
      IF (JRL(K3).NE.0) GO TO 250
      S(JROW,2)=S(JROW,2)+SMD(5,6)
250   IF (JRL(K3).NE.0) GO TO 60
      JROW=K3-JCRL(K3)
      S(JROW,1)=S(JROW,1)+SMD(6,6)
      GO TO 60
260   CALL DCOMBD (N,JUBW,S,IW)
      READ(5,*) NLCASE
      DO 10 LCASE = 1,NLCASE
      WRITE(6,523) LCASE
      WRITE (6,524)
```

```
      READ (5,*) NLJ,NLM
      WRITE (6,525) NLJ,NLM
      DO 13 J=1,NTDF
      AE(J)=0.
      AR(J)=0.
      AC(J)=0.
   13 A(J)=0.
      DO 14 J=1,M
      LML(J)=0
      DO 14 K=1,6
   14 AML(J,K)=0.
      IF (NLJ.EQ.0) GO TO 315
      WRITE (6,526)
      WRITE (6,527)
      SUMA=0.
      DO 310 J=1,NLJ
      READ (5,*) K,A(3*K-2),A(3*K-1),A(3*K)
      SUMA=SUMA+A(3*K)
  310 WRITE (6,537) K,A(3*K-2),A(3*K-1),A(3*K)
      WRITE(6,566) SUMA
  566 FORMAT (1H0,30HTOTAL.........................,E13.6)
  315 IF (NLM.EQ.0) GO TO 355
      WRITE (6,530)
      WRITE (6,531)
      SUMN=0.
      SUMF=0.
      DO 325 J=1,NLM
      READ (5,*) I,AML(I,1),AML(I,2),AML(I,3),AML(I,4),AML(I,5),
     *AML(I,6)
      WRITE (6,534)I,AML(I,1),AML(I,2),AML(I,3),AML(I,4),AML(I,5),
     *AML(I,6)
      SUMN=SUMN+AML(I,3)
      SUMF=SUMF+AML(I,6)
  325 LML(I)=1
      WRITE(6,567) SUMN,SUMF
  567 FORMAT (1H0,30HTOTAL.........................,D13.6,26H...........
     *...............,D13.6)
      DO 350 I=1,M
      IF (LML(I).NE.1) GO TO 350
```

```
      JJI=JJ(I)
      JKI=JK(I)
      AE(3*JJI  -2)=AE(3*JJI  -2)-R(I,1)*AML(I,1)-R(I,4)*AML(I,2)
     * -R(I,7)*AML(I,3)
      AE(3*JJI  -1)=AE(3*JJI  -1)-R(I,2)*AML(I,1)-R(I,5)*AML(I,2)
     *-R(I,8)*AML(I,3)
      AE(3*JJI  )=AE(3*JJI  )-R(I,3)*AML(I,1)-R(I,6)*AML(I,2)-R(I,9)
     **AML(I,3)
      AE(3*JKI  -2)=AE(3*JKI  -2)-R(I,1)*AML(I,4)-R(I,4)*AML(I,5)
     *-R(I,7)*AML(I,6)
      AE(3*JKI  -1)=AE(3*JKI  -1)-R(I,2)*AML(I,4)-R(I,5)*AML(I,5)
     *-R(I,8)*AML(I,6)
      AE(3*JKI )=AE(3*JKI  )-R(I,3)*AML(I,4)-R(I,6)*AML(I,5)-R(I,9)
     **AML(I,6)
  350 CONTINUE
  355 NNR=N+NR
      DO 360 J=1,NNR
      IF (JRL(J).NE.0) GO TO 358
      K=J-JCRL(J)
      GO TO 360
  358 K=N+JCRL(J)
  360 AC(K)=A(J)+AE(J)
      WRITE (6,535)
      WRITE (6,536)
      DO 15 J=1,N
   15 D(J)=0.
      CALL SOLVBD (N,JUBW,S,AC,D)
  370 J=N+1
      JOE=N+NR
      MC=0
      MM=2*JOE-1
      DO 380 JE=JOE,MM
      JEE=JE-MC
      IF (JRL(JEE).EQ.0) GO TO 375
      DJ(JEE)=0
      GO TO 380
  375 J=J-1
      DJ(JEE)=D(J)
  380 MC=MC+2
```

```
      JOB=3*NJ
      DO 390 JE=3,JOB,3
      JOC=JE/3
  390 WRITE (6,537) JOC,DJ(JE-2),DJ(JE-1),DJ(JE)
      WRITE (6,540)
      WRITE (6,541)
      I=0
  400 I=I+1
      IF (I.GT.M) GO TO  460
      J1=3*JJ(I)-2
      J2=3*JJ(I)-1
      J3=3*JJ(I)
      K1=3*JK(I)-2
      K2=3*JK(I)-1
      K3=3*JK(I)
      SCM1B=G*KT(I)/AL(I)
      SCM2Y=4.0*E*FIY(I)/AL(I)
      SCM3Y=1.5*SCM2Y/AL(I)
      SCM4Y=2.0*SCM3Y/AL(I)
      SM(1,1)=SCM1B
      SM(4,4)=SCM1B
      SM(1,4)=-SCM1B
      SM(4,1)=-SCM1B
      SM(2,2)=SCM2Y
      SM(5,5)=SCM2Y
      SM(2,5)=SCM2Y/2.0
      SM(5,2)=SCM2Y/2.0
      SM(2,6)=SCM3Y
      SM(6,2)=SCM3Y
      SM(5,6)=SCM3Y
      SM(6,5)=SCM3Y
      SM(2,3)=-SCM3Y
      SM(3,2)=-SCM3Y
      SM(3,5)=-SCM3Y
      SM(5,3)=-SCM3Y
      SM(3,3)=SCM4Y
      SM(6,6)=SCM4Y
      SM(3,6)=-SCM4Y
      SM(6,3)=-SCM4Y
```

```
      KOO=2*NDJ/3
      KII=2*NDJ
      DO 410 K=1,KOO
      DO 410 J=1,KII
      SMR(J,3*K-2)=SM(J,3*K-2)*R(I,1)+SM(J,3*K-1)*R(I,4)+SM(J,3*K)*
     *R(I,7)
      SMR(J,3*K-1)=SM(J,3*K-2)*R(I,2)+SM(J,3*K-1)*R(I,5)+SM(J,3*K)*
     *R(I,8)
  410 SMR(J,3*K)=SM(J,3*K-2)*R(I,3)+SM(J,3*K-1)*R(I,6)+SM(J,3*K)*R(I,9)
      DO 420 J=1,6
  420 AMD(J)=SMR(J,1)*DJ(J1)+SMR(J,2)*DJ(J2)+SMR(J,3)*DJ(J3)+SMR(J,4)*
     *DJ(K1)+SMR(J,5)*DJ(K2)+SMR(J,6)*DJ(K3)
      DO 425 J=1,6
  425 AAA(J)=AML(I,J) + AMD(J)
  430 WRITE (6,550) I,(AAA(J),J=1,6)
      IF (JRL(J1).NE.1) GO TO 435
      AR(J1)=AR(J1)+R(I,1)*AMD(1)+R(I,4)*AMD(2)+R(I,7)*AMD(3)
  435 IF (JRL(J2).NE.1) GO TO 440
      AR(J2)=AR(J2)+R(I,2)*AMD(1)+R(I,5)*AMD(2)+R(I,8)*AMD(3)
  440 IF (JRL(J3).NE.1) GO TO 445
      AR(J3)=AR(J3)+R(I,3)*AMD(1)+R(I,6)*AMD(2)+R(I,9)*AMD(3)
  445 IF (JRL(K1).NE.1) GO TO 450
      AR(K1)=AR(K1)+R(I,1)*AMD(4)+R(I,4)*AMD(5)+R(I,7)*AMD(6)
  450 IF (JRL(K2).NE.1)GO TO 455
      AR(K2)=AR(K2)+R(I,2)*AMD(4)+R(I,5)*AMD(5)+R(I,8)*AMD(6)
  455 IF (JRL(K3).NE.1) GO TO 400
      AR(K3)=AR(K3)+R(I,3)*AMD(4)+R(I,6)*AMD(5)+R(I,9)*AMD(6)
      GO TO 400
  460 WRITE (6,555)
      WRITE (6,560)
      DO 480 K=1,NNR
      IF (JRL(K).NE.1) GO TO 480
  470 AR(K)=AR(K)-A(K)-AE(K)
  480 CONTINUE
      NOT=3*NJ
      SUMR=0.
      DO 490 KE=3,NOT,3
      IF (JRL(KE-2).EQ.1) GO TO 496
      IF (JRL(KE-1).EQ.1) GO TO 496
```

```
      IF (JRL(KE).EQ.1) GO TO  496
      GO TO 490
  496 JOB=KE/3
      SUMR=SUMR+AR(KE)
      WRITE (6,565) JOB,AR(KE-2),AR(KE-1),AR(KE)
  490 CONTINUE
      WRITE(6,568) SUMR
  568 FORMAT (1H0,30HTOTAL.......................,D13.6)
   10 CONTINUE
  503 FORMAT(/15H STRUCTURE DATA)
  504 FORMAT (/44H    M   NJ   NR  NRJ      E        G                 )
  511 FORMAT (/22H COORDINATES OF JOINTS)
  512 FORMAT (/24H JOINT     X          Y )
  514 FORMAT (I5,2E11.4)
  515 FORMAT(/19H MEMBER INFORMATION)
  516 FORMAT (/44H MEMBER JJ   JK     KT        FIY       AL     )
  518 FORMAT (3I5,3E10.3)
  519 FORMAT(/17H JOINT RESTRAINTS)
  520 FORMAT (/20H JOINT   X    Y    Z)
  522 FORMAT (4I5)
  523 FORMAT (/1X,'LOADING NO.',I5)
  524 FORMAT (/12H  NLJ  NLM  )
  525 FORMAT (2I5)
  526 FORMAT(/27H ACTIONS APPLIED AT JOINTS )
  527 FORMAT (/39H JOINT     A1           A2           A3)
  530 FORMAT(/43H ACTIONS AT RESTRAINED MEMBERS DUE TO LOADS)
  531 FORMAT (/79H MEMBER    AM1          AM2          AM3          AM4
     *         AM5          AM6)
  534 FORMAT (I5,6D13.6)
  535 FORMAT(/20H JOINT DISPLACEMENTS)
  536 FORMAT (/39H JOINT     D1           D2           D3)
  537 FORMAT (I5,3D13.6)
  540 FORMAT(/19H MEMBER END ACTIONS)
  541 FORMAT (/79H MEMBER    AM1          AM2          AM3          AM4
     *         AM5          AM6)
  550 FORMAT (I5,6D13.6)
  555 FORMAT(/18H SUPPORT REACTIONS)
  560 FORMAT (/40H JOINT     AR1          AR2          AR3)
  565 FORMAT (I5,3D13.6)
```

```
      RETURN
      END
      SUBROUTINE SOLVBD (N,JUBW,U,B,C)
      IMPLICIT REAL*8 (A-H,O-Z)
      DIMENSION U(N,1),B(1),C(1)
      DO 100 I=1,N
      J=I-JUBW+1
      IF (I+1.GT.JUBW) GO TO 10
      J=1
   10 SUM=B(I)
      JOE=I-1
      IF (JOE.EQ.0) GO TO 100
      DO 20 K=J,JOE
   20 SUM=SUM-U(K,I-K+1)*C(K)
  100 C(I)=SUM*U(I,1)
      M=0
      MM = 2*N-1
      DO 200 I=N,MM
      IS=I-M
      J=IS+JUBW-1
      IF (J.LE.N) GO TO 30
      J=N
   30 SUM=C(IS)
      II=IS+1
      DO 40 K=II,J
   40 SUM=SUM-U(IS,K-IS+1)*C(K)
      C(IS)=SUM*U(IS,1)
  200 M=M+2
      RETURN
      END
      SUBROUTINE DCOMBD(N, JUBW,S,IW)
      IMPLICIT REAL*8 (A-H,O-Z)
      DIMENSION S(N,1)
      IW=0
      DO 10 I=1,N
      IP=N-I+1
      IF (JUBW.GE.IP) GO TO 20
      IP=JUBW
   20 CONTINUE
```

```
      DO 10 J=1,IP
      IQ=JUBW-J
      IF (I-1.GE.IQ) GO TO 30
      IQ=I-1
   30 SUM=S(I,J)
      IF (IQ.EQ.0) GO TO 45
      DO 40 K=1,IQ
   40 SUM=SUM-S(I-K,1+K)*S(I-K,J+K)
   45 IF (J.NE.1) GO TO 50
      IF (SUM.LE.0) GO TO 60
      TEMP=1./(DSQRT(SUM))
      S(I,J)=TEMP
      GO TO 10
   50 S(I,J)=SUM*TEMP
   10 CONTINUE
      GO TO 70
   60 IW=1
   70 CONTINUE
      RETURN
      END
```

APPENDIX G

APPENDIX G

CALCULATION OF COMPOSITE SECTION PROPERTIES

This appendix illustrates the calculations of the composite section properties for the longitudinal and transverse members of the grid models. The cross sections used for the calculations are shown in Figures G1 and G2.

Calculations for Longitudinal Members:

Girder Properties:

$A = 30\ in^2$

$I = 2700\ in^4$

$k_t = 5\ in^4$

$d = 24\ in$

Neutral Axis Location:

$y = [(A_{girder} \times d/2) + (A_{deck} \times (d + 3\ in))] / A_{total}$

$y = [(6\ in)\ (8\ in)\ (27\ in) + (30\ in^2)\ (12\ in)] / 78\ in^2 = 21.2\ in$

Composite Moment of Inertia:

$I = I_{girder} + (A_{girder})\ (y - d/2)^2 + I_{deck} + (A_{deck})\ [(d + 3) - y]^2$

$I = 2700\ in_4 + 30\ in^2\ (21.2 - 12)^2 + (6\ in)^3\ (8\ in) / 12 +$

$(6\ in)\ (8\ in)\ (27\ in - 21.2\ in)^2 = 6998\ in^4$

Torsional Constant:

$k_t = K_{t\ girder} + k_{t\ deck}$

$k_{t\ deck} = (6\ in)^3\ (8\ in) / 3$

$k_t = 5\ in^4 + 576\ in^4 = 581\ in^4$

Concrete Deck Measurements:

$d' = 1.8\ in$

$d = 1.3\ in$

$t = 6.5\ in$

$A_{top\ steel} = A_{bottom\ steel} = 2\ in^2$

$w = 4.33\ ft = 52\ in$

Transformed Width of Concrete Deck:

$n = 6$

$w = 52\ in / 6 = 8.67\ in$

Neutral Axis Location:

$(w_{deck})\ (y^2) / 2 + (A_{top\ steel})\ (y - d') = (A_{bottom\ steel})\ (t - d - y)$

$(8.67\ in)\ (y^2) / 2 + (2\ in^2)\ (y - 1.8) = (2\ in^2)\ (5.2 - y)$

Solving for y gives: $y = 1.4\ in$

Moment in Inertia:

$I = (w)\ (y)^3 / 3 + (A_{top\ steel})\ (d' - y)^2 + (A_{bottom\ steel})\ (t - d - y)^2$

$I = (8.67\ in)\ (1.4\ in)^3 / 3 + (2\ in^2)\ (1.8\ in - 1.4\ in)^2 + (2\ in^2)\ (5.2\ in - 1.4\ in)^2 = 37\ in^4$

Torsional Constant:

$k_t = k_{t\ deck}$

$k_{t\ deck} = (8.67\ in)\ (6.5\ in)^3 / 3$

$k_t = 794\ in^4$

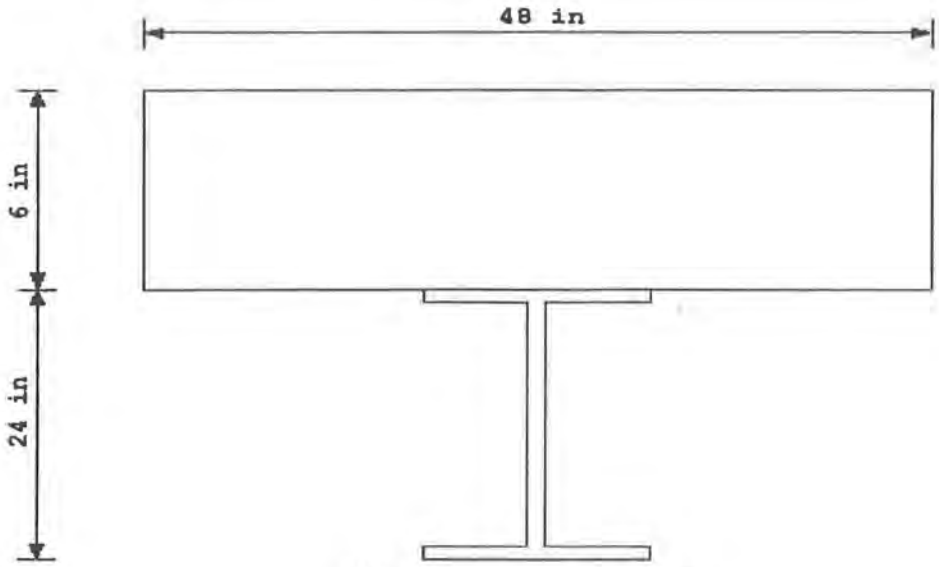

Longitudinal Section

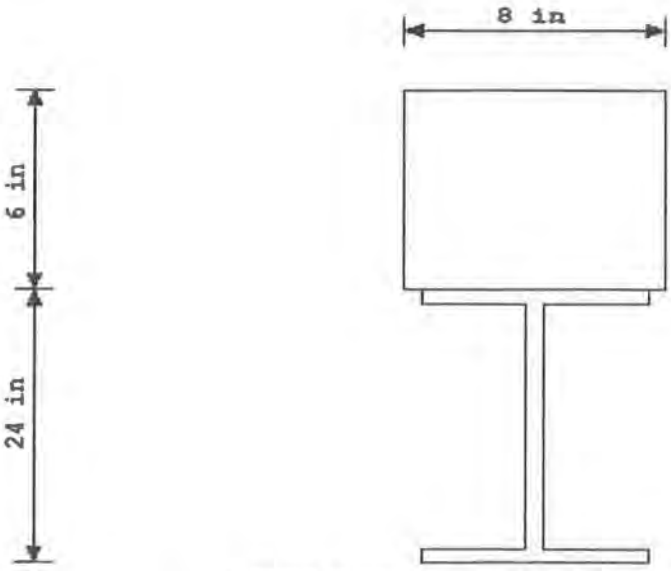

Transformed Longitudinal Section

Figure G1. Longitudinal Section

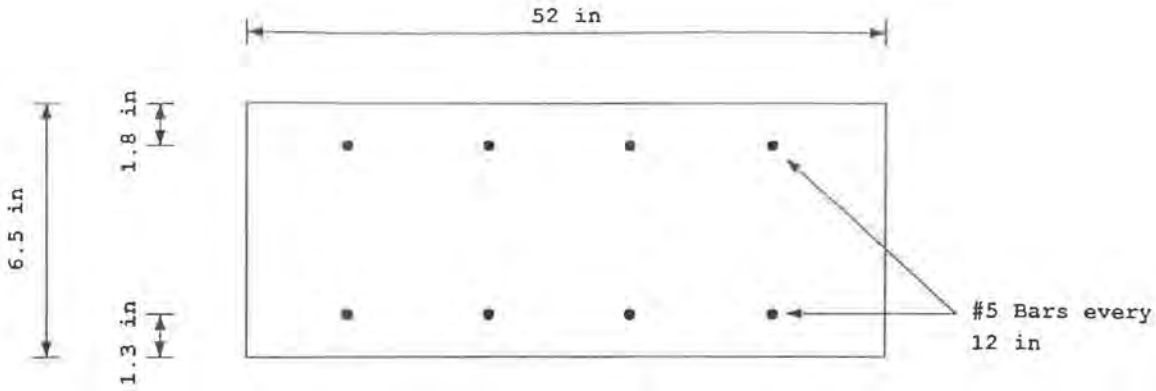

Transverse Section

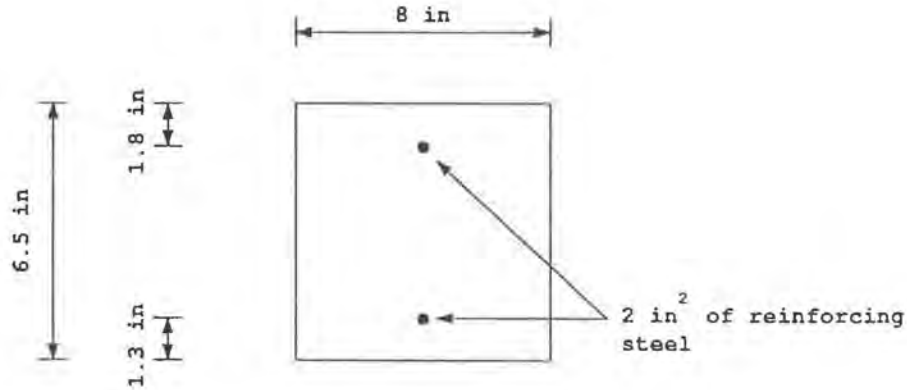

Transformed Transverse Section

Figure G2. Transverse Section

LIST OF TABLES

Table 1. Bridges Tested 2
Table 2. Girder Cross Section 14
Table 3. Measured Strains and Deflections from Ashville Bridge Test 15
Table 4. Observed Impact Factors from Ashville Bridge Test 18
Table 5. Girder Cross Section Properties 21
Table 6. Measured Strains and Deflections from Vincent Bridge Test, Stationary Truck Tests 24
Table 7. Measured Strains and Deflections from Vincent Bridge Test, Moving Truck Tests 25
Table 8. Girder Cross Section Properties 26
Table 9. Measured Strains and Deflections from Childersburg Bridge Test, 44 ft Span 30
Table 10. Measured Strains and Deflections from Childersburg Bridge Test, 77 ft Span 31
Table 11. Girder Cross Section Properties 38
Table 12. Measured Strains and Deflections from Mulberry Fork Bridge Test, 34 ft Span 39
Table 13. Measured Strains and Deflections from Mulberry Fork Bridge Test, 44 ft Span 40
Table 14. Girder Cross Section Properties 44
Table 15. Measured Strains and Deflections from Locust Fork Bridge Test, 49 ft Span 48
Table 16. Measured Strains and Deflections from Locust Fork Bridge Test, Continuous Spans 49
Table 17. Comparison of Measured and Calculated Strains and Deflections, Ashville Bridge 55
Table 18. Comparison of Measured and Calculated Strains and Deflections, Vincent Bridge 56
Table 19. Comparison of Measured and Calculated Strains and Deflections, Childersburg Bridge, 44 ft Span 59
Table 20. Comparison of Measured and Calculated Strains and Deflections, Childersburg Bridge, 77 ft Span 60
Table 21. Comparison of Measured and Calculated Strains and Deflections, Mulberry Fork Bridge, 34 ft Span 63
Table 22. Comparison of Measured and Calculated Strains and Deflections, Mulberry Fork Bridge, 44 ft Span 64
Table 23. Comparison of Measured and Calculated Strains and Deflections, Locust Fork Bridge, 49 ft Span 66
Table 24. Comparison of Measured and Calculated Strains and Deflections, Locust Fork Bridge, Continuous Spans 67
Table 25. Comparison of Moment Ratios from Grid and Simple Beam Analysis
Table 26. Estimated Dead Loads, Ashville 71
Table 27. Estimated Dead Loads, Vincent 74
Table 28. Estimated Dead Loads, Childersburg 74
Table 29. Estimated Dead Loads, Mulberry Fork 74
Table 30. Estimated Dead Loads, Locust Fork 75
Table 31. Allowable Operating Stresses 75
Table 32. M_{test} Values 75
Table 33. Ashville Operating Ratings 79
Table 34. Childersburg Operating Ratings, 44 ft Span 79
Table 35. Childersburg Operating Ratings, 77 ft Span 79

LIST OF TABLES (continued)

Table 36. Vincent Operating Ratings. 80
Table 37. Mulberry Fork Operating Ratings, 34 ft Span 80
Table 38. Mulberry Fork Operating Ratings, 44 ft Span 80
Table 39. Locust Fork Operating Ratings, 49 ft Span. 81
Table 40. Locust Fork Operating Ratings, Continuous Spans 81
Table 41. BARS and AASHTO Ratings, Childersburg, 44 ft Span. 82
Table 42. BARS and AASHTO Ratings, Mulberry Fork, 34 ft Span. 83
Table 43 BARS and AASHTO Ratings, Mulberry Fork, 44 ft Span. 83

LIST OF FIGURES

Figure 1. Strain Gage. 6
Figure 2. Deflectometer 8
Figure 3. Measuring and Recording Equipment. 8
Figure 4. AHD Two-Axle Dump Trucks 10
Figure 5. Ashville Bridge. 12
Figure 6. Ashville Bridge Cross Section. 12
Figure 7. Strain Gage and Deflectometer Locations. 16
Figure 8. Test Truck Axle Loads and Spacings. 16
Figure 9. Longitudinal Positions of Test Trucks 19
Figure 10. Vincent Bridge. 22
Figure 11. Vincent Bridge Cross Section. 22
Figure 12. Strain Gage and Deflectometer Locations. 27
Figure 13. Test Truck Axle Loads and Spacings. 27
Figure 14. Longitudinal Positions of Test Trucks 28
Figure 15. Childersburg Bridge. 32
Figure 16. Childersburg Bridge Cross Section 32
Figure 17. Strain Gage and Deflectometer Locations. 33
Figure 18. Text Truck Axle Loads and Spacings. 33
Figure 19. Longitudinal Positions of Test Trucks 34
Figure 20. Mulberry Fork Bridge. 36
Figure 21. Mulberry Fork Bridge Cross Section. 36
Figure 22. Strain Gage and Deflectometer Locations. 41
Figure 23. Test Truck Axle Loads and Spacings. 41
Figure 24. Longitudinal Positions of Test Trucks 42
Figure 25. Locust Fork Bridge. 42
Figure 26. Locust Fork Bridge Cover Plates. 45
Figure 27. Locust Fork Bridge Cross Section. 45
Figure 28. Strain Gage and Deflectometer Locations. 46
Figure 29. Test Truck Axle Loads and Spacings. 46
Figure 30. Longitudinal Positions of Test Trucks 50
Figure 31. Grid Model of Bridge Deck System. 53
Figure 32. Cross Sections Used for Ashville Sections. 57
Figure 33. Cross Section Used for Vincent Section Properties. 57
Figure 34. Cross Sections Used for Childersburg Section Properties 61
Figure 35. Cross Sections Used for Mulberry Fork Section Properties. 61
Figure 36. Cross Sections Used for Locust Fork Section Properties 68
Figure 37. Position of Standard Trucks on Vincent Grid Model 69
Figure 38. Position of Standard Trucks on Mulberry Fork Grid Model 69
Figure 39. Position of Standard Trucks on Locust Fork Grid Model. 72
Figure 40. Standard Truck Types. 83